DISSERTATION

INFLUENCE OF CO-DISPOSING OIL AND GAS EXPLORATION AND PRODUCTION WASTE AND MUNICIPAL SOLID WASTE ON HYDRAULIC CONDUCTIVITY

Submitted by

Sajjad Karimi

Department of Civil & Environmental Engineering

In partial fulfillment of the requirements

For the Degree of Doctor of Philosophy

Colorado State University

Fort Collins, Colorado

Summer 2022

Doctoral Committee:

Advisor: Christopher Bareither
Co-Advisor: Joseph Scalia

Sybil Sharvelle
Joe von Fischer

ABSTRACT

INFLUENCE OF CO-DISPOSING OIL AND GAS EXPLORATION AND PRODUCTION WASTE AND MUNICIPAL SOLID WASTE ON HYDRAULIC CONDUCTIVITY

The most common method of municipal solid waste (MSW) disposal in the U.S. is still landfilling. Co-disposal of MSW with other non-MSWs in solid waste landfills requires engineering design to reduce the risks associated with the stability and functionality of solid waste landfills. Hydraulic conductivity is one of the engineering parameters required to assess the stability of a landfill. This study evaluated the effects of addition of oil and gas exploration and production wastes (E&PW) to municipal solid waste (MSW) landfills on hydraulic behavior of mixed waste. Hydraulic conductivity of solid waste is a function of vertical stress, waste composition, mixture ratio of MSW to E&PW based on total mass (e.g., 20% MSW + 80% E&PW), and mixing methods. A series of laboratory experiments were conducted to assess the impacts of these factors on the hydraulic conductivity of solid waste. Exploration and production waste was prepared to two moisture contents for laboratory testing: (i) as-received, which had a dry weight water content of 18%; and (ii) wet, which had a target moisture content of 32% to 36%. Wet E&PW prepared to the water content threshold represented the upper bound of water content for which the HMW met regulations for direct disposal in an MSW landfill. Hydraulic conductivity of the as-received E&PW measured in a large-scale permeameter decreased from 7.3×10^{-5} m/s to 1.1×10^{-8} m/s with an increase in vertical stress from 1 kPa to 394 kPa. The k_s of as-received E&PW in small scale a small-scale permeameter reduced from 1.2×10^{-7} to 1×10^{-9} m/s with increasing stress to 50 kPa, and then k_s stabilized at 7.5×10^{-10} m/s with increasing effective stress to 400 kPa. Although k_s of the small-scale E&PW specimen was two to three orders-of-magnitude lower relative to the large-scale specimen as a function of vertical stress, the data align when evaluating k_s as a function of

dry unit weight. This indicated similar response of small-scale and large-scale specimens to hydraulic conductivity with respect to dry unit weight. The effects of E&PW hydration can be observed via the wet E&PW. The initial dry unit weight of the wet E&PW specimen was approximately 14 kN/m^3, with a k_s similar to the trend in k_s versus dry unit weight for the as-received (dryer) E&PW specimen. However, k_s of the wet E&PW specimen reduced two orders of magnitude (6.6×10^{-6} m/s to 5.4×10^{-9} m/s) as the effective vertical stress was increased to 17 kPa and dry unit weight increased to 15 kN/m^3. Subsequently, k_s of the wet E&PW decreased one order of magnitude to 2.8×10^{-10} m/s as vertical effective stress was increased from 17 kPa to 389 kPa. The ks of the wet E&PW specimen was two orders of magnitude lower than as-received E&PW under 394 kPa effective vertical stress. The overall trends for all E&PW mixture ratios for both the as-received and wet E&PW were similar and exhibited an as-expected decrease in hydraulic conductivity with increasing vertical effective stress. Hydraulic conductivity for MSW-E&PW mixtures with 20% and 40% E&PW contents reduced from 3×10^{-5} m/s to 1×10^{-7} m/s under effective vertical stress ranged from 0 to 400 kPa. An increase in the mixture ratio above 60% resulted in an additional order-of-magnitude decrease in k_s to 1×10^{-8} m/s as vertical effective stress increased above 200 kPa. The lowest k_s at each stress level was measured for MSW mixed with 80% wet E&PW. Findings from this study indicate that addition of an E&PW did not change the hydraulic behavior of MSW. Mixture of E&PW and MSW creates a waste matrix such that hydraulic behavior still is controlled by MSW components at low stresses (and low dry densities). However, if vertical stress exceeds 50 kPa, mixtures of MSW + 80% (and above) E&PW were observed to produce a low permeability (i.e., $k_s < 1\times10^{-9}$ m/s). If the E&PW is disposed in discrete layers without rigorous mixing with MSW, increasing vertical stress may substantially reduce the E&PW hydraulic conductivity producing water and vapor barriers within the landfill. These findings represent the specific E&PW tested in this study, however, when combined with other data in the literature, illustrate the need for establishing mixture ratio thresholds and intentionally co-disposing E&PWs.

ACKNOWLEDGMENTS

I would like to thank my advisor, Dr. Bareither, for his support and guidance during the last five years. I do appreciate him for giving me the opportunity to work with him and providing an excellent atmosphere for me to conduct my research. What I learned from him during my Ph.D. journey was invaluable. I would like to thank my co-advisor, Dr. Scalia, for his support during my Ph.D. project. I would like to thank Dr. Von Fischer for his willingness to be on my Ph.D. committee and for his guidance.

I am grateful to my colleagues and friends in the Geo-group at Colorado State University, especially Mohammad Reza and Kelechi, for their constant cooperation and assistance throughout my Ph.D. in the last six years. I would like to thank my best friend, Mohammad Javad, with whom we had a memorable time in the US. I would like to thank my brothers, Dr. Sina, Dr. Hossein, and Dr. Zakaria, for their everlasting encouragement, support, and motivation. They are always my best mentors. I would like to offer a special thank you to my wife, Arefeh, who, without her patience, understanding, and support, I would never have been able to finish my dissertation. Thank you for helping me in the laboratory until late at night to conduct my laboratory tests. Thank you, Arefeh, for the sacrifices you have made for me to pursue my Ph.D.

Last but not least, my warm and heartfelt thanks go to my parents for the tremendous support and unconditional love they have given me; they mean the world to me. I am thankful for my grandmother, who remembered me in their prayers for the ultimate success, and unfortunately, I was not able to visit her before she passed away. I would like to thank my father, Professor Abbas Ali Karimi, and my mother, Zohreh Rabbani, who inspired me to pursue higher education. My accomplishments and success are because they believed in me. I am forever thankful for their love and support throughout my entire life.

DEDICATION

This dissertation is dedicated to

my wife, Arefeh,

and my mother, Zohreh Rabbani,

and my father, Professor Abbas Ali Karimi.

TABLE OF CONTENTS

LIST OF TABLES

LIST OF FIGURES

CHAPTER 1: EXECUTIVE SUMMARY

1.1. Introduction

Final disposal of 50% of municipal solid waste (MSW) generated in the U.S. is still in landfills. Proper operation and management of landfills are critical to landfill owners to reduce the risks associated with landfilled waste. In addition, providing a safe and healthy environment is essential for society working and living in an adjacent area. A method implemented by landfills practitioners to develop a sustainable landfill is to promote waste decomposition to (i) accelerate waste neutralization (i.e., reduce the risks associated with solid waste), (ii) convert the solid waste to energy (e.g., biogas and electricity), and (iii) increase waste settlement, which provides more airspace for waste disposal that increases landfills revenue. Moisture enhancement has a pivotal role in increasing MSW decomposition rate (Karimi and Bareither 2021).

The initial intent of adding non-MSW to solid waste landfills is to provide a sustainable solution for disposing non-MSW. However, non-MSW can provide benefits for landfills. Non-MSWs such as municipal sludge, biosolids, or wastes with a high-moisture content (HMW) can potentially elevate the moisture content in a landfill; or provide nutrients or microorganisms to a landfill, which enhances the decomposition rate. Municipal solid waste landfills in arid regions employ bulk or stabilized waste with high-moisture content as a daily cover to reduce the need for additional daily cover materials. These wastes also increase the overall moisture content of landfills to enhance the degradation of organic materials.

Despite the fact that increasing moisture level in a landfill or co-disposing MSW with other types of waste can enhance the waste decomposition rate, introducing liquid waste or non-MSW can affect landfill stability and functionality. For instance, the ability of a landfill to transfer liquid waste or leachate is a key factor for the addition of liquid waste, landfill slope stability analysis, leachate collection systems, and gas extraction wells. The impacts of co-disposing MSW with other types of waste on biogas generation are important for operating a landfill. Therefore, the chemical and biological compatibility of liquid and solid waste mixtures and landfill stability must be evaluated.

The stability and functionality of a landfill are the main factors that engineers consider in designing and monitoring a landfill. The hydraulic behavior of solid waste directly affects landfill stability and functionality. For instance, low permeable layers of waste prevent liquid from percolating into waste mass and create perched water tables within the landfill. Perched water zones introduce liquid to gas wells and impede biogas extraction. Low permeable layers reduce the efficiency of leachate distribution and collection systems throughout a landfill. Furthermore, perched water tables can potentially lead to positive pore water pressure buildup, reducing the effective stress and subsequently landfill stability.

Hydraulic conductivity of solid waste can decrease where solid waste landfills are allowed to accept non-MSW materials such as industrial sludge, biosolids, or low permeable wastes. The decrease in MSW hydraulic conductivity can potentially cause negative consequences. For instance, mixing solid waste with a low permeable sludge can substantially reduce the hydraulic conductivity and form a lens of the perched water table. Co-disposing MSW with biosolids enhances biogas generation, and the accumulation of biogas under low permeable layers can lead to excess gas pressure in landfills. These issues lie at the root of low hydraulic conductivity wastes. Therefore, understanding the hydraulic behavior of solid waste and other mixed wastes is critical to the effective operation of landfills.

As solid waste decomposes, the physical, chemical, and biological characteristics of solid waste change. For instance, degradation of solid waste and conversion of solid mass to gas reduces the waste particle size, decreases the organic fraction of waste, and increases the dry unit weight of solid waste. The degradation of solid waste can have effects on hydraulic conductivity as well.

The objectives of this study were to (i) evaluate the impacts of stress and degradation on hydraulic conductivity of MSW, (ii) evaluate the geotechnical characteristics of oil and gas exploration and production waste (E&PW), and (iii) determine the hydraulic conductivity of MSW mixed with E&PW. To achieve the mentioned objectives, first, a literature review was carried out to assess the impacts of stress, unit weight, composition, and degradation on MSW hydraulic conductivity. Then, geotechnical engineering laboratory tests, including modified Proctor compaction test, specific gravity, and hydraulic conductivity tests were performed on E&PW to characterize the waste. The strength of MSW and E&PW were measured by conducting shear strength and vane shear tests (Ciraula 2022). After that, a series of hydraulic conductivity experiments were conducted on MSW, E&PW, and mixtures of MSW and E&PW to assess hydraulic behavior.

1.2. Major findings

The findings from this research are presented in three chapters, (1) critical review of MSW hydraulic conductivity, (2) influence of oil and gas exploration and production waste on municipal solid waste hydraulic conductivity, (3) practical implications regarding management and disposal of E&PW in MSW landfills. Supplemental information to this study is compiled in five appendices: Appendix A – the influence of moisture enhancement on solid waste biodegradation, which was published as a journal publication in Waste Management (Karimi and Bareither 2021); Appendix B – summaries of hydraulic conductivity experiments that assessed the impacts of vertical stress, dry unit weight, and degradation on hydraulic conductivity of MSW; and a summary of studies reporting the hydraulic conductivity of landfill-scale experiments, Appendix C – a collection of photographs, tables, and figures documenting the waste preparation and testing procedures; Appendix D – summary of modified Proctor compaction tests; Appendix D – summary of compaction testes on MSW, E&PW and mixtures of MSW-E&PW; and Appendix E – summary of hydraulic conductivity tests on MSW, E&PW, and mixtures of MSW and E&PW. The result from a set of experiments to assess the influence of co-disposal of MSW with different solid/liquid wastes on biodegradation and biochemical compatibility was published as a journal publication in Waste Management (Rohlf, Karimi, and Bareither 2021).

1.2.1. Influence of Moisture Enhancement on Solid Waste Degradation

The influence of moisture enhancement strategies on biodegradation of municipal solid waste was assessed in laboratory-scale reactors. Moisture enhancement strategies were varied with respect to dose volume (40, 80, 160, and 320 L/Mg-MSW) and dose frequency (dosing every ½, 1, 2, and 4 weeks). Biodegradation was evaluated based on methane generation to assess (i) the lag-time between the start of liquid dosing and onset of methane generation and (ii) the first-order decay rate for methane generation. In general, the decay rate increased with an increase in dose volume for a given dose frequency. In addition, trends of increasing decay rate and decreasing lag-time were observed for an increase in dose frequency for reactors operated with dose volumes of 40, 80, and 160 L/Mg-MSW. A key conclusion was that reactors with more aggressive moisture enhancement attained more rapid methane generation that initiated at shorter elapsed times following the onset of dosing. An assessment of liquid dosing per month indicated that there were more pronounced impacts of increasing decay rate and decreasing lag-time as moisture enhancement increased from 40 L/Mg-MSW/month to 320 L/Mg-MSW/month as compared to the impact on both variables for an increase in liquid dosing above 320 L/Mg-MSW/month (Karimi and Bareither 2021).

1.2.2. Influence of Stress and Decomposition on Solid Waste Hydraulic Conductivity

The impacts of stress and unit weight on MSW hydraulic conductivity were consistent. In general, hydraulic conductivity reduces when stress and unit weight increase. The extent of reduction in hydraulic conductivity is dependent on stress, waste composition, and decomposition state. Solid waste degradation can have two opposing effects on hydraulic behavior. Some studies indicated that an increase in MSW decomposition results in particle size reduction and settlement that reduces the void ratio (i.e., the ratio of void volume to solid volume), such that MSW hydraulic conductivity decreases. On the other hand, some studies indicated that waste decomposition reduces the solid mass, which increases the void ratio and creates larger flow paths, which subsequently increases hydraulic conductivity. As a result, the overall effect of degradation on hydraulic conductivity is determined by changes in void ratio.

1.2.3. Impacts of Co-Disposing Exploration and Production Waste and Municipal Solid Waste on Hydraulic Conductivity

The hydraulic conductivity of MSW-E&PW mixtures for both the as-received and wet E&PW mixtures reduced with a similar trend from 1×10^{-5} m/s to 1×10^{-8} m/s by applying 400 kPa vertical stress. Hydraulic conductivity of mixed MSW-E&PW reduced by an additional order-of-magnitude relative to MSW, as the mixture ratio exceeded 60% and vertical effective stress increased above 200 kPa. The lowest k_s at each stress level was measured for MSW mixed with 80% wet E&PW. The results of this study indicated that when E&PW is mixed with MSW, the hydraulic behavior of MSW does not change. Mixing E&PW with MSW creates a waste matrix such that hydraulic behavior still is controlled by MSW materials. Only if vertical stress exceeds 50 kPa, mixtures of MSW + 80% and above E&PW content may create a low permeable layer (i.e., $k_s < 1\times10^{-9}$ m/s). However, the hydraulic conductivity of E&PW can reduce substantially if the dry unit weight decreases to 14 kN/m^3. Disposal of E&PW in discrete layers can potentially create a low permeable layer, form perched water lenses, and consequently causes water accumulation in landfill. Accumulation of water may lead to pore water pressure buildup, reduce the safety factor of landfill and cause instability at landfills. Several landfills or slope failures have been reported due to excessive pore water pressure generation in solid waste landfills (Hendron et al., 1999; Koerner and Soong 2000; Bonaparte et al., 2020; Bareither et al., 2020). The potential consequences associated with landfill instability can yield serious issues which threaten human health and the environment.

1.3. References

Bareither, C. A., Benson, C. H., Rohlf, E. M., & Scalia, J. (2020). Hydraulic and mechanical behavior of municipal solid waste and high-moisture waste mixtures. *Waste Management,* 105, 540–549. https://doi.org/10.1016/j.wasman.2020.02.030

Bonaparte, R., Bachus, R. C., & Gross, B. A. (2020). Geotechnical Stability of Waste Fills: Lessons Learned and Continuing Challenges. *Journal of Geotechnical and Geoenvironmental Engineering*, 146(11), 05020010. https://doi.org/10.1061/(ASCE)gt.1943-5606.0002291

Ciraula A. (2022). *Influence of co-disposing oil and gas exploration and production waste and municipal solid waste on shear strength*, MS Thesis, Colorado State University, Fort Collins, CO, USA.

Hendron, D. M., Fernandez, G., Prommer, P. J., Giroud, J. P., & Orozco, L. F. (1999). INVESTIGATION OF THE CAUSE OF THE 27 SEPTEMBER 1997 SLOPE FAILURE AT THE DONA JUANA LANDFILL. *Proceeding Sardiana 99, Seventh International Waste Management and Landfill Symposium*, October.

Karimi, S., & Bareither, C. A. (2021). The influence of moisture enhancement on solid waste biodegradation. *Waste Management,* 123, 131–141. https://doi.org/10.1016/j.wasman.2021.01.022

Koerner, R. M. H., Soong, T.-Y., Robert M. Koernerl-Hon, & Soong, T.-Y. (2000). Stability Assessment of Ten Large Landfill Failures. *Geo-Denver; Advances in Transportation and Geoenvironmental Systems Using Geosynthetics*. https://doi.org/10.1061/40515(291)1

Rohlf, E. M., Karimi, S., & Bareither, C. A. (2021). Implications of municipal solid waste co-disposal experiments on biodegradation and biochemical compatibility. *Waste Management*, 129, 62–75. https://doi.org/10.1016/j.wasman.2021.05.009

CHAPTER 2: A REVIEW OF HYDRAULIC CONDUCTIVITY OF MUNICIPAL SOLID WASTE

2.1. Introduction

The hydraulic conductivity of MSW is an important engineering parameter that aids engineers in analyzing landfill stability, designing leachate distribution and collection systems, and gas extraction systems (Hendron et al., 1999; Dixon and Jones 2005; Jain et al., 2006; Wu et al., 2012; Townsend et al., 2015; Bonaparte et al., 2020), and operating landfills effectively to avoid adverse environmental consequences associated with waste disposal. Due to the coupled nature of municipal solid waste (MSW) behavior during the life of a landfill, physical, hydraulic, chemical, and biological processes are interdependent. Thus, a comprehensive evaluation is needed to obtain a reliable prediction of hydraulic behavior of MSW. For instance, hydraulic behavior of solid waste depends on the solid waste composition and particle size (Gao et al., 2015; Gavelyte et al., 2016) as well as the amount and rate of decomposition (Ke et al., 2017; Breitmeyer et al., 2019).

Hydraulic conductivity of MSW is a function of stress (overburden pressure), waste composition, degradation, particle size, unit weight, water content, field capacity, void ratio, porosity, drainable porosity, compression, and landfill operations (Landva et al., 1998; Powrie and Beaven 1999; Beaven 2000; Powrie et al., 2005; Machado et al., 2010; Ke et al., 2017; Zhang et al., 2018; Miguel et al., 2018; Breitmeyer et al., 2019). Past research indicates that vertical stress, waste composition, and waste decomposition are the most influential factors on MSW hydraulic conductivity (Fungaroli and Steiner 1979; Korfiatis et al., 1984; Bleiker et al., 1993; Chen and Chynoweth 1995; Bleiker et al., 1995; Gabr and Valero 1995; Landva et al., 1998, Powrie and Beaven 1999; Jang et al., 2002; Powrie et al., 2005; Durmusoglu et al., 2006; Powrie et al., 2008; Hossain et al., 2008; Reddy et al., 2009a, Reddy et al., 2009b; Stoltz et al., 2010; Machado et al., 2010; Reddy et al., 2011; Jie YX et al., 2013; Zhang et al., 2016; Ke et al., 2017; Miguel et al., 2018; Breitmeyer et al., 2019; Bareither et al., 2020). Stress, waste composition, and waste decomposition are interrelated and dependent on additional factors. For instance, stress is a function of unit weight, composition, and landfill height, whereas degradation depends on composition, water content, particle size, climate, and landfill operations, among other factors.

The potential negative impacts associated with disposing low hydraulic conductivity waste in solid waste landfills are shown in Fig. 2.1. Municipal solid waste with low hydraulic conductivity can affect landfill performance, whereby lower hydraulic conductivity materials can lead to leachate mounding and perched water tables, which can generate positive pore pressure that reduces landfill stability and/or generates leachate seeps (Hendron et al., 1999; Koerner and Soong 2000; Bonaparte et al., 2020; Bareither et al., 2020). Low hydraulic conductivity materials also reduce gas permeability that can result in gas accumulation and elevated gas pressures (Merry et al., 2006; Powrie et al., 2008; Hudson et al., 2009; Zhan et al., 2017). The buildup of positive pore water and/or air pressure within a landfill can lead to failure, which is a serious threat to human health and the environment (Bonaparte et al., 2020).

2.2. Background:

Bonaparte et al. (2020) evaluated several landfill failures in the last four decades in the U.S., and two of the failures were directly related to hydraulic behavior of the landfill. In one failure, a lateral expansion of a landfill was developed on top of the intermediate cover, which impeded vertical percolation of leachate from the expansion zone to the leachate collection system at the bottom of the original landfill. Lack of a drainage system at the bottom of the expansion area coupled with low hydraulic conductivity of the existing intermediate cover caused pore water pressure buildup and increased liquid levels, which subsequently led to a slope failure. Another landfill failure occurred in the northeast of the U.S, which incorporated low permeability materials (i.e., drill cutting mixed with lime) employed as an intermediate soil cover. This material created relatively impervious layers, resulting in gas and liquid pressure buildup that consequently led to a landfill slope failure.

Additional landfill failures were analyzed by Hendron et al. (1999), Koerner and Soong (2000), and Jafari et al. (2013). Hendron et al. (1999) indicated that leachate recirculation, high initial waste saturation, and low permeability intermediate cover layers allowed a rapid pore water pressure buildup that caused a slope failure at Dona Juana Landfill in Bogota, Colombia. Jafari et al. (2103) evaluated a landfill slope failure in Quezon City, Philippines. High leachate levels within the landfill after a two-week rainfall coupled with gas pressure buildup due to waste degradation and an over-steepened landfill slope contributed to the landfill slope failure.

Koerner and Soong (2000) assessed the stability of four large landfill failures due to leachate buildup in the waste mass. The first failure likely occurred due to an estimated 5-m leachate level buildup in an old decomposed solid waste landfill. The second landfill failure occurred in Ohio, U.S. and has been discussed by Kenter et al. (1997), Stark and Evans (1997), Schmucker and Hendron (1997), Stark et al. (1998), and Stark et al. (2000), Eid et al. (2000), Chugh et al. (2007), and Bonaparte et al. (2020). One of the root causes of the Ohio failure was again leachate level buildup that reduced effective stress in the waste mass. The third failure evaluated by Koerner and Soong (2000) was a co-disposed municipal and hazardous waste landfill. Active leachate recycling coupled with a 48-hour rainfall saturated the landfill to the point that waste actually liquified which resulted in slope failure. The failure surface was between the old and new waste slopes that were already saturated due to excessive addition of liquid waste. The fourth failure was due to aggressive pressure injection of leachate. Koerner and Soong (2000) identified an increase in leachate head in the waste mass as the triggering mechanism of failure.

All of the aforementioned failures share a common characteristic, which is the introduction of excessive leachate or rainwater to the waste mass can generate pore water pressure that reduces effective stress and subsequently the stability of landfills. These failures emphasize the importance of understanding and predicting landfill hydraulic behavior to promote effective and safe landfill operations that enhance physical stability.

The objectives of this study were to (i) compile a comprehensive review of the hydraulic conductivity of MSW and (ii) evaluate the influence of MSW and landfill characteristics on MSW hydraulic conductivity. A total of 52 studies were compiled that included laboratory-, pilot-, and landfill-scale hydraulic conductivity experiments. The data compilation, observations, and key findings from this study are beneficial for solid waste engineers to improve design, analysis, and operation of MSW landfills to prevent the future failures in landfills.

2.3. Study Selection and Screening

The 56 studies collected were reviewed to assess the influence of various factors on MSW hydraulic conductivity. Studies that did not provide data on MSW or experiment characteristics (e.g., age, experiment size, test methods) were omitted from the analysis. A total of 47 studies were included as these studies provided sufficient information on MSW and/or landfill characteristics to make inferences and comparisons regarding factors influencing the measured hydraulic conductivity.

Studies initially were categorized based on two characteristics: (i) magnitude and range of vertical stress and (ii) state of waste degradation. The impacts of stress and unit weight on MSW hydraulic conductivity were assessed in 34 studies. These 34 studies were further categorized based on the age of MSW and/or state of decomposition, scale of experiments (i.e., laboratory-, pilot-, and landfill-scale), specimen size, and MSW particle size. The influence of degradation on MSW hydraulic conductivity was evaluated separately.

Data of hydraulic conductivity tests collected from 56 studies summarized in three categories presented in three reference tables in Appendix B. The results of studies that assessed the impacts of stress and dry unit weight on MSW hydraulic conductivity are in Table. B1. Studies that reported hydraulic conductivity of landfills compiled in Table B2 separately, as these data are representative of actual hydraulic behavior of landfills which are valuable references. A summary of studies measured the hydraulic conductivity of waste in different decomposition states is in

Table B3. The summaries include method of experiment, waste composition, range of stress and dry unit weight, hydraulic conductivity, details of hydraulic conductivity test (e.g., depths of exhumed samples, diameter of specimen, and particle size), and decomposition state of MSW (for studies evaluated the impacts of degradation on hydraulic conductivity). A graph-reader tool (www.graphreader.com) was used to extract the data from the figures. If results had been reported in tables, the results were extracted directly from tables.

2.4. Impacts of Stress and Unit Weight on Hydraulic Conductivity

A summary of hydraulic conductivity experiments that assessed the impacts of vertical stress and unit weight on hydraulic conductivity of MSW is in Table B.1 (Appendix B). The summary includes test method, source of MSW and composition, range of vertical stress, unit weight or dry unit weight, hydraulic conductivity, and description of test procedures. The influence of stress and MSW unit weight on hydraulic conductivity were separately evaluated for wastes characterized as fresh, semi-decomposed, and decomposed.

The unit weight of landfilled MSW initially increases via waste compaction at the working face of a landfill (Hanson et al., 2010; Li et al., 2013). Compacting waste increases the unit weight and reduces the void volume, resulting in narrower flow paths and reducing the infiltration of liquid such as rainwater. After compaction, waste compresses as vertical stress increases via placement of subsequent waste layers and interim daily cover. The rate of vertical stress increase from the surface of a landfill downward depends on MSW unit weight, which is a function of waste composition, climate, compaction energy, and landfill operation (Zekkos et al., 2006). In general, higher fractions of soil or soil-like material increase MSW unit weight. Kavazanjian (1999) reported that total unit weight of MSW in relatively dry landfills ranged from 4 kN/m^3 to 6.5 kN/m^3 and with addition of daily or interim soil covers the total unit weight of MSW with soil increased to 8 kN/m^3 to 13 kN/m^3. The later range on unit weight assumed a 1:1 ratio of MSW-to-soil.

Hanson et al. (2010) indicated that MSW disposed during winter tended to reach higher unit weight because of freezing and thawing cycles. Higher waste moisture contents in wetter climates and landfills with leachate recirculation also yield higher MSW unit weight (Kavazanjian 2001) via more effective compaction at the working face (Hanson et al., 2010).

2.4.1. Fresh MSW

Relationships of saturated hydraulic conductivity (k_s) versus vertical stress and dry unit weight for fresh MSW are shown in Fig. 2.2. Data compiled in Fig. 2.2 are segregated into three types of experiments to compare the influence of specimen preparation and scale: (i) laboratory-scale experiments on shredded waste; (ii) laboratory-scale experiments on unshredded waste; and (iii) pilot-scale experiments on unshredded waste. The k_s reported for fresh MSW ranges from 1×10^{-4} m/s to 1×10^{-7} m/s under zero applied stress and decreases to a range of 1×10^{-7} m/s to 1×10^{-9} m/s for vertical stress equal to 600 kPa (Fig. 2.2a). The variation in k_s for a given vertical stress is attributed to initial dry unit weight, MSW composition, and particle size. For example, smaller MSW particles can facilitate more effective MSW compaction by filling larger void spaces that cannot easily be filled with larger waste particles. A reduction in MSW particle size can lead to higher initial unit weight for the same MSW composition. In general, an increase in unit weight reduces porosity, which reduces the size of pore spaces (i.e., flow channels) and consequently the hydraulic conductivity (Fig. 2.2b).

2.4.1.1. *Laboratory-Scale Hydraulic Conductivity*

The measurement of MSW hydraulic conductivity in laboratory-scale permeameters commonly requires waste shredding to adhere to particle size testing constraints or the use of a larger-scale permeameter that can accommodate unshredded waste particles (Reddy et al., 2009b; Ke et al., 2017; Breitmeyer et al., 2019). ASTM D5856 specifies that the diameter of soil particles must be less than 1/6 the specimen diameter when using a compaction-mold permeameter. Considering that there is no standard for the measurement of MSW hydraulic conductivity, the 1/6 particle-to-specimen diameter ratio has been adopted by some researchers (e.g., Reddy et al., 2009b; Breitmeyer et al., 2019) and not adopted by others (Stoltz et al., 2010; Ke et al., 2017; Reddy et al., 2009a; Reddy et al., 2009b). Furthermore, standard methods for laboratory-scale hydraulic conductivity measurement vary throughout the world. Zhang et al. (2018) adhered to a ratio of particle-to-specimen diameter < 1/8 based on Chinese practice. The subsequent discussion focuses on studies that adhered to particle-to-specimen diameter ratio ≤ 1/6 as these experiments are argued to have similar influence between the scale of MSW particles and laboratory permeameters.

As fresh MSW is shredded for laboratory testing, the void spaces can be filled with smaller particles, which reduces hydraulic conductivity. Breitmeyer et al. (2019) reported two orders of magnitude differences in k_s for specimens with similar composition and approximately similar dry unit weight, but with different particle size. They measured $k_s = 7\times10^{-5}$ m/s for shredded fresh MSW (dry unit weight = 5.5 kN/m^3) and $k_s = 7.7\times10^{-3}$ m/s for unshredded fresh MSW (dry unit weight = 5.2 kN/m^3) under zero vertical stress. The smaller waste particles decreased the size of void spaces available for flow while also increasing tortuosity.

In general, conducting hydraulic conductivity tests on unshredded fresh MSW tends to yield higher hydraulic conductivity (Fig. 2.2). Landva et al. (1998) tested unshredded MSW exhumed from landfills. Hydraulic conductivities measured by Landva et al. (1998) plot in the upper range of k_s for shredded MSW (Fig. 2.2a). Machado et al. (2010) used unshredded MSW exhumed from a landfill that consisted of 50% of waste particles smaller than 30 mm diameter. The small particles in the MSW evaluated by Machado et al. (2010) yielded lower k_s (1×10^{-5} m/s to 1×10^{-8} m/s) relative to Landva et al. (1998). The main difference in this comparison of k_s for unshredded MSW is the size of the waste particles, whereby larger waste particles, and lower percentage of finer particles, correspond to larger void spaces that serve as flow paths to yield higher hydraulic conductivity.

Municipal solid waste composition includes materials such as paper, plastic, wood, rubber, metal, and soil, which all have different specific gravities (Wong 2009). Variation in the MSW composition directly influencing the unit weight that can be achieved during placement in a landfill or compacted in a laboratory specimen, as well as the change in unit weight with increasing stress. Relationships between vertical stress and dry unit weight for laboratory specimens prepared with fresh MSW are shown in Fig. 2.3. Zhang et al. (2018) reported an increase in dry unit weight from 5.4 kN/m^3 to 8.3 kN/m^3 under 0 to 300 kPa vertical stress, whereas Reddy et al. (2009b) reported that dry unit weight increased from 4.1 kN/m^3 to 13.4 kN/m^3 for the same increase in vertical stress. Furthermore, Breitmeyer et al. (2019) reported an initial dry unit weight of 6.4 kN/m^3 to 10.1 kN/m^3 for varying compaction effort, which subsequently increased to 7.9 kN/m^3 to 11 kN/m^3 as vertical stress increased from 0 to 400 kPa. The higher dry unit weights reported by Reddy et al. (2009b) and Breitmeyer et al. (2019) were due to higher percent contributions of high-density materials (e.g., soil), whereas the lower dry unit weights reported by Zhang et al. (2018) were attributed to the use of synthetic MSW that consisted 61.5% food waste.

The hydraulic conductivity measurements reported by Zhang et al. (2018) are higher relative to other laboratory-scale k_s results (Fig. 2.2a, b). The high fraction of food waste resulted in low compacted specimens with relatively lower unit weight (Zhang et al., 2018) than MSW specimens contained high-density materials. Furthermore, food wastes are more permeable than other waste materials. Then, initially, the moisture content of food waste increases the saturation degree in waste mass which can aid the transfer of flow. Afterward, hypothetically, rapid degradation of food waste can provide more void spaces for liquid flow and increases the k_s. This indicates the effect of MSW components on the hydraulic behavior of MSW.

In summary, although there is a large range of k_s for a given vertical stress, there is a better relationship between k k_s and dry unit weight for most of the laboratory data on shredded

MSW. The only outlier in laboratory-scale k_s tests on shredded MSW is the data set from Reddy et al. (2019). The initial unit weight of MSW specimen was 3.1 kN/m^3 which reduce to 10 kN/m^3 by increasing vertical stress to 35 kPa resulting in reduction of k_s from 2×10^{-3} to 3.7×10^{-6} and then k_s reduced to 5×10^{-7} m/s via increasing stress up to 276 kPa, and dry unit weight increase to 13.4 kN/m^3. Low initial compaction energy (15 standard Proctor hammer blows per layer) and MSW specimen containing 30% non-MSW with high unit weight (17% construction and demolition waste and 11% soils) were potentially the main reasons for the significant increase in dry unit weight (Fig. 3.3b).

2.4.1.2. *Pilot-scale Hydraulic Conductivity*

Hydraulic conductivities measured in pilot-scale tests fall within the upper boundary of the compiled k_s results in Fig. 2.2. Pilot-scale k_s tests were conducted by Beaven and Powrie (1995), Powrie and Beaven (1999), and Hudson et al. (2001). They used similar compression cell with a 2-m diameter to evaluate the effect of stress on MSW hydraulic conductivity. Applying 600 kPa stress increased the dry unit weight from 2.5 kN/m^3 to 5.9 kN/m^3 and reduced hydraulic conductivity from 1×10^{-4} m/s to between 1×10^{-7} and 1×10^{-9} m/s (Fig. 2.2b). For a given vertical stress, k_s varied two orders of magnitude, which is mainly attributed to variation in waste composition. For given k_s, the dry unit weight of MSW specimen in pilot-scale tests were lower than laboratory-scale experiments. Small waste particles tend to be compacted and compressed less than small, shredded particles.

The order of magnitude change in hydraulic conductivity [log(k_s/k_{si})] with respect to increase of dry unit weight [(γ_d / γ_{di}) -1] for the laboratory-scale k_s tests on unshredded MSW and pilot-scale k_s tests are shown in Fig. 2.4. The dry unit weight (γ_d) and k_s were normalized based on the initial conditions of hydraulic conductivity (k_{si}) and dry unit weight (γ_{di}). The x-axis is representative of an increase in dry unit weight (e.g., 0.6 represents a 60% increase in dry unit weight relative to the initial dry unit weight) and the corresponding order of magnitude reduction in k_s is identified by the slope (M) of a linear regression between log(k_s/k_{si}) and ([(γ_d / γ_{di}) -1]. For instance, M = -3 indicates three orders of magnitude reduction in k_s for 100% increase in dry unit weight. The average of the slopes for the unshredded MSW specimens in laboratory-scale tests was similar to the unshredded MSW specimens in pilot-scale tests. This indicates that the ratio of change in k_s by increasing dry unit weight is similar if the MSW is unshredded, regardless of whether the experiment is conducted at laboratory-scale or pilot-scale. The reduction in k_s of fresh shredded MSW was higher than unshredded MSW (M= -5.4 and -6.3) (Fig. 2.4). The higher rate of reduction in k_s for fresh, shredded MSW with a similar magnitude increase in dry unit weight is attributed to the smaller particle size. The small particles of shredded waste can fill void spaces that cannot be filled with large particles, which reduces the size and increases tortuosity of flow paths.

Breitmeyer et al. (2019) determined hydraulic conductivity of MSW at field-scale using a 2.4-m diameter by 8.2-m tall lysimeter. The k_s was 1.2×10^{-8} m/s with a dry unit weight of 7.5 kN/m^3 and void ratio of 1.0. The field-scale hydraulic conductivity was in the same range as the pilot-scale k_s on unshredded MSW (Fig. 2.2). The k_s was determined in a manner that the MSW matrix was neither saturated nor at field capacity. Therefore, the k_s was underestimated relative to saturated hydraulic conductivity tests, and the actual k_s was likely higher than 1.2×10^{-8} m/s. Breitmeyer et al. (2019) stated that if the void ratio and unit weight of MSW specimens are representative of field conditions, laboratory tests provide a reasonable representation of field-scale k_s.

There appears to be limited data in the literature pertaining to the direct measurement of the void ratio of landfilled MSW. Feng et al. (2016) measured the void ratio of relatively fresh MSW (0.3 yr) exhumed at a depth of 4 meters via a large-diameter bucket auger. The average void ratio was 2.33 and average dry unit weight was 6 kN/m^3. Hartwell et al. (2021) reported that void ratio of landfilled waste ranged from 2.21 to 0.75 for waste exhumed from depths of 1.5 m to

26 m, which corresponded to dry unit weights of 5.1 kN/m^3 to 9.7 kN/m^3. The difference in MSW void ratio is attributed to waste composition and particle size.

There is no data regarding the hydraulic conductivity of fresh MSW at landfill scale because field-scale hydraulic conductivity tests are usually conducted when landfill operators drill a well to inject liquid waste or extract the biogas. Based on landfill operation, drilling a well is conducted after months or years when MSW has begun decomposition and hence MSW is not considered a fresh waste.

Increasing stress is the first factor that affects MSW hydraulic conductivity, then composition, decomposition, and particle size become more significant as vertical stress increases (Beaven 2000). Conducting experiments using unshredded MSW requires larger-scale equipment. Therefore, the results of laboratory-scale hydraulic conductivity tests on fresh MSW can be used considering the following points: (i) the results of k_s tests in laboratory-scale can be overestimated by two to three orders of magnitude. However, variation in k_s results is less varied as stress increases. This is because increasing stress will change the pores spaces distribution and reduce the flow paths, (ii) actual vertical hydraulic conductivity is lower in landfills than in laboratory experiments due to horizontal flow in landfilled waste, and (iii) unsaturated condition in landfill yields lower hydraulic conductivity relative to saturated hydraulic conductivity tests.

2.4.2. Semi-Decomposed MSW

Relationships of k_s measured in laboratory- and landfill-scale tests versus vertical stress and dry unit weight for semi-decomposed waste are shown in Fig. 2.5. Data were categorized based on experiment scale and MSW particle size to evaluate their influence on k_s. The reported results for hydraulic conductivity of semi-decomposed MSW are in the range of 1×10^{-1} m/s to 1×10^{-7} m/s for vertical stress between 0 and 400 kPa. In general, the compilation of k_s for semi-decomposed MSW indicates a two order-of-magnitude increase in k_s relative to the fresh MSW for a range of vertical stress from 0 to 400 kPa. However, there are less data available for the hydraulic conductivity of semi-decomposed MSW relative to fresh waste, particularly for vertical stress > 200 kPa.

Solid waste decomposition changes the physical characteristics and overall composition of waste. Increasing decomposition corresponds to an increase in MSW specific gravity because the majority of non-degradable materials have higher specific gravity than degradable materials (Wong 2009). The size of individual MSW particles reduces due to both degradation and compression. The waste particles break down into smaller, more soil-like materials. Hence, a reduction in particle size via waste degradation and compression would imply a reduction in k_s based on mechanisms of decreasing void size and increasing tortuosity. On the other hand, the conversion of solid organic waste to gaseous end-products via anaerobic biodegradation increases the void ratio (McDougall et al., 2004; Bareither et al., 2012), which can increase pore volume and connectivity within the waste skeleton that reduces tortuosity among flow paths and increases k_s. These two competing factors occur simultaneously during waste degradation and may result in an increase or decrease k_s based on the state of stress, degradation, and waste composition. In the following subsections, the impacts of factors affecting k_s at different test scales are discussed.

2.4.2.1. *Laboratory-Scale Hydraulic Conductivity*

Hydraulic conductivity tests on shredded, semi-decomposed MSW tend to yield higher k_s compared with hydraulic conductivity tests on unshredded MSW or pilot-scale tests, particularly under 0 to 200 kPa stress (Fig. 2.5). Results of hydraulic conductivity tests on shredded MSW yielded k_s ranging between 1×10^{-1} m/s to 1×10^{-3} m/s under zero vertical stress, and k_s decreased to as low as 1×10^{-5} m/s by increasing stress to 400 kPa. However, k_s measured on unshredded MSW under a similar range of stress ranged between 1×10^{-5} m/s to 1×10^{-7} m/s.

The two data sets compiled in Fig. 2.5 for k_s measured on shredded, semi-decomposed MSW in laboratory-scale experiments are from Breitmeyer et al. (2019) and Durmusoglu (2006).

Breitmeyer et al. (2019) reported that void enlargement due to waste degradation was the main reason for the higher k_s measured on semi-decomposed MSW relative to the k_s they measured on fresh MSW (Fig. 2.2). The three data sets compiled from Breitmeyer et al. (2019) in Fig. 2.5 are for semi-decomposed MSW specimens prepared with reduced, standard, and modified Proctor compaction energies. Although the highly compacted MSW specimens yielded a 2-order of magnitude decrease in k_s under zero vertical stress (Fig. 2.5a), all three data sets merge to a similar trend of k_s versus dry unit weight (Fig. 2.5b). Thus, regardless of the variation in initial compacted dry unit weight (ranging from 5.2 kN/m^3 to 7.9 kN/m^3), the trend of k_s versus dry unit weight for the three semi-decomposed MSW specimens was similar. The k_s values reported by Durmusoglu et al. (2006) were in the same range as Breitmeyer et el. (2019). Durmusoglu used landfilled MSW with particle size similar to the Breitmeyer et al. (2019) k_s tests on shredded MSW.

The composition of incoming waste stream and the non-degradable fraction of MSW could cause different hydraulic behavior. Landva et al. (1998) reported that MSW specimens contained a high fraction of plastic bags and wood wastes that could create obstructed vertical flow paths and reduce hydraulic conductivity. MSW landfills with high kitchen waste content (i.e., more than 40%) potentially can generate significant amount of leachate Zairi et al. (2014) and Xu et al. (2014). Significant leachate production coupled with low k_s landfilled waste can cause leachate mounding in landfills, clogging leachate collection and gas extraction systems, and change the stress distribution in landfills. (Gao et al., 2015).

In general, the existence of soil via daily or interim cover (Bogner 1990; Townsend et al., 1995; Burrows et al., 1997) combined with an increased fraction of soil-like materials due to MSW decomposition resulted in a reduction in hydraulic conductivity. These small particles contribute to decrease the size of void spaces and can occlude the connectivity of pores within a waste mass. Bareither et al. (2020) reported hydraulic conductivity for waste exhumed from an active landfill for testing that included 20% municipal sewage sludge and 13% special residual waste, on average. The special residual waste was exploration and production waste from the oil and gas industry, which was shown to dramatically reduce MSW k_s as the total mass fraction of the exploration and production waste increased above 40%. Thus, the inclusion of trace amounts of this residual waste and sewage sludge likely reduced k_s relative to the experiments conducted by Breitmeyer et al. (2019) (Fig. 2.5.a, b).

Other laboratory permeability tests were conducted by Durmusoglu et al. (2006), Reddy et al. (2009b), Reddy et al. (2011), Zhan et al. (2014), Feng et al. (2016), and Ke et al. (2017) on semi-decomposed MSW. A summary of these studies is included in Table B.1 and Table B.3. These studies used MSW specimens with particles < 5-mm diameter (Durmusoglu et al., 2006) or used synthetic MSW with particles < 10-mm diameter (Reddy et al., 2011). These studies are not included in Fig. 2.5 because the 1/6 particle-to-specimen diameter ratio was not followed. In general, the smaller waste particles produce dense specimens that yield lower k_s, which was not in agreement with trends from other reported hydraulic conductivity data.

2.4.2.2. *Landfill-Scale Hydraulic Conductivity*

Olivier et al. (2009) measured k_s in a landfill-scale test on semi-decomposed MSW. The experiment was conducted as a field pumping test in 5- to 7-year-old landfilled waste under 80 kPa and 150 kPa which yielded k_s, on average, 2.8×10^{-6} m/s. Although the landfilled waste consisted of other non-MSW such as mixture of industrial and commercial waste (52%), sewage sludge (8%), and inert materials (8%), the k_s was in a similar range with unshredded MSW laboratory-scale tests.

There are limited data on field-scale hydraulic conductivity of semi-decomposed MSW for which the unit weight or overburden pressure (stress) were reported. Field data are extremely valuable as they represent actual hydraulic behavior of landfilled MSW. A summary of studies reporting hydraulic conductivity of landfilled MSW is in Table B.2 (Appendix B). The data pertain to landfill-scale hydraulic conductivity tests ranged between 1×10^{-5} m/s to 1×10^{-8} m/s, which are in similar range to unshredded MSW laboratory-scale and landfill-scale ks tests. The variation in reported k_s is attributed to variation in waste composition, landfill operations, and state of degradation.

2.4.3. Decomposed MSW

Relationships of hydraulic conductivity versus vertical stress and dry unit weight for decomposed MSW from laboratory-, pilot-, and landfill-scale experiments are shown in Fig. 2.6. The relationship of k_s versus vertical stress exhibits a clean distinction between laboratory experiments on shredded, decomposed MSW, a pilot-scale experiment on unshredded MSW conducted by Beaven (2000), and a landfill-scale experiment on decomposed MSW conducted by Machado et al. (2010). The hydraulic conductivity measured in these three experiment scales decreases with an increase in experiment scale.

The decrease in k_s with increase in experiment scale was attributed to differences in MSW particle size and composition. The shredded, decomposed MSW tested by Breitmeyer et al. (2019) included a maximum particle diameter of 25 mm. Beaven (2000) used 20-year-old household waste that included a particle size distribution (by weight) of 18% > 80 mm, 52% > 40 mm, and approximately 34% < 10 mm. Although the maximum particle size used by Beaven (2000) was larger than that used by Breitmeyer et al. (2019), the larger fraction of smaller particles likely occupied void spaces between the larger particles and contributed to a lower k_s.

The landfill-scale k_s reported by Machado et al. (2010) were measured via infiltration tests. The authors reported 85% of the MSW was at least 15 years old with particles less than 30-mm diameter and total volatile solids content of approximately 23%. The range of k_s measured by Machado et al. (2010) was justified based on the presence of small MSW particles that were similar to soil, the presence of plastic components that obstructed flow, and MSW heterogeneity. Furthermore, the landfill evaluated included soil as daily and interim cover, which introduced soil particles to the waste mass and created vertical layers with lower hydraulic conductivity.

An additional data set from Breitmeyer et al. (2019) is included in the relationship of k_s versus dry unit weight, which is representative of laboratory-scale hydraulic conductivity tests conducted on unshredded, decomposed MSW. The trends of k_s versus dry unit weight for the shredded and unshredded, decomposed MSW from Breitmeyer et al. (2019) overlap to form a single relationship. Although decomposition of waste changes MSW particle size and shape, the comparison from Breitmeyer et al. (2019) suggests that more advanced states of MSW decomposition reduced the variation of particle size between shredded and unshredded MSW.

Interestingly, the range of MSW dry unit weight for the pilot-scale experiments conducted by Beaven (2000) is similar to that of Breitmeyer et al. (2019); however, the k_s are consistently two to nearly four orders of magnitude lower. The difference in k_s may attribute to the particles size distribution of waste materials and age of the waste. Beaven (2000) used MSW that 6.3% of particles were larger than 160 mm, but 34% were less than 10 mm. The MSW specimen consisted of waste particle sizes that were distributed over a wide range. The small particles filled the void spaces that cannot be filled with large particles and created a dense specimen at which small particles occupied the majority of interconnected void spaces and caused a pronounced reduction in k_s. The flowpath became narrower relative to MSW specimens that contained mainly waste particles with similar sizes.

Although there are limited data regarding k_s of decomposed MSW, the overall variation of k_s increased for the entire range of vertical stress by increasing the experiment size. An increase in variation is mainly related to an increase in heterogeneity of landfilled MSW. Incoming waste streams to landfills can vary significantly based on the season, adjacent industries, and environmental regulations. Thus, the heterogeneity of landfilled wastes can change the hydraulic behavior of waste in different zones of a landfill.

In summary, compacting waste and increasing vertical stress change the waste particles geometry and pore size distribution, reshape the pore networks throughout the waste matrix, reduce the void ratio and flow paths, and increase tortuosity. All these changes can lead to a reduction in MSW hydraulic conductivity. However, the magnitude of reduction in MSW k_s depends on waste composition and state of decomposition. Changes in mentioned parameters can influence hydraulic behavior of MSW, and replicating these parameters in laboratory is not practical. Therefore, the results of hydraulic conductivity tests in solid waste landfills can be a credible reference for landfill practitioners (Table B2, Appendix B).

2.5. Impacts of Decomposition

Solid waste is a dynamic material whereby physical, hydraulic, chemical, and biological behavior change as waste decomposition progress. Several studies evaluated the influence of decomposition on MSW unit weight, particle size, void ratio, compression, and hydraulic behavior (Olivier et al., 2007; Reddy et al., 2011; Machado et al., 2010; Xu et al., 2014; Fei et al., 2014; Ke et al., 2017; Miguel et al., 2018; Breitmeyer et al., 2019; Liu et al., 2019; Breitmeyer et al., 2020; Beentjes 2021). A summary of studies that evaluated the influence of different degrees of degradation on MSW hydraulic conductivity is in Table B.3 (Appendix B). Past studies have documented that conversion of degradable waste to gas increases settlement (Bareither et al., 2013), reduce waste particles size, and eliminate void spaces, which can contribute to reduction in k_s (Reddy et al., 2009b; Mousavi et al., 2021).

On the other hand, removing solid mass via decomposition of organic matter creates void space within the waste skeleton, which can increase k_s (Miguel et al., 2018; Breitmeyer et al., 2019). Hydraulic conductivities measured by Breitmeyer et al. (2019) for two different laboratory scale experiments (150-mm and 300-mm diameter) are compiled in Fig. 2.7. Results from the 150-mm-diameter permeameter are for shredded MSW (Fig. 2.7a), whereas results from the 300-mm-diameter permeameter are for unshredded MSW (Fig. 2.7b). In both data sets compiled from Breitmeyer et al. (2019), there is an increase in k_s with more advanced state of waste degradation, which the authors attributed to an increase in void ratio due to solid conversion to gas that was more pronounced than a corresponding reduction in void ratio due to waste settlement. The influence of these aforementioned mechanisms on increasing or decreasing hydraulic conductivity depends on the waste composition, degradation rate, and landfill operations.

2.5.1. Particle size

Reduction in MSW particles size is a natural occurrence due to decomposition of the degradable fraction of MSW and compression of non-degradable materials, which potentially can reduce the MSW permeability via reducing the flow paths. The decrease in MSW particle size with decomposition has been reported in numerous studies (Fungaroli and Steiner 1979; Olivier and Gourc 2007; Hossain et al., 2009; Machado et al., 2010; Reddy et al., 2011; Xu et al., 2014; Ke et al., 2017; and Breitmeyer et al., 2019). Breitmeyer et al. (2019) reported that the fraction of waste materials with particle sizes < 25 mm increased 20% (from 48.2% to 69.3%) after three years of decomposition.

The particle size of decomposed MSW extracted from landfills have been reported by numerous researchers (e.g., Landva et al., 1998; Reddy et al., 2009b; Reddy et al., 2011; Machado et al., 2010; Xu et al., 2014). Xu et al. (2014) reported 40% of waste particles were smaller than 40 mm and wastes mainly consisted of small particles and soil-like materials. Reddy et al. (2009b) reported 16% of landfilled MSW were smaller than 50 mm. Machado et al. (2010) performed sieve analysis on 15-year-old landfilled waste and approximately 18% passed a 1-mm sieve. Reduction in particle size leads to rearrangement and geometric changes in waste particles, which lower the strength of waste skeleton and cause a collapse in waste mass (McDougall et al., 2004). Therefore, the small particles and soil-like materials can occupy the void spaces and increase the pore-tortuosity, resulting in a reduction in hydraulic conductivity.

2.5.2. Void ratio

With the initiation of waste degradation, readily degradable materials (i.e., food waste, yard waste, paper) decompose and convert to biogas (Kim and Pohland 2003). This process results in solid waste mass loss and an increase of void spaces throughout the waste matrix

(Bareither et al., 2012; Breitmeyer et al., 2019). The reduction of solid mass creates more air space and potentially more interconnected pores network, which provide less tortuous flow paths. These occurrences yield an increase in hydraulic conductivity. Bareither et al. (2012) indicated that the waste matrix under a small constant vertical stress (i.e., 2 kPa) is possibly resisted more waste settlement during the active decomposition phase, which indicates an increase in the void ratio.

Settlement due to decomposition of MSW, known as biocompression (Bareither et al., 2013), also contributes to a reduction in MSW void ratio. However, the impact of settlement on decreasing void ratio and influence of decomposition on increasing void ratio depend on the waste composition and landfill operation. Hence, the overall changes in void ratio represent the hydraulic behavior of MSW. Breitmeyer et al. (2019) conducted a pilot-scale test on MSW and simultaneously observed the compression and hydraulic behavior of landfilled waste. They reported that MSW hydraulic conductivity increased due to decomposition.

Breitmeyer et al. (2019) also carried out a series of laboratory-scale k_s tests on MSW with different degrees of degradation. They reported that for a given dry unit weight, MSW with a higher degree of decomposition had a higher void ratio and subsequently higher hydraulic conductivity than MSW with a lower degree of decomposition. Miguel et al. (2018) conducted permeability tests on MSW that were under degradation process. Similarly, they reported two orders of magnitude increase in permeability of MSW samples with an initial unit weight of 7.2 kN/m^3 during the first three months of the degradation process.

2.6. Conceptual model of Solid Waste Hydraulic conductivity

A graphical representation of the influence of stress and waste degradation on MSW hydraulic conductivity is shown in Fig. 2.8. The schematics in Fig. 2.8 were based on the review and analysis completed for this study and capture the state-of-knowledge for MSW hydraulic conductivity. The relative magnitude of hydraulic conductivity between the schematics in Fig. 2.8

(i.e., a through i) relates to the thickness of the blue flow lines, whereby thicker flow lines correspond to higher hydraulic conductivity.

A summary of the average MSW composition in U.S. landfills (US EPA 2018) and general descriptions of degradability and compressibility of each waste component is in Table 2.1. Waste components in Table 2.1 were segregated into four groups based on similarity of degradability and compressibility characteristics, and these groups are differentiated by color in Fig. 2.8: light green = degradable and compressible; dark green = degradable and incompressible; orange = non-degradable and compressible; and black = non-degradable and incompressible. The composite particle surface area of the four waste groups in the fresh waste under low stress (Fig. 2.8a) is approximately representative of the average MSW composition disposed in U.S. landfills (e.g., Group 1 ≈ 46% of total MSW). The small brown particles are representative of soil introduced into MSW via daily cover or soil-like materials that exist in MSW and are not distinguishable. The particle sizes in each waste group in Figs. 2.7b through 2.7i were modified based on anticipated changes due to stress increase or waste degradation.

Vertical stress was separated into three levels in Figs. 2.7a, b, c: (a) low stress = 0 to 50 kPa; (b) medium stress = 50 kPa to 200 kPa; and (c) high stress = greater than 200 kPa. These stress levels were inferred from the literature review and represent where substantial changes were generally observed in MSW hydraulic conductivity. However, due to variability in waste composition, the transition in hydraulic behavior of MSW may occur under different ranges of vertical stress. The vertical overburden stress in a landfill is due to the thickness and unit weight of waste and other material placed in the landfill (e.g., daily cover). Unit weight profiles in landfills vary as a function of compaction effort and waste composition (Zekkos et al., 2006). Therefore, evaluating the hydraulic conductivity of MSW versus stress is more universal than evaluating hydraulic conductivity versus MSW unit weight.

The effect of increasing vertical stress on MSW hydraulic conductivity is consistent in literature, whereby hydraulic conductivity reduced six orders of magnitude, from 1×10^{-3} m/s to

1×10^{-9} m/s, by increasing vertical stress from 0 to 600 kPa. The decrease in MSW hydraulic conductivity with increasing stress (Fig. 2.8b and Fig. 2.8c) is attributed to decreasing the pore sizes and remolding the pore networks. Breakage and slippage of waste particles assist in eliminating macropores and constricting flow pathways. As vertical stress elevates to a high level (i.e., 200 kPa), soil-like particles tend to occupy available void spaces. Powrie et al. (2005) reported that at higher vertical stress (> 400 kPa), the impacts of particle size and waste degradation become more significant than vertical stress on hydraulic conductivity. However, the composition, particle size, and state of degradation of MSW vary among landfills. Therefore, the pronounced impacts of changing particle size and waste degradation can occur at lower stress (i.e., 200 kPa). In summary, the magnitude of reduction in hydraulic conductivity depends on the initial solid waste unit weight, composition, particle size, and state of degradation.

Waste degradation in MSW landfills commonly progresses through anaerobic processes and includes five sequential phases (Kim and Pohland 2003): stabilization, transition, acid formation, methane fermentation, and final maturation. However, waste degradation was simplified to three states in Fig. 2.8d through 2.7i to illustrate the effects of MSW degradation on hydraulic conductivity more concisely: (i) fresh waste = waste disposed in a landfill; (ii) semi-decomposed waste = actively degrading waste in the acidogenic and methanogenic phase; and (iii) decomposed waste = fully decomposed waste that has reached organic stabilization (Barlaz et al., 1990; Kim and Pohland 2003).

Decomposition of MSW can yield two consequences: (i) settlement of the waste matrix due to biocompression (Bareither et al., 2013) that reduces available pore space and reduces k_s; or (ii) conversion of solid waste to gas, which increases void ratio and pore connectivity that increases k_s. Waste settlement and void ratio increase during waste degradation are competing mechanisms on MSW hydraulic behavior that occur simultaneously; however, the more dominant mechanism will control flow. The schematics in Figs. 2.7d, e, f represent a waste matrix for which waste settlement due to biocompression is dominant, and schematics in Figs. 2.7g, h, i represent a condition at which void ratio increase during MSW degradation is dominant. Settlement of MSW due to biocompression can lead to smaller decomposed waste particles that compress and reduce available macropores, which leads to a decrease in k_s. In contrast, MSW decomposition that leads to an increase in void space without substantial settlement can create a more porous waste medium with interconnected pores capable of transferring liquid flow at a higher rate, which means an increase in void ratio is more influential on MSW k_s relative to the settlement. This mechanism is less prevalent in MSW landfills. Hence, the overall impacts of degradation on hydraulic conductivity depend on waste composition, waste decomposition rate, overburden pressure, and landfill operation.

2.7. Summary

Landfill practitioners require hydraulic conductivity of MSW to determine landfill slope stability, design leachate collection and recirculation systems, and gas extraction systems. Hydraulic conductivity of MSW varies in landfills and making a reliable prediction or measurement of hydraulic conductivity aids in landfill design and operation. A comprehensive review was conducted to evaluate the influence of stress, composition, and decomposition on municipal solid waste hydraulic conductivity. The findings from 47 research studies were assessed regarding the impacts of stress, unit weight, and decomposition on MSW hydraulic conductivity. A summary of 14 studies that reported hydraulic conductivities of landfilled MSW is compiled in Table B.2 (Appendix B). Furthermore, impacts of other factors such as composition, experiment scale, particle size, and specimen size on MSW hydraulic conductivity have been evaluated.

In general, the effects of increasing stress and reduction in unit weight on MSW hydraulic conductivity were consistent for MSW at varying states of decomposition in that both caused a reduction in hydraulic conductivity. However, the magnitude of reduction in k_s depends on the state of stress, amount of decomposition, and MSW composition. Degradation of MSW can have two contrary effects on MSW hydraulic behavior. Some studies indicate that an increase in MSW decomposition results in particle size reduction and settlement, which reduce the MSW permeability. However, there are studies that indicate waste decomposition increases flow paths and increase hydraulic conductivity. Both of these mechanisms are rationale and have contrasting influence on MSW hydraulic conductivity. General schematics were developed that document key mechanisms of stress and degradation on liquid flow in a solid waste matrix.

Table 2.1. Summary of Waste Composition and Classification of Waste based on Degradability and Compressibility.

Composition	Percentage (%)	Degradability	Compressibility	Group
Paper and Cardboard	13.1	✓	✓	1
Glass	4.9	-	-	4
Metals	9.9	partially	partially	3
Plastic (rigid, soft)	19.2	-	✓	3
Rubber/leather/textiles	11.5	partially	partially	4
Wood	8.7	partially	-	2
Food	21.9	✓	✓	1
Yard trimmings	6.2	✓	✓	1
Miscellaneous inorganic wastes and other materials	4.5	-	partially	3
Total	100			

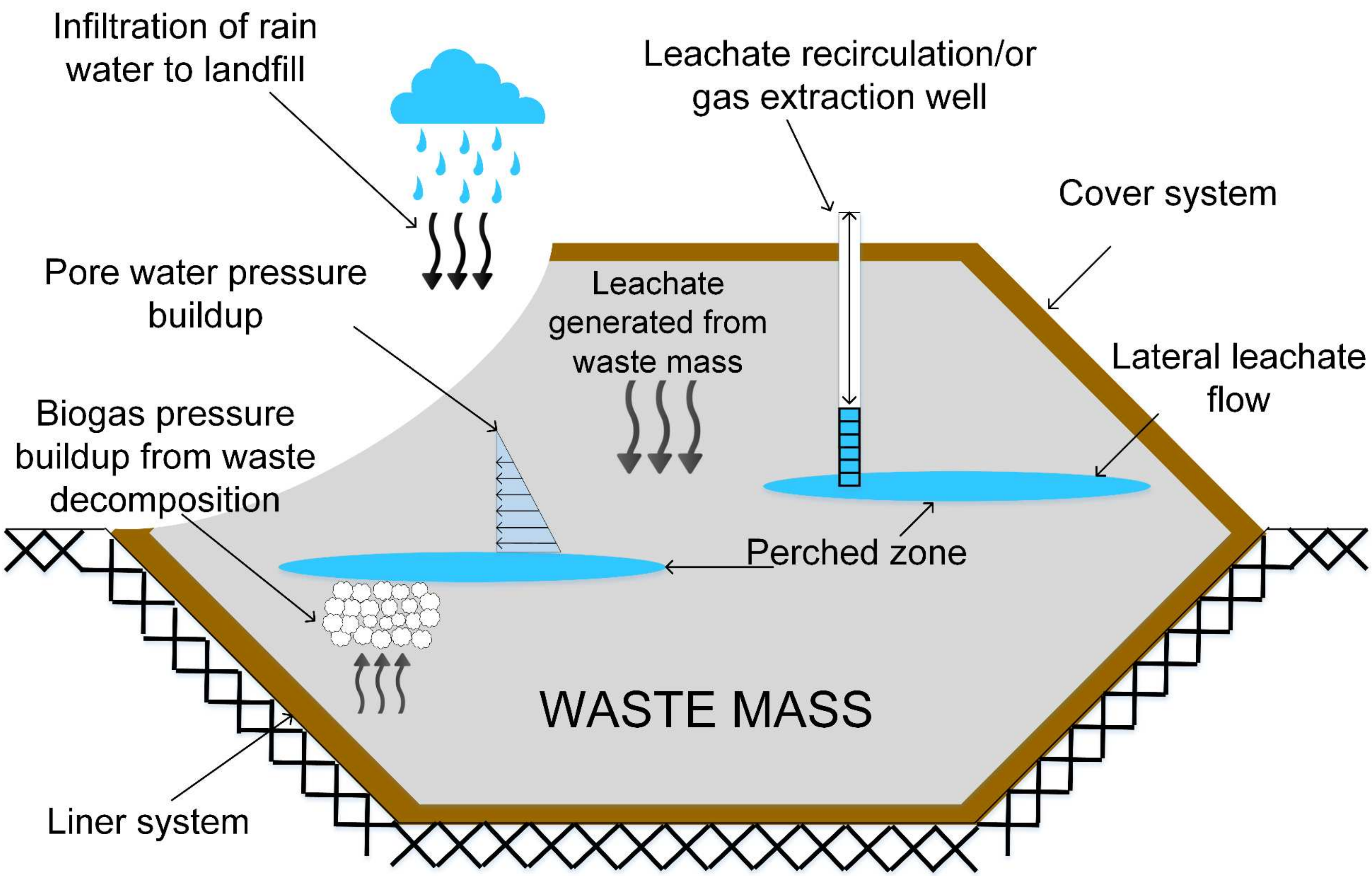

Fig. 2.1 Schematic of solid waste landfill illustrating the potential negative consequences related to disposal of low permeable waste.

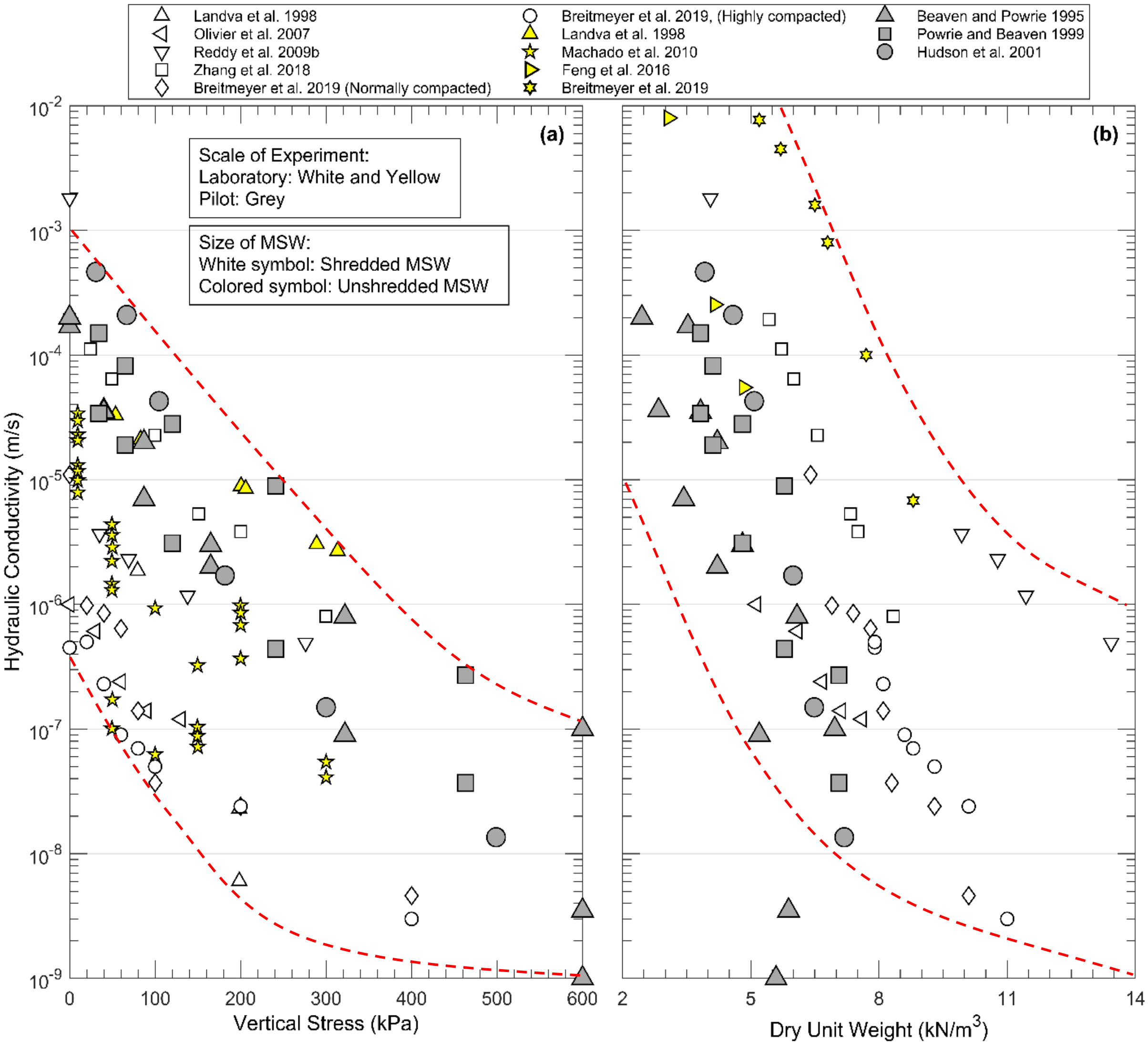

Fig. 2.2 Relationships of municipal solid waste (MSW) hydraulic conductivity versus (a) vertical stress and (b) dry unit weight.

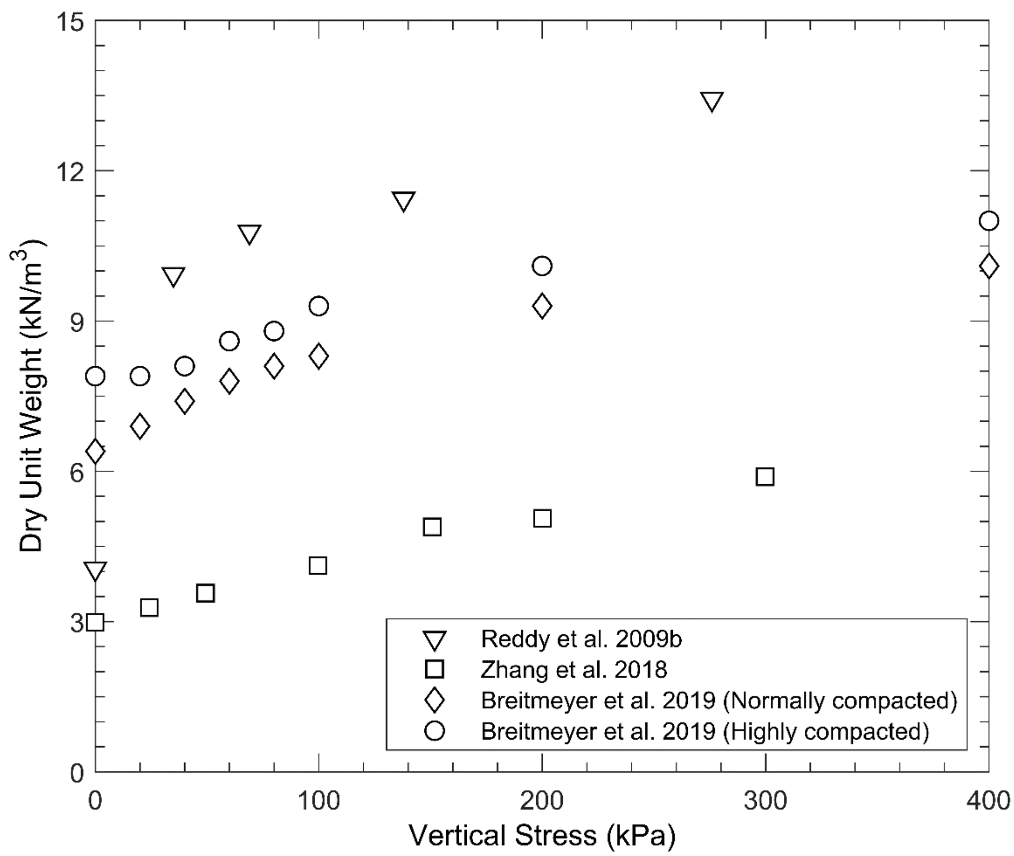

Fig. 2.3 Relationships of vertical stress versus dry unit weight for fresh MSW.

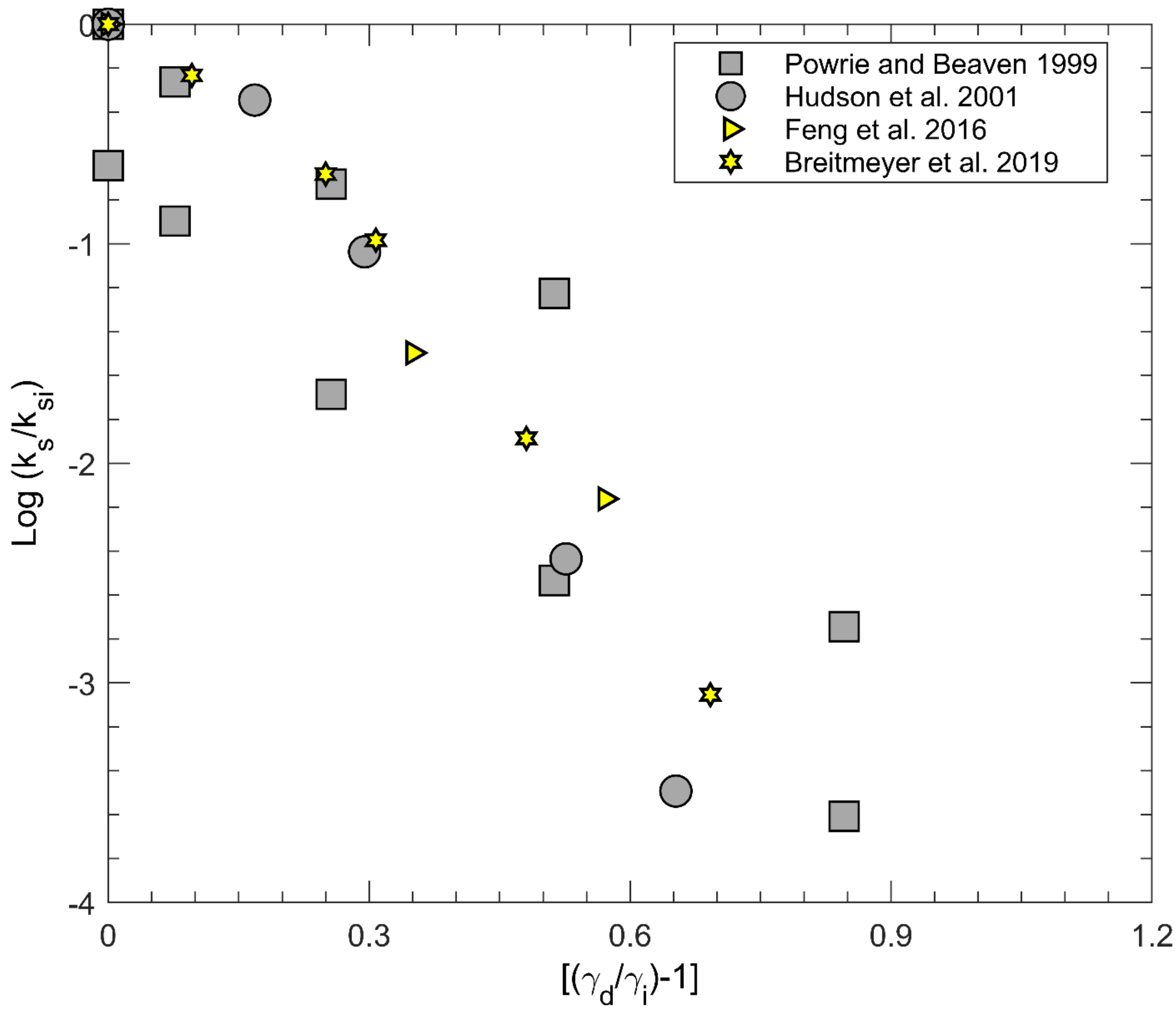

Fig. 2.4 Hydraulic conductivity versus dry unit weight normalized to initial condition for the laboratory- and pilot-scale k_s test on unshredded MSW.

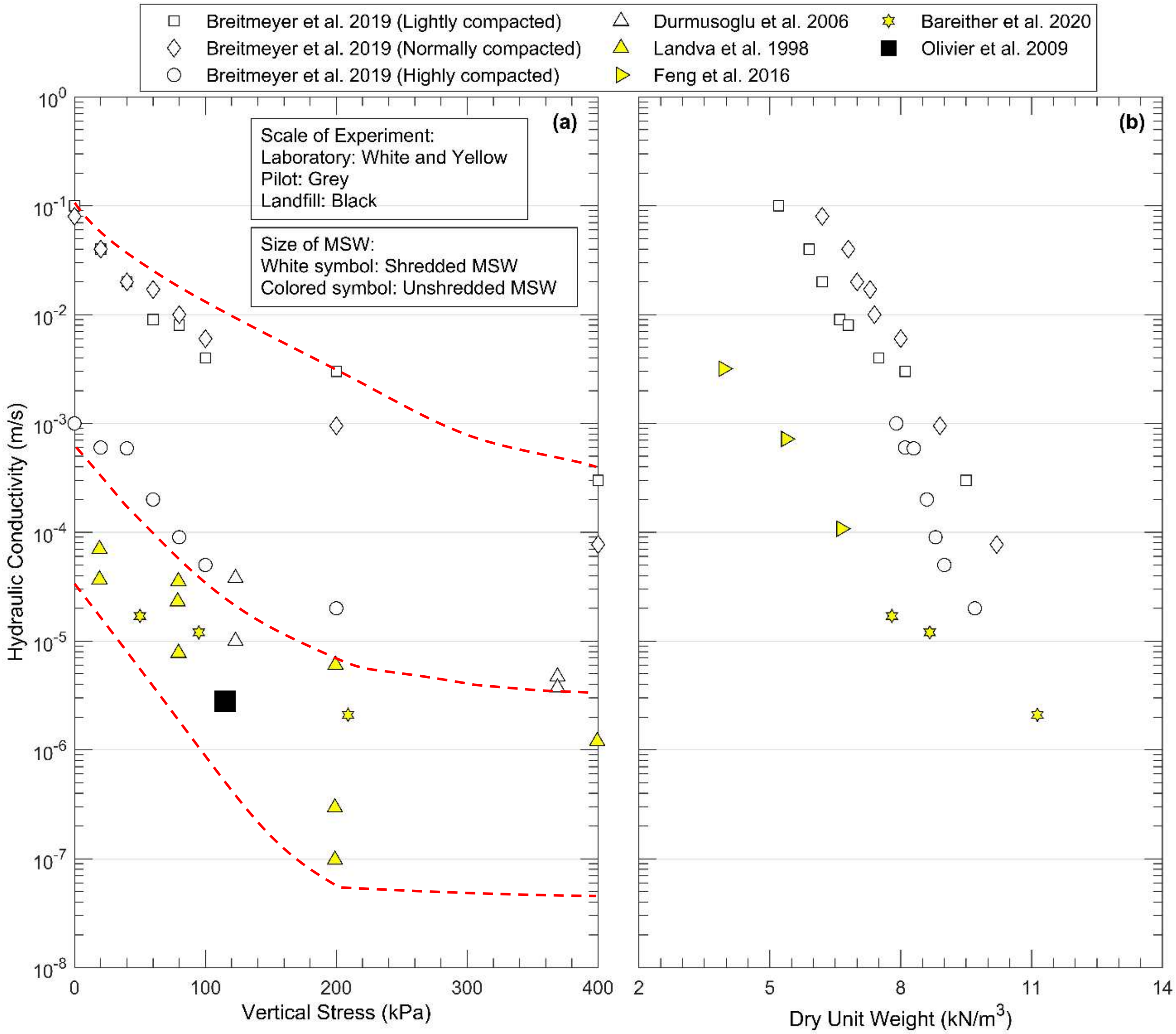

Fig. 2.5 Relationships of hydraulic conductivity versus (a) vertical stress and (b) dry unit weight for semi-decomposed MSW.

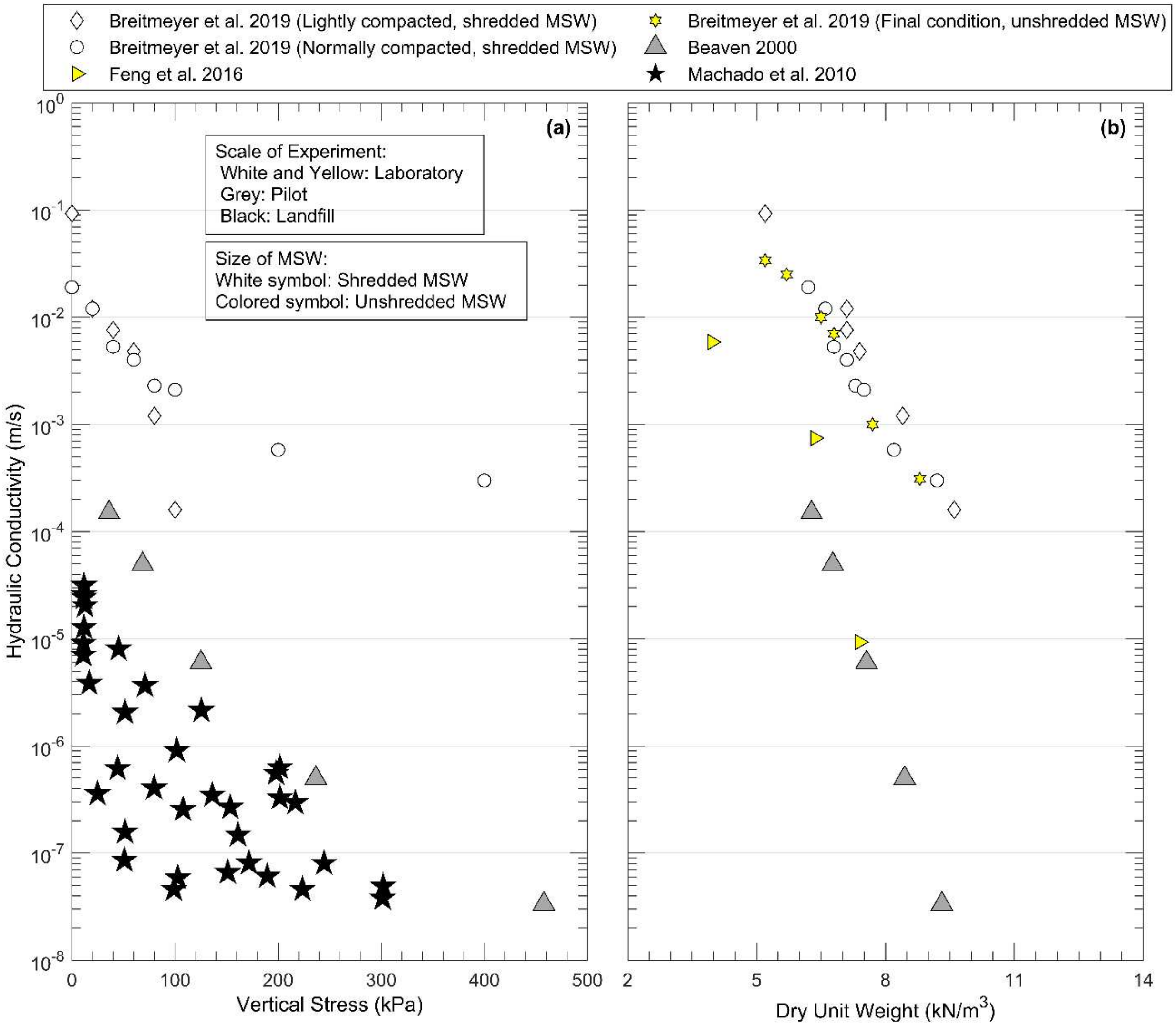

Fig. 2.6 Relationships of hydraulic conductivity versus (a) vertical stress and (b) dry unit weight for decomposed MSW.

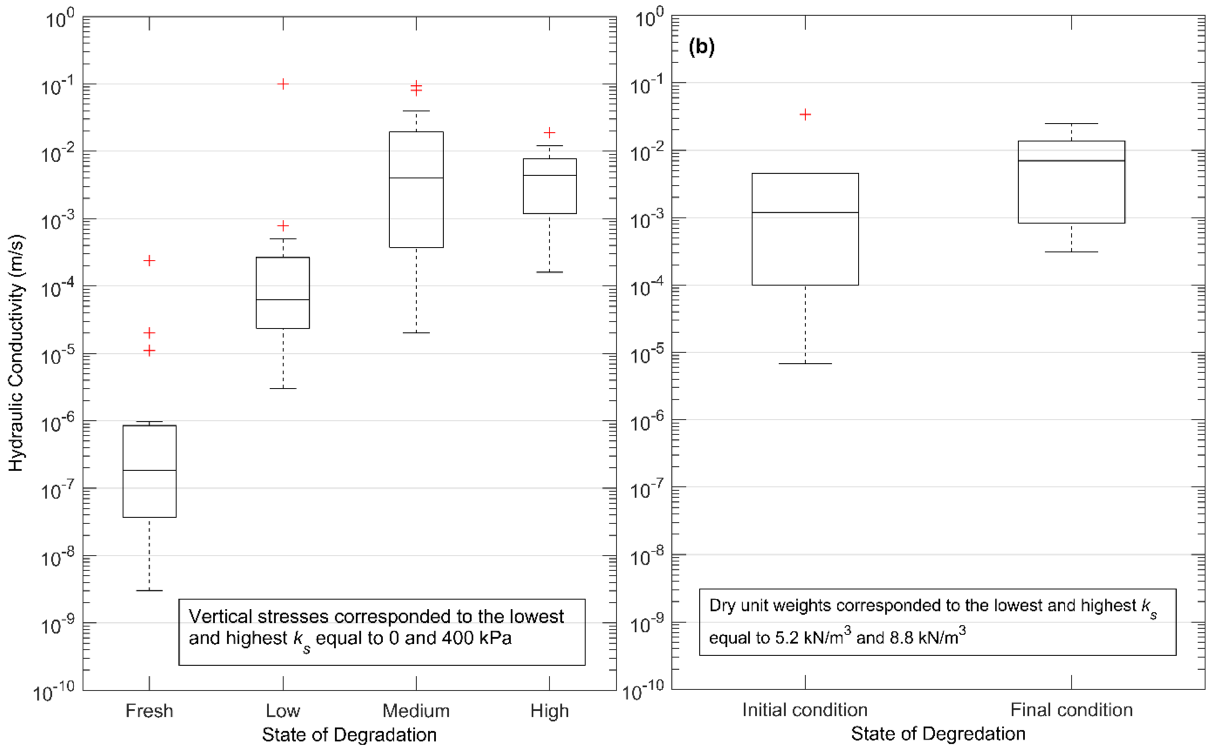

Fig. 2.7 Relationships of MSW degradation and hydraulic conductivity (a) hydraulic conductivity tests using a 150-mm-diameter permeameter and shredded MSW; (b) hydraulic conductivity tests using a 300-mm-diameter permeameter and unshredded MSW.

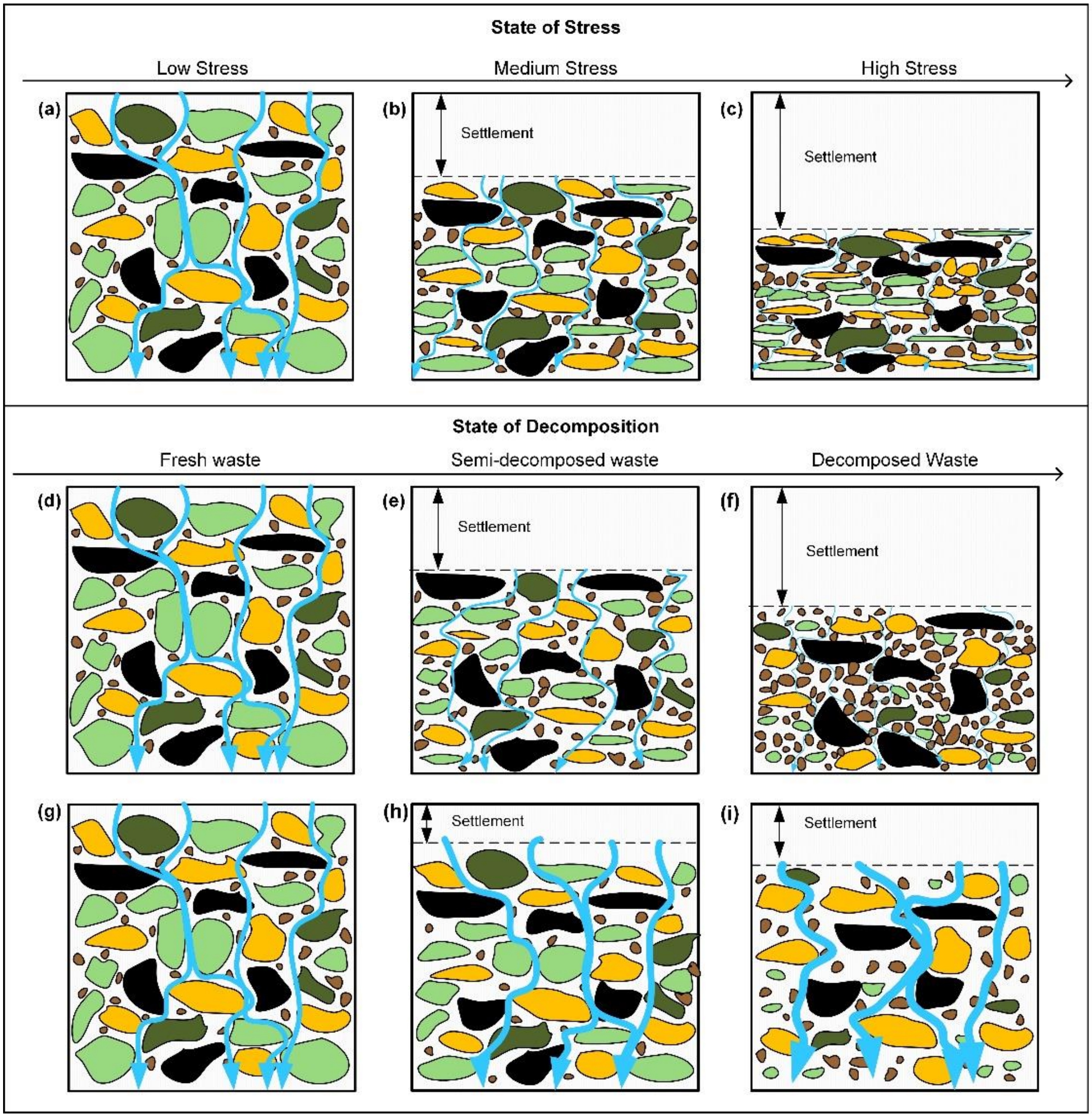

Fig. 2.8 A graphical representation of the influence of stress and waste degradation on MSW hydraulic conductivity, the relative magnitude of hydraulic conductivity is related to the thickness of the blue flow lines; light green shapes are representative of degradable and compressible MSW; dark green shapes are representative of degradable and incompressible MSW; orange shapes are representative of non-degradable and compressible MSW; black shapes are representative of non-degradable and incompressible; and small brown particles are representative of soil and soil-like materials. The composite particle surface area of the shapes in Fig. 2.8a is approximately representative of the average MSW composition disposed in US landfills.

2.7. References

ASTM. (2012). Standard Test Methods for Laboratory Compaction Characteristics of Soil Using Standard Effort. *ASTM International*, 1–13. https://doi.org/10.1520/D0698-12E01.1

ASTM International. (2003). Standard Test Methods for Laboratory Compaction Characteristics of Soil Using Modified Effort. *ASTM Standard Guide*, *3*, 1–10. https://doi.org/10.1520/D1557-12.1

Bareither, C. A., Benson, C. H., & Edil, T. B. (2013). Compression of Municipal Solid Waste in Bioreactor Landfills : Mechanical Creep and Biocompression. *Journal of Geotechnical and Geoenvironmental Engineering*, 139(July), 1007–1021. https://doi.org/10.1061/(ASCE)GT.1943-5606.0000835.

Bareither, C. A., Benson, C. H., & Edil, T. B. (2012). Compression Behavior of Municipal Solid Waste: Immediate Compression. *Journal of Geotechnical and Geoenvironmental Engineering*, *138*(9), 1047–1062. https://doi.org/10.1061/(ASCE)GT.1943-5606.0000672

Bareither, C. A., Benson, C. H., Rohlf, E. M., & Scalia, J. (2020). Hydraulic and mechanical behavior of municipal solid waste and high-moisture waste mixtures. *Waste Management*, 105, 540–549. https://doi.org/10.1016/j.wasman.2020.02.030

Bareither, C. A., Benson, C. H., & Edil, T. B. (2012). Comparison of Waste Settlement Parameters for Bioreactor Landfills Derived from Physical, Chemical, and Biological Processes. *Global Waste Management Symposium*, 1–5.

Barlaz, M. A., Ham, R. K., & Schaefer, D. M. (1990). Methane production from municipal refuse - a review of enhancement techniques and microbial dynamics. *Critical Reviews in Environmental Control*, 19(6), 557–584. https://doi.org/https://doi.org/10.1080/10643389009388384

Beaven, R. P., & Powrie, W. (1995). The hydrogeological and geotechnical properties of household waste in relation to sustainable landfilling. *International Landfill Symposium*.

Beaven, R. P. (2000). The hydrogeological and geotechnical properties of household waste in relation to sustainable landfilling. (Issue January) [University of London]. http://qmro.qmul.ac.uk/jspui/handle/123456789/1698

Bleiker, D. E., Farquhar, G., & Mcbean, E. (1995). Landfill settlement and the impact on site capacity and refuse hydraulic conductivity. *Waste Management & Research*, 13(6), 533–554. https://doi.org/10.1177/0734242X9501300604

Bleiker, D. E., McBean, E., & Farquhar, G. (1993). Refuse Sampling and Permeability Testing at the Brock West and Keele Valley Landfills. *Proceedings, Sixteenth International Madison Waste Conference : Municipal & Industrial Waste*, 548–567.

Bogner, J. E. (1990). Controlled study of landfill biodegradation rates using modified BMP assays. *Waste Management and Research*, 8(5), 329–352. https://doi.org/10.1016/0734-242X(90)90073-V

Bonaparte, R., Bachus, R. C., & Gross, B. A. (2020). Geotechnical Stability of Waste Fills: Lessons Learned and Continuing Challenges. *Journal of Geotechnical and Geoenvironmental Engineering*, 146(11), 05020010. https://doi.org/10.1061/(asce)gt.1943-5606.0002291

Breitmeyer, R. J., Benson, C. H., & Edil, T. B. (2019). Effects of Compression and Decomposition on Saturated Hydraulic Conductivity of Municipal Solid Waste in Bioreactor Landfills. *Journal of Geotechnical and Geoenvironmental Engineering*, 145(4), 1–15. https://doi.org/10.1061/(ASCE)GT.1943-5606.0002026

Breitmeyer, R. J., Benson, C. H., & Edil, T. B. (2020). Effect of Changing Unit Weight and Decomposition on Unsaturated Hydraulics of Municipal Solid Waste in Bioreactor Landfills. *Journal of Geotechnical and Geoenvironmental Engineering*, 146(5), 1–18. https://doi.org/10.1061/(ASCE)GT.1943-5606.0002244

Burrows, M. R., Joseph, J. B., & D., M. J. (1997). The hydraulic properties of in-situ landfilled waste. *Proceedings Sardinia 97, Sixth International Landfill Symposium*, 53(9), 78–83. https://doi.org/10.1017/CBO9781107415324.004

Chen, T. Hong, & Chynoweth, D. P. (1995). Hydraulic conductivity of compacted municipal solid waste. *Bioresource Technology*, 51(2–3), 205–212. https://doi.org/10.1016/0960-8524(94)00127-M

Choi, H. J., Choi, Y., & Rhee, S. W. (2019). Estimation on migration characteristics of leachate using analysis of hydraulic conductivity at bioreactor landfill. *Waste Management and Research*, 38(1), 59–68. https://doi.org/10.1177/0734242X19873705

Chugh, A. K., Stark, T. D., & DeJong, K. A. (2007). Reanalysis of a municipal landfill slope failure near Cincinnati, Ohio, USA. *Canadian Geotechnical Journal*, 44(1), 33–53. https://doi.org/10.1139/T06-089

Dixon, N., & Jones, D. R. V. (2005). Engineering properties of municipal solid waste. *Geotextiles and Geomembranes*, 23(3), 205–233. https://doi.org/10.1016/j.geotexmem.2004.11.002

Durmusoglu, E., Sanchez, I. M., & Corapcioglu, M. Y. (2006). Permeability and compression characteristics of municipal solid waste samples. *Environmental Geology*, 50(6), 773–786. https://doi.org/10.1007/s00254-006-0249-6

Eid, H. T., Stark, T. D., Evans, W. D., & Sherry, P. E. (2000). MUNICIPAL SOLID WASTE SLOPE FAILURE. I: WASTE AND FOUNDATION SOIL PROPERTIES By. *Journal of Geotechnical and Geoenvironmental Engineering*, 126(2010), 397–407.

Fei, X., Zekkos, D., & Raskin, L. (2014). An experimental setup for simultaneous physical, geotechnical, and biochemical characterization of municipal solid waste undergoing biodegradation in the laboratory. *Geotechnical Testing Journal*, 37(1). https://doi.org/10.1520/GTJ20130084

Feng, S., Gao, K., Chen, Y., Li, Y., Zhang, L. M., & Chen, H. X. (2016). Geotechnical properties of municipal solid waste at Laogang Landfill , China. *Waste Management*. https://doi.org/10.1016/j.wasman.2016.09.016

Fungaroli, A. A., & Steiner, R. L. (1979). Investigation of Sanitary Landfill Behavior. *Environmental Protection Technology Series. EPA*, 1.

Gabr, M. a., & Valero, S. N. (1995). Geotechnical properties of synthetic municipal solid waste. *Geotechnical Testing Journal*, 18(2), 241–251. https://doi.org/10.3328/IJGE.2009.03.03.429-438

Gao, W., Chen, Y., Zhan, L., & Bian, X. (2015). Engineering properties for high kitchen waste content municipal solid waste. *Journal of Rock Mechanics and Geotechnical Engineering*, 7(6), 646–658. https://doi.org/10.1016/j.jrmge.2015.08.007

Gavelyte, S., Dace, E., & Baziene, K. (2016). The Effect of Particle Size Distribution on Hydraulic Permeability in a Waste Mass. *Energy Procedia*, 95, 140–144. https://doi.org/10.1016/j.egypro.2016.09.035

Han, B., Scicchitano, V., & Imhoff, P. T. (2011). Measuring fluid flow properties of waste and assessing alternative conceptual models of pore structure. *Waste Management*, 31(3), 445–456. https://doi.org/10.1016/j.wasman.2010.09.021

Hanson, J. L., Yesiller, N., Von Stockhausen, S. a., & Wong, W. W. (2010). Compaction Characteristics of Municipal Solid Waste. *Journal of Geotechnical and Geoenvironmental Engineering*, 136(8), 1095–1102. https://doi.org/10.1061/(ASCE)GT.1943-5606.0000324

Hartwell, J., Mousavi, M. S., Eun, J., & Bartelt-Hunt, S. (2021). Evaluation of depth-dependent properties of municipal solid waste using a large diameter-borehole sampling method. *Journal of the Air and Waste Management Association*, 71(4), 433–446. https://doi.org/10.1080/10962247.2020.1848942

Hendron, D. M., Fernandez, G., Prommer, P. J., Giroud, J. P., & Orozco, L. F. (1999). Investigation of the cause of the 27 September 1997 slope failure at the Dna Jana landfill. *Proceeding.*Sardinia 99, Seventh International Waste Management and Landfill Symposium, October.

Hossain, M. S., Penmethsa, K. K., & Hoyos, L. (2008). Permeability of municipal solid waste in bioreactor landfill with degradation. *Geotechnical and Geological Engineering*, 27(1), 43–51. https://doi.org/10.1007/s10706-008-9210-7

Jafari, N. H., Stark, T. D., & Merry, S. (2013). The July 10 2000 Payatas Landfill Slope Failure. *International Journal of Geoengineering Case Histories*, 2(3), 208–228. https://doi.org/10.4417/IJGCH-02-03-03

Jain, P., Powell, J., Townsend, T. G., & Reinhart, D. R. (2006). Estimating the Hydraulic Conductivity of Landfilled Municipal Solid Waste Using the Borehole Permeameter Test. *Journal of Environmental Engineering*, 132(JUNE), 645–652. https://doi.org/10.1061/(ASCE)0733-9372(2006)132

Jang, Y. S., Kim, Y. W., & Lee, S. I. (2002). Hydraulic properties and leachate level analysis of Kimpo metropolitan landfill, Korea. *Waste Management*, 22(3), 261–267. https://doi.org/10.1016/S0956-053X(01)00019-8

Jie, Y. X., Xu, W. J., Dunzhu, D., Wei, Y. F., Peng, T., & Zhou, Z. Y. (2013). Laboratory testing of a densified municipal solid waste in Beijing. *Journal of Central South University*, 20(7), 1953–1963. https://doi.org/10.1007/s11771-013-1695-4

Karimi, S., & Bareither, C. A. (2021). The influence of moisture enhancement on solid waste biodegradation. *Waste Management*, 123, 131–141. https://doi.org/10.1016/j.wasman.2021.01.022

Kavazanjian Jr., E., & Matasovic, N. (1995). Seismic analysis of solid waste landfills. *Geotechnical Special Publication*, 46 /2.

Kavazanjian, E. (1999). Seismic Design of Solid Waste Containment Facilities. *Proceedings of the Eight Canadian Conference on Earthquake Engineering*, June, 51–89.

Kavazanjian, E., Matasovic, N., Stokoe, K., & Bray, J. (1996). In-Situ Shear Wave Velocity of Solid Waste from Surface Wave Measurements. *2nd International Congress on Environmental Geotechnics*, Vol. 1, 97 102.

Kavazanjian, E., Jr. (2001). “Mechanical properties of municipal solid waste.” Proc., *Sardinia 2001, 8th Int. Landfill Symposium*

Ke, H., Hu, J., Xu, X. B., Wang, W. F., Chen, Y. M., & Zhan, L. T. (2017). Evolution of saturated hydraulic conductivity with compression and degradation for municipal solid waste. *Waste Management*, 65, 63–74. https://doi.org/10.1016/j.wasman.2017.04.015

Kenter, R. J., Schmucker, B. O. and Miller, K. R. (1997), "The Day the Earth Didn't Stand Still: the Rumpke Landslide," *Waste Age*, March, 28 (3): 66–81.

Kees Beentjes. (2021). *Intercepting Landfill Leachate for Recirculation: An Initial Assessment of Experimental Design Parameters*. University of Canterbury.

Kim, J., & Pohland, F. G. (2003). Process enhancement in anerobic bioreactor landfills. *Water Science and Technology*, 48(4), 29–36.

Koerner, G. R., & Eith, A. W. (2002). Drainage Capability of Fully Degraded MSW with respect to Various Leachate Collection and Removal Systems. *Geo-Frontiers Congress* 2005, 512, 2–7.

Koerner, R. M. H., Soong, T.-Y., Robert M. Koernerl-Hon, & Soong, T.-Y. (2000). Stability Assessment of Ten Large Landfill Failures. *Geo-Denver; Advances in Transportation and Geoenvironmental Systems Using Geosynthetics*. https://doi.org/10.1061/40515(291)1

Korfiatis, G. P., Demetracopoulos, A. C., Bourodimos, E. L., & Nawy, E. G. (1984). Moisture transport in a solid waste column. *Journal of Environmental Engineering (United States)*, 110(4), 780–796. https://doi.org/10.1061/(ASCE)0733-9372(1984)110:4(780)

Landva, A., Pelkey, S., & Valsangkar, A. (1998). Coefficient of permeability of municipal refuse. *Environmental Geotechnics: Proceedings of the Third International Congress on Environmental Geotechnics*, 63–72.

Li, Y. C., Liu, H. L., Cleall, P. J., Ke, H., & Bian, X. C. (2013). Influences of operational practices on municipal solid waste landfill storage capacity. *Waste Management and Research*, 31(3), 273–282. https://doi.org/10.1177/0734242X12472705

Liu, X., Zhang, L., Wu, S., Shao, Y., Wu, X., & Li, Z. (2020). Changes in municipal solid waste pore structure during degradation: Analysis of synthetic waste using X-ray computed microtomography. *Science of the Total Environment*, 708(5), 135089. https://doi.org/10.1016/j.scitotenv.2019.135089

Machado, S. L., Karimpour-Fard, M., Shariatmadari, N., Carvalho, M. F., & Nascimento, J. C. F. d. (2010). Evaluation of the geotechnical properties of MSW in two Brazilian landfills. *Waste Management*, 30(12), 2579–2591. https://doi.org/10.1016/j.wasman.2010.07.019

McDougall, J. R., Pyrah, I. C., Yuen, S. T. S., Monteiro, V. E. D., Melo, M. C., & Juca, J. F. T. (2004). Decomposition and settlement in landfilled waste and other soil-like materials. *Geotechnique*, 54(9), 605–609. https://doi.org/10.1680/geot.2004.54.9.605

Merry, S. M., Fritz, W. U., Budhu, M., & Jesionek, K. (2006). Effect of Gas on Pore Pressures in Wet Landfills. *Journal of Geotechnical and Geoenvironmental Engineering*, 132(May), 553–561. https://doi.org/10.1061/(ASCE)1090-0241(2006)132:5(553)

Miguel, M. G., Mortatti, B. C., Da Paixão Filho, J. L., & Pereira, S. Y. (2018). Saturated Hydraulic Conductivity of Municipal Solid Waste Considering the Influence of Biodegradation. *Journal of Environmental Engineering*, 144(9), 1–8. https://doi.org/10.1061/(ASCE)EE.1943-7870.0001432

OLIVIER, F., OXARANGO, L., MUGNIER, V., TINET, A. J., & MARCOUX, M. A. (2009). Estimating the Drawdown of Leachate in a Saturated Landfill : 3D Modeling Based on Field Pumping Tests. *Sardinia 2009, Twelfth International Waste Management and Landfill Symposium*, October 2009.

Olivier, F., Marcoux, M., Gourc, J., & Machado, S. L. (2007). Attempt for a Comprehensive Interdisciplinary Analysis of a Mechanically Pretreated Msw Confined Two Years in a Large-Scale Laboratory Reactor. *Proceedings Sardinia 2007, Eleventh International Waste Management and Landfill Symposium*, 1(5).

Olivier, F., & Gourc, J.-P. (2007). Hydro-mechanical behavior of Municipal Solid Waste subject to leachate recirculation in a large-scale compression reactor cell. *Waste Management*, 27(1), 44–58. https://doi.org/10.1016/j.wasman.2006.01.025

Oweis, I. S., Smith, D. A., Ellwood, B. R., & Greene, D. S. (1990). Hydraulic Characteristics of Municipal Refuse. *Journal of Geotechnical Engineering*, 116(4), 539–553. https://doi.org/10.1061/(ASCE)0733-9410(1990)116

Powrie, W., & Beaven, R. P. (1999). Hydraulic properties of household waste and implications for landfills. *Proceedings of the Institution of Civil Engineers: Geotechnical Engineering*, 137(4), 235–247. https://doi.org/10.1680/geng.1997.137.4.235

Powrie, W., Beaven, R. P., & Hudson, A. P. (2005). Factors affecting the hydraulic conductivity of waste. *In: International Workshop "Hydro-Physico-Mechanics of Landfills.*," March, 1–5.

Powrie, W., Beaven, R., & Hudson, A. (2008). The influence of landfill gas on the hydraulic conductivity of waste. *Geotechnical Special Publication*, 177, 264–271. https://doi.org/10.1061/40970(309)33

Reddy, K. R., Hettiarachchi, H., Gangathulasi, J., & Bogner, J. E. (2011). Geotechnical properties of municipal solid waste at different phases of biodegradation. *Waste Management*, 31(11), 2275–2286. https://doi.org/10.1016/j.wasman.2011.06.002

Reddy, K. R., Hettiarachchi, H., Parakalla, N. S., Gangathulasi, J., & Bogner, J. E. (2009). Geotechnical properties of fresh municipal solid waste at Orchard Hills Landfill, USA. *Waste Management*, 29(2), 952–959. https://doi.org/10.1016/j.wasman.2008.05.011

Reddy, K. R., Hettiarachchi, H., Parakalla, N., Gangathulasi, J., Bogner, J., & Lagier, T. (2009). Hydraulic Conductivity of MSW in Landfills. *Journal of Environmental Engineering*, 135(8), 677–683. https://doi.org/10.1061/(ASCE)EE.1943-7870.0000031

Rohlf, E. M., Karimi, S., & Bareither, C. A. (2021). Implications of municipal solid waste co-disposal experiments on biodegradation and biochemical compatibility. *Waste Management*, 129, 62–75. https://doi.org/10.1016/j.wasman.2021.05.009

Schmucker, B. O., and D. M. Hendron. 1997. “Forensic analysis of 9 March 1996 landslide at the Rumpke sanitary landfill, Hamilton County, Ohio.” In Proc., *ASCE Central Ohio and Toledo Sections 1997 Fall Seminar Slope Stability in Waste Systems*. Reston, VA: ASCE.

Stark, T. D. and Evans, W. D. (1997), "Balancing Act," *Civil Engineering, ASCE*, August, pp 8A-11A.

Stark, T. D., H. T. Eid, W. D. Evans, and P. E. Sherry. 2000. “Municipal solid waste slope failure. II: Stability analyses.*” J. Geotech. Geoenviron. Eng.* 126 (5): 408–419. https://doi.org/10.1061/(ASCE)1090 -0241(2000)126:5(408).

Stark, T. D., D. Arellano, W. D. Evans, V. L. Wilson, and J. M. Gonda. 1998. “Unreinforced geosynthetic liner case history.” *Geosynthetics Int.* 5 (5): 521–544. https://doi.org/10.1680/gein.5.0135.

Staub, M., Galietti, B., Oxarango, L., Khire, M. V, & Gourc, J.-P. (2009). Porosity and Hydraulic Conductivity of MSW Using Laboratory-Scale Tests. *The International Workshop “Hydro-Physico-Mechanics of Landfills,”* March 20*09*, 1–9.

Stoltz, G., Gourc, J. P., & Oxarango, L. (2010). Liquid and gas permeabilities of unsaturated municipal solid waste under compression. *Journal of Contaminant Hydrology*, 118(1–2), 27–42. https://doi.org/10.1016/j.jconhyd.2010.07.008

Townsend, T. G., Miller, W. L., & Earle, J. F. K. K. (1995). Leachate-recycle infiltration ponds. *Journal of Environmental Engineering (United States)*, 121(6), 465–471. https://doi.org/10.1061/(ASCE)0733-9372(1995)121:6(465)

Townsend, T. G., Powell, J., Jain, P., Xu, Q., Tolaymat, T., & Reinhart, D. (2015). *Sustainable Practices for Land ll Design and Operation*. Springer.

Wong, W. W. Y. (2009). *Investigation of the Geotechnical Properties of Municipal Solid* (Issue September). California Polytechnic State University.

Wu, H., Chen, T., Wang, H., & Lu, W. (2012). Field air permeability and hydraulic conductivity of landfilled municipal solid waste in China. *Journal of Environmental Management*, 98(1), 15–22. https://doi.org/10.1016/j.jenvman.2011.12.008

Xu H, Zhan LT, Guo RY, Shen SL, Lin WA, Chen P, Chen YM. Large-scale model experiments on multi-field interactions in landfill of municipal solid waste. In: *The 7th International Congress on Environmental Geotechnics*, Melbourne; 2014. p. 810e7

Xu, X. B., Zhan, T. L. T., Chen, Y. M., & Beaven, R. P. (2014). Intrinsic and relative permeabilities of shredded municipal solid wastes from the Qizishan landfill, China. *Canadian Geotechnical Journal*, 51(11), 1243–1252. https://doi.org/10.1139/cgj-2013-0306

Zairi, M., Aydi, A., & Dhia, H. Ben. (2014). Leachate generation and biogas energy recovery in the Jebel Chakir municipal solid waste landfill, Tunisia. *Journal of Material Cycles and Waste Management*, 16(1), 141–150. https://doi.org/10.1007/s10163-013-0164-3

Zeiss, C., Uguccioni, M., Zeiss, Chris, Uguccioni, M., Zeiss, C., & Uguccioni, M. (1995). Mechanisms and Patterns of Leachate Flow in Municipal Solid Waste Landfills. *Journal of Environmental Systems and Engineering*, 23(3), 247–270. https://doi.org/10.2190/jw1m-a901-l1x9-t15f

Zekkos, D., Bray, J. D., Jr, E. K., Matasovic, N., Rathje, E. M., Riemer, M. F., & Stokoe Ii, K. H. (2006). Unit Weight of Municipal Solid Waste. *Journal of Geotechnical and Geoenvironmental Engineering*, 132(10), 1250–1261.

Zhang, Z., Wang, Y., Xu, H., Fang, Y., & Wu, D. (2018). Influence of effective stress and dry density on the permeability of municipal solid waste. *Waste Management and Research*. https://doi.org/10.1177/0734242X18763520

Zhu, Y., Zhang, Y., Luo, D., Chong, Z., Li, E., & Kong, X. (2020). A review of municipal solid waste in China: characteristics, compositions, influential factors and treatment technologies. *Environment, Development and Sustainability*, https://doi.org/10.1007/s10668-020-00959-9

CHAPTER 3: INFLUENCE OF OIL AND GAS EXPLORATION AND PRODUCTION WASTE ON MUNICIPAL SOLID WASTE HYDRAULIC CONDUCTIVITY

3.1. Introduction

In 1991, the US Environmental Protection Agency (EPA) promulgated that municipal solid waste (MSW) landfills are allowed to receive and dispose other types of RCRA Subtitle D wastes (EPA 1991). These wastes were identified as non-hazardous and non-MSW, which included commercial and industrial solid wastes. The most commonly disposed non-MSW wastes in MSW landfills are construction and demolition wastes (41 states), industrial wastes (33 states), municipal sludge/biosolids (27 states), and ash (20 states) (Environmental Research Education Foundation (EREF), 2018). Revenue from tipping fees is a key benefit to landfill owners by disposing non-MSW solids wastes, and disposal in engineered landfills mitigates risks to human health and the environment. Additional benefits can be achieved from the disposal of select wastes with high moisture content, which can increase compaction, overall waste unit weight and storage of incoming waste, and also can accelerate biogas generation (Hanson et al., 2010).

Non-hazardous waste with high moisture content, i.e., high-moisture waste (HMW), can be disposed in MSW landfills if the HMW does not contain free liquids. The paint filter test, which assesses the presence of free liquids in a sample of HMW is used by landfill operators to permit disposal of HMWs in MSW landfills (SW-846 Method 9095b, EPA 2004). However, wastes such as sludges or oil and gas exploration and production wastes (E&PW) can have high moisture content, low hydraulic conductivity, and low shear strength compared to MSW (Bareither et al., 2020). The variation in waste properties can affect landfill operation, which requires further assessment regarding the waste characteristics.

A summary of geotechnical laboratory tests conducted on HMW and dewatered HMW is shown in Table C.1 (Appendix C). There are limited data regarding the characteristics of HMW; however, available research suggests that there could be issues with the permeability and strength of these waste materials. Oil and gas exploration and production wastes are generated during the exploration, development, and production of crude oil, natural gas, and geothermal energy. Bareither et al. (2020) reported characteristics of an E&PW that included dry weight water contents of 125% to 155% (i.e., dry weight water content = mass of water per mass of solid), saturated hydraulic conductivity (k_s) of 1×10^{-11} m/s, and friction angle (ϕ_s) of 2° (Bareither et al., 2020). Chiado (2014) reported that hydraulic conductivity of E&PWs from the Marcellus Shale ranged from 2×10^{-7} m/s to 1×10^{-11} m/s. The potential low strength of E&PWs (i.e., low friction angle) combined with low permeability can affect the stability and functionality of MSW landfills.

The potential negative impacts associated with disposing low hydraulic conductivity waste in solid waste landfills are shown in Fig. 3.1. Low hydraulic conductivity wastes (e.g., E&PWs) may create low permeability layers, which can lead to perched water tables and generate positive pore water pressure that reduces landfill stability and/or produces leachate seeps (Hendron et al., 1999; Koerner and Soong 2000; Bonaparte et al., 2020; Bareither et al., 2020). Waste materials with low hydraulic conductivity also have a lower gas permeability, which can result in excessive increase in gas pressure (Merry et al., 2006; Powrie et al., 2008; Hudson et al., 2009; Zhan et al., 2017). Disposing wastes with lower hydraulic conductivities may lead to landfill instability (Benson 2018), which poses risks to human health and the environment.

Hendron et al. (1999) indicated that low permeability intermittent cover layers allowed rapid pore pressure buildup that produced a slope failure at Dona Juana landfill located in Bogota, Colombia. Bonaparte et al. (2020) reported that placing a cover soil layer over deposited low permeable materials (i.e., drill cutting mixed with lime) created a relatively impervious layer, which resulted in gas and liquid pressure buildup that led to landfill slope failure. Landfill instability issues associated with low hydraulic conductivity HMWs can be mitigated if the hydraulic and mechanical behaviors of MSW, HMW, and MSW-HMW mixtures are understood prior to landfill disposal.

The main factors that influence the engineering properties of HMWs and MSW-HMW mixtures are (i) stress, (ii) mixture ratio, (iii) composition, and (iv) disposal methods. Current recommendations in industry for HMW management include the following: (i) dispose less than

20% concentrated non-MSW in a particular area relative to the total mass or spread the HMW in thin layers to avoid a concentrated zone, and (ii) avoid non-MSW disposal in proximity of final slopes (Chiado, 2014; EREF, 2018). However, the mixture ratio of MSW and a given HMW that introduces pronounced changes in physical and hydraulic behavior varies considering the waste composition and vertical stress. Bareither et al. (2020) reported mixture ratio below 40% HMW + MSW is an appropriate mixture ratio threshold to co-dispose HMW and MSW, provided that the vertical stress is below 200 kPa.

A hypothesis based on the current perspective of industry and relevant research is that an appropriate MSW-HMW mixture ratio can be determined based on stress, composition, and mixture methods that satisfy requirements for landfill stability and functionality. The appropriate mixture ratio must (i) maintain landfill stability such that the safety factors of landfill slopes meet criteria, (ii) not change hydraulic behavior such that leachate collection, liquid addition, and/or gas extraction remain effective, and (iii) not affect landfill disposal at the working face. If an appropriate mixture ratio is identified for co-disposed HMWs with MSW, co-disposing HMW and MSW can simultaneously help to reduce the negative consequences associated with disposing HMW wastes in MSW landfills and increase the efficiency of MSW landfills.

Although past research has provided valuable insight on laboratory- and field-scale MSW hydraulic conductivity, limited research has been conducted to evaluate factors that influence the hydraulic conductivity of MSW co-disposed with HMW. In particular, one of the most common HMWs disposed in MSW landfills is E&PW (personal communication, Waste Management). The objectives of this study included the following: (i) identify the influence of stress, waste composition, mixing method, and MSW-E&PW mixture ratios on hydraulic conductivity; (ii) develop a practical index test to estimate the hydraulic conductivity of MSW-E&PW mixtures; and (iii) recommend disposal strategies for E&PW.

The aforementioned objectives were evaluated via conducting hydraulic conductivity experiments in 305-mm-diameter permeameters for MSW and MSW-E&PW, as well as 102-mm-diameter permeameters for pure E&PW. Experiments were conducted at low (0 to 10 kPa), medium (10 to 100 kPa), and high (100 kPa to 400 kPa) vertical stress to evaluate the impact of stress and dry unit weight on hydraulic conductivity. Four mixture ratios for MSW-E&PW mixtures (i.e., 20%, 40%, 60%, and 80% E&PW content based on the total mass) were chosen to assess hydraulic behavior of mixtures. The E&PW was tested in two conditions: (i) *as-received E&PW*, which represented the moisture content of the bulk E&PW stream received at an MSW landfill; and (ii) *wet E&PW*, which represented the E&PW prepared to the maximum potential moisture content that met landfill disposal requirements (i.e., just passed the paint-filter test). Wet E&PW was prepared from as-received E&PW mixed with additional water. Geotechnical characteristics were determined on the MSW and E&PW separately, which aided in relating material characteristics to hydraulic conductivity.

3.2. Materials and Methods

3.2.1. Solid Waste Collection, Composition, and Preparation

3.2.1.1. *Municipal Solid Waste*

Synthetic MSW was used in this study due to health and safety issues related to Covid-19. Municipal solid waste materials were obtained from the Colorado State University (CSU) recycling center. Wastes were hand sorted into relevant categories (e.g., paper, cardboard, metals, glass, plastics) and air-dried. Food waste was collected from a CSU dining hall as pre-consumer food waste. Rubber mulch and wood mulch were obtained locally in Fort Collins, Colorado and used in lieu of rubber and leather wastes. A collection of photographs documenting the MSW collection and preparation process are included in Appendix C (Fig. C1 and Fig. C2).

The MSW composition used in this study is in Table 3.1, which reflected the average MSW composition reported in the 2015 US Environmental Protection Agency (USEPA) solid waste database (USEPA 2015). All waste materials were shredded with a slow-speed, high-torque shredder and sieved through a 20-mm screen. Screened food wastes were squeezed to reduce the moisture content, packed in Ziploc bags, and frozen until used to create MSW. Food waste was defrosted at room temperature the day before MSW preparation. All other MSW materials were dried and stored in sealed barrels after shredding and sieving. Waste components were mixed thoroughly to obtain a homogenous MSW mixture. A photograph of the mixed MSW is shown in Fig. C3, Appendix C.

3.2.1.2. *Exploration and Production Waste*

Exploration and production waste was obtained from a local landfill in Weld County, Colorado, USA. The E&PW consisted of contaminated soil with oil from well drilling and was collected in buckets directly from haul trucks entering the landfill. A total of 30 x 5-gallon buckets were collected, which were all mixed together on a large plastic tarp to create a homogenous E&PW used throughout the laboratory testing program (Fig. 3.1 and Fig. C4). After mixing, the homogenized E&PW was stored in sealed buckets.

High-moisture or wet wastes can be disposed in MSW landfills if they meet the paint filter liquids test criteria (EPA Method 9095B). The highest water content at which the wet E&PW passed the paint filter test was defined as the water content threshold. The water content threshold was determined by adding pre-determined amounts of water to E&PW, followed by thorough mixing and hydration for three days in sealed buckets. Subsequently, a 100-g sample was placed in a paint filter and allowed to drain freely. If the material did not drain freely after 5 minutes, the wet E&PW passed the test (Fig. C5). The water content threshold for wet E&PW was approximately 32% to 36% (Fig. C6).

Exploration and production waste was prepared to two moisture contents for laboratory testing: (i) as-received, which had a target dry weight water content of 18%; and (ii) wet, which had a target moisture content of 32% to 36% that represented the moisture content threshold. Wet E&PW prepared to the water content threshold represented the upper bound of water content for which the HMW met regulations for direct disposal in an MSW landfill. This elevated moisture content relative to the as-received state also represented more conservative geotechnical behavior for landfilled E&PW (i.e., potentially lower hydraulic conductivity and strength).

3.2.1.3. *Preparation of E&PW and MSW mixtures*

Four mixture ratios were used to evaluate the influence of E&PW addition on the hydraulic conductivity of MSW. The MSW-E&PW mixtures were prepared with as-received E&PW and wet E&PW mixed with MSW at E&PW contents of 20%, 40%, 60%, and 80% based on total mass. A known mass of E&PW was added to MSW to obtain the target mixture ratio and mixed thoroughly to create a homogeneous material.

3.2.2. Waste Characteristics

3.2.2.1. *Water Content and Unit Weight*

Water content (w_d) was measured via drying representative samples for 24 hr at 105 °C, and afterward, a volatile solid test was performed via combusting the dry waste for 2 hr at 550 °C. Water content of MSW samples were performed 24 hr after waste preparation to allow wastes particles to absorb moisture from the food waste. Water contents reported herein were calculated based on the mass of water per mass of dry solid. The volatile solid test reflects the organic/combustible fraction of a given waste sample.

3.2.2.2. *Specific Gravity*

Specific gravity (G_s) of E&PW was measured via a water pycnometer (ASTM D854). The "moist specimen" procedure (Method A) was used for measuring particle density. The G_s of E&PW was 2.64, which agrees with the upper boundary of G_s for E&PW as reported by Chiado (2014).

The G_s of MSW was estimated using Eq. 1, and G_s of individual waste materials assumed based on recommendations in Wong (2009) and Yesiller et al. (2014):

$$G_s = \frac{\left(\sum_{i=1}^{n} M_{si}\right)}{\left[\sum_{i=1}^{n} \frac{M_{si}}{G_{si} \cdot \rho_w}\right] \cdot \rho_w} \tag{1}$$

where Ms_i is the initial mass of an individual component, Gs_i is the specific gravity of an individual component, and ρ_w is the density of water (1 g/cm^3). This approach yielded G_s = 1.26 for the MSW used in the study, which is similar to past studies by Karimi and Bareither (2021) and Rohlf et al. (2021).

3.2.2.3. *Compaction tests*

A series of modified Proctor compaction tests (ASTM D1557-Method C) was performed to determine a target dry unit weight of MSW and MSW-E&PW mixtures to prepare specimens for hydraulic conductivity tests. Prior to compaction, MSW was mixed thoroughly with pre-determined amounts of water and hydrated for 24 hr. Mixtures of MSW and E&PW were compacted immediately after mixing without additional hydration time. The maximum dry unit weights for compaction tests and hydraulic conductivity specimens of MSW and MSW-E&PW mixtures are shown in Fig. D2, Appendix D. The maximum dry unit weights obtained from compaction tests were used as target dry unit weights for preparing hydraulic conductivity specimens. The target dry unit weight for MSW specimen was 3.3 kN/m^3 and for the MSW-E&PW specimens with 20%, 40%, 60%, and 80% E&PW content were 4.3 kN/m^3, 5.9 kN/m^3, 8.1 kN/m^3, and 12.4 kN/m^3, respectively.

The specimens of hydraulic conductivity test were prepared with target unit weights obtained from the compaction tests. However, target unit weights for the MSW-E&PW hydraulic conductivity specimens were lower than target unit weight from compaction tests. The 20% E&PW specimen was compacted to 76% of target dry unit weight, and the ratio of specimen unit weight to modified Proctor unit weigh ($\gamma_{dc} / \gamma_{ds}$) reduced to 64%, on average, for the specimens with 40% 60%, and 80% E&PW content. The reduction in the ratio of $\gamma_{dc/} \gamma_{ds}$ was attributed to increase in E&PW content which is less compressible than MSW materials; and decrease in moisture content of specimens which reduced the compressibility of the waste materials. Details of testing procedures, results, and analysis are in Appendix D.

3.2.3. Hydraulic Conductivity Testing

3.2.3.1. *Large-Scale Permeameter*

The large-scale permeameter in this study was a 305-mm-diameter consolidation-mold permeameter, which was used to conduct hydraulic conductivity tests on MSW and MSW-E&PW mixtures. Two methods were implemented to measure hydraulic conductivity: (i) constant-headwater constant-tailwater was used to measure hydraulic conductivities > 10^{-7} m/s; and (ii) falling-headwater constant-tailwater was used to measure hydraulic conductivities < 10^{-7} m/s. Vertical stress applied to the test specimens ranged from 2 kPa to 400 kPa to capture a trend of hydraulic behavior as a function of stress ranging from daily cover (e.g., 2 kPa) to an approximately 40-m-thick landfill (e.g., 400 kPa). Hydraulic gradients employed for each loading step were in accordance with ASTM D5856.

A schematic of the hydraulic conductivity apparatus for the falling-headwater constant-tailwater test is shown in Fig. 3.2. The only difference between the falling-headwater and the constant-headwater test apparatuses was the upper reservoir. The upper reservoir was attached to an adjustable vertical trolley that allowed control on the hydraulic gradient (*i*) for different ranges of hydraulic conductivities (Table B1, Appendix B). For the falling-headwater test, the upper reservoir was a graduated cylinder with 350-mL capacity that contained sufficient water for at least one hydraulic conductivity test. For the constant-headwater test, a constant head of water was applied to specimen using an overflow reservoir. The effluent liquid was collected in a 100-mL graduated cylinder or a 5-L container based on the outflow volume. Measurements of inflow volume and outflow volume during a given hydraulic conductivity test were recorded manually. The outflow mass was measured and converted to an outflow volume assuming the density of water = 1 g/cm^3.

A pore water pressure transducer was connected to the base of the permeameter (Fig. 3.2). Pore pressure was monitored upon load application at each step to assure that any excess pore pressure generated during loading dissipated before beginning the hydraulic conductivity test. A valve also was installed at the base of the permeameter to vent entrapped air during the specimen saturation process, which helped expedite specimen saturation. The permeameters were equipped with 6.4-mm inner diameter tubing and valves to control flow. The tubing and valves permitted measurement of hydraulic conductivities as high as 10^{-3} m/s.

A 305-mm-diameter pneumatic air cylinder was used to apply vertical force, which was distributed on a test specimen via a load distribution plate. A target vertical stress was achieved on a given test specimen via feedback control between the load cell and digital pressure regulator that was controlled by MICAS-X (Original Code Consulting, Boulder, CO, USA). A proportional-integral-derivative controller (i.e., PID controller) was used to prevent overshooting the target vertical stress on a given specimen. The MICAS-X program was written in LabVIEW (National Instruments Inc., Austin, TX, USA) and all output data were recorded using data acquisition (NI USB 6002). Measurements of vertical force and vertical displacement were recorded continuously during hydraulic conductivity testing. Displacement was monitored using a 150-mm linear variable displacement transducer (Omega Engineering, Poland). Compression of each component residing between the load rod and permeameter base (i.e., load distribution plates, geocomposite drainage layers, and PVC plates) was measured without a test specimen present. Component compression was less than 1% relative to compression measured in a given test specimen, and was considered negligible in the data analysis.

The initial specimen dimensions of all hydraulic conductivity test specimens were 152-mm tall by 305-mm diameter. Solid waste was shredded such that the maximum ratio of particle diameter to specimen diameter (d_{max}/D_{max}) was less than 1:6 (ASTM D5856) for hydraulic conductivity experiments. Given the lack of a standard for measuring MSW hydraulic conductivity, several researchers have followed the 1/6 particle-to-specimen diameter ratio (e.g., Reddy et al., 2009b; Breitmeyer et al., 2019; Bareither et al., 2020). All E&PW particles larger than 20 mm were also broken into smaller particles to follow the ASTM standard as the ratio of particles size to the diameter of specimen must be less than 1/6 (ASTM D5856).

Specimens were sandwiched between two geocomposite drainage layers and included a perforated PVC plate at the top of the specimen. The geocomposites prevented clogging of the permeameter and helped establish one-dimensional flow through test specimens. The specimen height at the beginning and end of a given vertical stress application, under which hydraulic conductivity was measured, was determined to assess volume change. The duration for which stress was maintained constant to measure a given hydraulic conductivity ranged from 1 to 20 hr, and volume changes in all specimens for all stress increments were < 1%, which was deemed negligible in the data analysis.

All test specimens were subjected to a 2 kPa vertical stress for one day prior to testing, and then hydraulic conductivity was measured under eight vertical stresses: 2, 6.25, 12.5, 25, 50, 100, 200, and 400 kPa. Specimens were saturated under the 2-kPa vertical stress by passing water through the specimens from the bottom-up to push air out. Specimens in as-received and wet conditions were prepared in loose conditions (not compacted) to compare their hydraulic behavior with changing stress and unit weight.

3.2.3.2. *Small-Scale Permeameter*

Hydraulic conductivity of E&PW was measured in a conventional rigid-wall permeameter, which contained specimens with dimensions of 102-mm diameter by 51-mm tall. The falling-headwater constant-tailwater method was used in an up-flow condition. The small-scale test provided the ability to measure hydraulic conductivity of E&PW at a higher stress and unit weight relative to the stress and unit weight of the large-scale specimen.

Similar termination criteria for small-scale and large-scale hydraulic conductivity tests were implemented. For hydraulic conductivity tests with $k_s > 1\times10^{-10}$ m/s, the ratio of Q_{out} to Q_{in} ranged between 0.9 to 1.1 while three or more consecutive k_s measurements were within ±25% of the mean. For hydraulic conductivity tests with $k_s < 1\times10^{-10}$ m/s, the ratio of Q_{out} to Q_{in} ranged between 0.75 to 1.25 while three or more consecutive k_s measurements were within ±50% of the mean (Daniel 1994; ASTM D5856).

3.3. Results

3.3.1. Water Content and Unit Weight

A summary of MSW and E&PW mixture ratios, initial dry weight water content, initial wet weight water content, and initial dry unit weight of the hydraulic conductivity specimens is in Table 3.2. The initial dry weight water content of MSW was 30%, on average, which is typical of incoming waste in US landfills (Tolaymat et al., 2013). The volatile solid content was 72%, on average, which is representative of fresh MSW.

The E&PW had a water content of 18%, on average, and was relatively dry. The addition of as-received E&PW to MSW resulted in a gradual reduction in the water content of MSW-E&PW mixtures (Fig. C6, Appendix C). However, mixing wet E&PW with MSW led to an increase in water content with increasing E&PW content due to the higher initial water content of wet E&PW (Fig. C6, Appendix C). The dry unit weight of the MWS-E&PW mixtures increased as the ratio of E&PW content increased due to the higher specific gravity of E&PW relative to MSW (Fig. C7).

3.3.2. Hydraulic Conductivity of Municipal Solid Waste

A compilation of hydraulic conductivity versus vertical stress and dry unit weight for MSW is shown in Fig. 3.3. The compilation includes relevant laboratory-scale studies and data from the current study. Details of each experiment, including experimental method, waste composition, vertical stress, dry unit weight, void ratio, and hydraulic conductivity are in Table 3.3. In general, the measured hydraulic conductivity of MSW agrees with k_s reported from previous studies. The hydraulic conductivity of fresh shredded MSW in the current study reduced from 4.4×10^{-5} m/s to 7.7×10^{-7} m/s as vertical stress increased from 2 kPa to 200 kPa. Hydraulic conductivity subsequently stabilized near 7×10^{-7} m/s with increasing vertical stress to 400 kPa. The approximately constant k_s between 200 kPa and 400 kPa was attributed to limited change in the dry unit weight of the MSW specimen after reaching 200 kPa. The compressible materials were sufficiently compacted at 200 kPa, after which the MSW specimen resisted compression.

Stress, dry unit weight, waste composition, and particle size are the main factors that influence hydraulic conductivity of fresh MSW. An increase in vertical stress compresses and reshapes waste particles, which reduces waste volume and increases unit weight. The reduction in waste volume primarily develops from reduced void volume, which decreased hydraulic conductivity due to a decrease in void spaces and available flow paths. The magnitude of reduction in hydraulic conductivity depends on waste composition and particle size. For instance, if MSW contains soil-like materials or small particles, these particles can occupy void spaces between the larger MSW particles and contribute to a more reduction in hydraulic conductivity with increased vertical stress.

The relationship between void ratio and vertical stress for the MSW hydraulic conductivity specimen is shown in Fig. 3.4. Approximately 80% of the total void ratio reduction occurred as the vertical stress increased from 2 kPa to 200 kPa, and the subsequent increase in vertical stress to 400 kPa only contributed a 20% reduction in the void ratio. The nearly constant hydraulic conductivity between 200 and 400 kPa suggests that the decrease in void ratio from 1.4 to approximately 1.0 did not considerably reduce the distribution or size of void spaces within the specimen. The data compiled in Fig. 3.3a show similar behavior, whereby the rate of decrease in hydraulic conductivity with increasing stress is higher for vertical stress less than approximately 200 kPa. Reddy et al. (2019) reported that k_s stabilized when vertical stress exceeded approximately 150 kPa. There appears to be a change in MSW compression that contributes to a reduction in hydraulic conductivity such that when MSW compresses adequately, the non-compressible or less-compressible materials resist compression and subsequent increasing stress has limited effect on hydraulic conductivity.

The relationship between hydraulic conductivity and dry unit weight in Fig. 3.3 indicates that as MSW dry unit weight increases, hydraulic conductivity decreases. Data from Breitmeyer et al. (2019) in Fig. 3.3 include two hydraulic conductivity tests on shredded MSW compacted with different energies (i.e., normally compacted and highly compacted). The shredded MSW specimens had initial dry unit weights of 6.4 kN/m^3 and 7.9 kN/m^3, which resulted in a two-order of magnitude difference in k_s (i.e., 1.1×10^{-5} m/s and 4.5×10^{-7} m/s) (Fig. 3.3b) for the initial specimens tested under negligible vertical stress. Feng et al. (2016) also reported an increase in MSW dry unit weight with higher compaction energy (i.e., 3.1 kN/m^3 to 4.8 kN/m^3) that produced a nearly two-order of magnitude decrease in k_s from 8.0×10^{-3} m/s to 5.5×10^{-5} m/s (Fig. 3.3b).

The magnitude of reduction in k_s due to an increase in stress or dry unit weight is a function of MSW particle size and composition. The hydraulic conductivity test conducted by Breitmeyer et al. (2019) on unshredded MSW yielded a two to three order-of-magnitude higher k_s than shredded MSW (Fig. 3.3b). Unshredded MSW has larger particles that create larger pore spaces, whereas shredded MSW and soil-like materials (i.e., particles < 25 mm diameter) can constrict available flow paths and reduce hydraulic conductivity. In addition, the presence of soil-like materials in MSW has a pronounced impact on MSW hydraulic conductivity at stress > 200 kPa (Powrie et al., 2005). Soil-like particles occupy the void spaces contribute to a reduction in MSW hydraulic conductivity.

Zhang et al. (2018) measured the k_s of the synthetic MSW consisted 61.5% food waste. The k_s ranged between 1.9×10^{-4} m/s to 8×10^{-7} m/s, which is on the upper range of k_s results (Fig. 3.3). The moisture from food waste affects the compaction of waste via hydrating the other waste components. However, food waste is inherently a permeable material and led to an increase in hydraulic conductivity. The solid waste composition can vary in landfills based on the incoming waste stream, landfill operation, and geographical location. For instance, Machado et al. (2010) reported the hydraulic conductivities for fresh landfilled wastes that varied by two orders of magnitude under similar vertical stress. The variation in k_s is attributed to the waste heterogeneity in the landfill.

The influence of stress level, dry unit weight, particle size and composition on k_s of fresh MSW were evaluated. The hydraulic conductivity is mainly a function of stress and dry unit weight, and then particle size. The influence of stress and particle size on k_s depends on composition of MSW. The results of hydraulic conductivity test in the current study are in the upper range of compiled data since the initial the dry unit weight of MSW specimen was low compared to other MSW specimens. Also, the specimen prepared in the current study did not include any soil or soli-like materials. The lack of these materials constrained the impact of increasing vertical stress on dry unit weight and k_s (Fig. 3.3a). The details of the MSW hydraulic conductivity test, including method, dry unit weight, effective vertical stress, void ratio, hydraulic conductivity are in Table E1. and Fig. E3 (Appendix E).

3.3.3. Hydraulic Conductivity of Oil and Gas Exploration & Production Waste

Relationships of hydraulic conductivity versus effective vertical stress and dry unit weight for the as-received E&PW and wet E&PW are shown in Figs. 3.6a and 3.6b. The data sets in Fig. 3.5 include two large-scale permeameter tests (i.e., 305-mm diameter) that were conducted on the as-received E&PW and wet E&PW, as well as a small-scale permeameter test (i.e., 102-mm diameter) on the as-received E&PW. The large-scale test specimens were prepared via loose placement and modest hand compaction, whereas the small-scale specimen was prepared via impact compaction with a tamping rod. The difference in specimen preparation and initial moisture content of the three test specimens contribute to the different trends of hydraulic conductivity versus vertical stress or dry unit weight.

Hydraulic conductivity of the as-received E&PW measured in the large-scale permeameter decreased from 7.3×10^{-5} m/s to 1.1×10^{-8} m/s with an increase in vertical stress from 1 kPa to 400 kPa. Although k_s of the small-scale E&PW specimen appear orders-of-magnitude lower relative to the large-scale specimen as a function of vertical stress, the data overlap perfectly when evaluating k_s as a function of dry unit weight. The initial dry unit weight of the small-scale, as-received E&PW specimen was 15.4 kN/m^3, which was considerably denser than the initial dry unit weight of 11.5 kN/m^3 for the large-scale specimen. The k_s of as-received E&PW under 1.2 kPa effective stress in small-scale test and under 200 kPa effective stress in the large-scale test were 1×10^{-7} m/s and both specimens had similar dry unit weights (Fig. 3.5b). This indicated similar response of small-scale and large-scale specimens to hydraulic conductivity regarding the dry unit weight. The k_s reduced to 1×10^{-9} m/s with increasing stress to 50 kPa, and then k_s stabilized at 7.5×10^{-10} m/s following increasing effective stress to 400 kPa. The changes in hydraulic conductivity as a function of dry unit weight for small-scale, as-received E&PW specimen were not recorded.

The effects of E&PW hydration can be observed in the wet E&PW specimen regarding the initial achieved dry unit weight and trend of k_s versus dry unit weight. The initial dry unit weight of the wet E&PW specimen was approximately 14 kN/m^3, and k_s measured on this initial specimen was, which agreed favorably with trend of k_s versus dry unit weight for the as-received E&PW specimen (Fig. 3.5b). However, k_s of the wet E&PW specimen reduced two orders of magnitude (6.6×10^{-6} m/s to 5.4×10^{-9} m/s) as the effective vertical stress increased to 17 kPa effective stress and dry unit weight increased to 15 kN/m^3. Subsequently, k_s of the wet E&PW decreased only one order of magnitude as vertical effective stress increased from 17 kPa to 389 kPa (i.e., k_s = 2.8×10^{-10} m/s under 389 kPa).

Trends of void ratio versus hydraulic conductivity for the as-received and wet E&PW measured in the large-scale permeameters are shown in Fig. 3.6. In both trends, a pronounced reduction in k_s was observed when the specimen void ratios were approximately 0.8 and hydraulic conductivity was on the order of 1×10^{-5} m/s. The pronounced change is indicative of change in flow mechanism and can be explained by clay clod theory and specimen remolding (Benson and Daniel. 1990). The reduction in k_s observed as void ratio decreased below 0.8 was attributed to the elimination of macropores that transmitted the flow. The increase in vertical stress compressed the E&PW specimens, which collapsed the macropores and transitioned flow to occur through a more microporous structure that consisted of smaller and more tortuous pathways. The more pronounced reduction in k_s for the wet E&PW at a void ratio of 0.8 was attributed to a wetter, softer specimen that was more remoldable. Even though the both E&PW specimens were completely saturated during hydraulic conductivity testing, the more rigid initial soil fabric of the as-received E&PW specimen consistently yielded higher k_s for a given void ratio < 0.8 related to the wet E&PW specimen.

3.3.4. Influence of addition of E&PW to MSW on Hydraulic Conductivity

Relationships of hydraulic conductivity versus vertical effective stress for the MSW, E&PW, and mixtures of as-received E&PW with MSW and wet E&PW with MSW are shown in Fig. 3.7. The vertical effective stress was calculated at the mid-depth of each specimen at the beginning of a hydraulic conductivity test for each stress increment. The data compiled in Fig. 3.7 are separated into mixtures with as-received E&PW (Fig. 3.7a) and mixtures with wet E&PW (Fig. 3.7b) to enhance clarity in visualizing all data points. The overall trends for all E&PW mixture ratios for both the as-received and wet E&PW are the same, and exhibit a decrease in hydraulic conductivity with increasing vertical effective stress. Hydraulic conductivity for MSW-E&PW

mixtures with 20% and 40% E&PW contents reduced from 3×10^{-5} m/s to 1×10^{-7} m/s under effective vertical stress ranged from 0 to 400 kPa. An increase in the mixture ratio above 60% resulted in an additional order-of-magnitude decrease in k_s to 1×10^{-8} m/s as vertical effective stress increased above 200 kPa. The lowest k_s at each stress level was measured for MSW mixed with 80% wet E&PW.

The hydraulic conductivity measured on all MSW-E&PW mixtures with different mixture ratios (i.e., 20% to 80% E&PW content) were approximately similar under 2 kPa vertical stress, and were within the same order of magnitude as the pure MSW and pure E&PW. The ranges of hydraulic conductivity for the mixed MSW-E&PW were relatively constant when comparing the as received E&PW and wet E&PW. For example, the k_s of MSW + 60% E&PW under 100 kPa was 4.8×10^{-6} m/s for both as-received and wet E&PW mixtures. However, a notable decrease in hydraulic conductivity between the as-received E&PW and wet E&PW was observed for the 80% E&PW mixtures (Fig. 3.7a and 3.8b). The k_s of MSW + 80% as-received E&PW specimen was 1×10^{-5} m/s under 100 kPa effective stress, whereas when MSW mixed with 80% wet E&PW, k_s decreased to 2.9×10^{-6} m/s. This decrease in k_s agrees with the lower k_s measured on wet E&PW relative to the as-received E&PW discussed previously (Figs. 3.6 and 3.7).

An additional comparison of the as-received and wet E&PW mixtures with MSW is shown in Fig. 3.8 as relationships between hydraulic conductivity and dry unit weight. All data sets exhibit trends of decreasing hydraulic conductivity with increasing dry unit weight. In addition, increasing the E&PW content from 20% to 80% increased the initial dry unit weight of MSW-E&PW specimens from approximately 3.2 kN/m^3 to 8.2 kN/m^3 for specimens under 2 kPa vertical stress. Negligible differences in the trends of k_s as a function of dry unit weight were observed between the as-received and wet E&PW mixtures for 20% and 40% E&PW contents. At these lower E&PW contents, the MSW constituted the majority of the specimens volume, and the E&PW predominantly occupied available void spaces between MSW particles. Although the range of k_s measured for the as-received and wet E&PW mixtures prepared with 60% and 80% E&PW were comparable, there was a notable difference in the wet E&PW mixtures yielding lower k_s for a given dry unit weight (Fig. 3.8). This observation is similar to that for pure E&PW (Fig. 3.5).

The coupled influence of E&PW content and vertical stress on hydraulic conductivity of MSW is shown in Fig. 3.9. The open and closed symbols in Fig. 3.9 are representative of MSW mixed with as-received E&PW and MSW mixed with wet E&PW, respectively. The increasing symbol size in Fig. 3.9 corresponds to increasing vertical stress from 2 kPa to 400 kPa. The breadth of the measured k_s for vertical stress ranging from 2 to 400 kPa increased with increasing E&PW content. The largest amount of variation in k_s was observed for pure E&PW. Increasing vertical stress from 2 kPa to 400 kPa reduced k_s of MSW from 4.4×10^{-5} m/s to 6.6×10^{-7} m/s, whereas k_s of pure E&PW reduced five orders of magnitude (i.e., from 7.3×10^{-5} to 2.8×10^{-10} m/s).

Municipal solid waste particles create a porous structure in which approximately 40% of the structure (in this study) consisted of non-compressible or less-compressible waste materials that resist compression. Then, while stress is increasing, the MSW matrix provides void areas that the E&PW particles can remain between the solid waste particles. The non-compressible waste materials do not let the E&PW significantly contribute to the flow mechanism. Hence, the structure of waste mass still maintains the flow paths to convey the flow, and the hydraulic behavior of MSW-E&P waste mixtures is controlled by MSW.

3.4. Discussion

Hydraulic conductivity measured for the MSW-E&PW mixtures prepared with as-received or wet E&PW were similar for mixture ratios of 20%, 40%, and 60% under effective vertical stress up to 400 kPa. Hydraulic conductivity of MSW-E&PW mixtures with 80% as-received or wet E&PW content and under 0 to 50 kPa vertical effective stress were also similar (Fig. 3.9). However, the difference between k_s of MSW + as-received E&PW and MSW + wet E&PW became one order of magnitude where effective stress went above 50 kPa. In summary, the results indicated that regardless of increasing E&PW content and dry unit weights, the hydraulic behavior of MSW-E&PW mixtures did not change substantially.

The justification for evaluating the hydraulic behavior of wet E&PW mixed with MSW was to simulate a potentially critical situation where E&PW that just passes a paint filter test is disposed in an MSW landfill. The hypothesis was that mixing wet E&PW with MSW decreased k_s relative to mixtures of as-received E&PW with MSW. However, the variation in k_s between the as-received and wet E&PW mixtures was minor, which was primarily attributed to having relatively similar mass of solid of E&PW. E&PW solid particles are more impactful in changing MSW hydraulic conductivity rather than the initial water content of E&PW. Solid particles of E&PW can occupy the voids of the waste matrix and narrow the flow path, and subsequently reduce the k_s. However, since the difference in mass of solid of E&PW in MSW + as-received E&PW and MSW + wet E&PW was negligible (i.e., 50 gr), therefore, they have similar response to hydraulic conductivity tests.

The hydraulic conductivity of E&PW is a function of dry unit weight as well as void ratio. The flow mechanism in E&PW changed as void ratio was near 0.8, and dry unit weight exceeded approximately 14 kN/m^3 (Fig. 3.5b and Fig. 3.6). This change in hydraulic conductivity of E&PW is hypothesized to be due to a shift from macropore to micropore flow. The dry unit weight of E&PW (and void ratio) is a function of compaction energy used to achieve the initial unit weight, water content, and vertical stress. For example, the small-scale, E&PW specimen prepared at the as-received water content was compacted to an initial dry unit weight of 15.4 kN/m^3, which yielded $k_s = 1\times10^{-7}$ m/s under 1 kPa effective stress. The large-scale, E&PW specimen prepared at the as-received water content as prepared loose (i.e., not compacted) at an initial dry unit weight of 11.5 kN/m^3 and yielded a $k_s = 1\times10^{-7}$ m/s at a vertical effective stress of 200 kPa, whereat the specimen reached a dry unit weight of approximately 15.4 kN/m^3. Furthermore, the large-scale, wet E&PW specimen prepared loose (initial dry unit weight of 14 kN/m^3) reached $k_s = 1\times10^{-7}$ m/s at a vertical stress = 3 kPa. These comparisons indicate that the initial dry unit weight and initial water content of E&PW bound the range over which k_s can vary as a function of vertical effective stress.

The composition of HMWs that can be disposed with MSW varies, which can lead to different hydraulic behavior for MSW-HMW mixtures. A summary of geotechnical properties of different HMWs is in Table C1 (Appendix C). Koenig et al. (1996), O'Kelly (2005), and Suthagaran et al. (2010) measured the hydraulic conductivity of municipal sewage sludge, biosolids, and dewatered wastewater sludge, and the results were 1×10^{-12} m/s, 1×10^{-9} m/s, and 1×10^{-7} m/s, respectively. Bareither et al. (2020) reported hydraulic conductivity of an exploration and production waste from the oil and gas industry to be on the order of 1×10^{-11} to 1×10^{-12} m/s for vertical stress between 50 and 100 kPa. The variation in hydraulic conductivity for different waste materials is mainly due to the composition. Hence, HMW composition is a key factor influencing the hydraulic conductivity of MSW-HMW mixtures.

Bareither et al. (2020) evaluated the influence of the addition of HMW from the oil and gas industry to MSW o hydraulic and mechanical behavior. A comparison of hydraulic conductivity versus vertical stress for MSW tested by Bareither et al. (2020) and in this study is shown in Fig. 3.10. The k_s from both studies were comparable and decreased from 1×10^{-5} m/s to 1×10^{-6} m/s with an increase in vertical stress from 50 kPa to 200 kPa. This similarity in MSW k_s provides a common basis for comparing the influence of HMW composition on k_s of MSW-HMW mixtures.

Relationships of hydraulic conductivity versus amount of HMW in MSW-HMW mixtures are shown in Fig. 3.11 that include data from the wet E&PW in this study and data from Bareither et al. (2020). The wet E&PW was used for comparison because the HMW tested by Bareither et al. (2020) was also an E&PW from the oil and gas industry that was tested at a high water content. Data in Fig. 3.11 are separated into three plots that correspond to low (50 kPa), medium (100 kPa), and high (200 kPa) vertical stress. Dashed lines have been added to the plots to identify the general trends and identify a threshold HMW content whereupon there is a pronounced decrease in the hydraulic conductivity of the HMW-MSW mixture. Findings from Bareither et al.

(2020) indicate that increasing vertical stress reduced the mixture ratio threshold of their MSW-HMW mixtures from approximately 75% at 50 kPa to 60% at 100 kPa and finally to 40% at 200 kPa. In contrast, the mixture ratio threshold in the current study was 80% for all three levels of stress evaluated.

In the current study, an approximately two to three order-of-magnitude decrease in k_s was observed between all of the MSW-HMW mixtures ratios and the pure E&PW (Fig. 3.11). The k_s of the HMW tested by Bareither et al. (2020) reduced from 1×10^{-11} m/s at 50 kPa vertical stress to a non-measurable value under 200 kPa. Although the hydraulic properties of the E&PW tested in the current study was considerably different from the E&PW tested by Bareither et al. (2020), a similar mechanism corresponding to a transition from macropore flow in MSW to micropore flow in HMW was hypothesized to control the position of the threshold HMW content (Bareither et al. 2020). As vertical stress increased, macropores within the waste mass were eliminated, which transferred flow through HMW fraction of waste.

Table 3.1. Summary of waste composition.

Composition	Component	Percentage (%)
Paper	Newsprint	1.7
	Office Paper	0.8
	Magazines	0.4
	Corrugated Containers	2.2
	Other Paper	11.6
Metals	Aluminum Cans	0.4
	Steel Cans	0.4
	Other Metals	6
Plastics	Rigid	11.3
	Soft	7.6
Glass	Glass Containers and Other Glass	5.4
Other Wastes	Rubber and Leather	4.2
	Textiles	8.2
	Food Waste	22.6
	Yard Waste	8.7
	Wood	8.5
Total		100

Table 3.2. A summary of MSW-E&PW, MSW-Wet E&PW mixture ratios, initial dry weight water content, initial wet weight water content, and initial dry unit weight of specimens for hydraulic conductivity tests.

Specimen	Initial Dry Weight Water Content (%)	Initial Wet Weight Water Content (%)	Initial Dry Unit Weight (kN/m^3)
MSW*	29.6	22.8	3.3
80% MSW + 20% E&PW	28.4	22.1	3.2
80% MSW + 20% wet E&PW	36.9	27.0	3.0
60% MSW + 40% E&PW	31.0	23.7	3.7
60% MSW + 40% wet E&PW	38.0	27.6	3.5
40% MSW + 60% E&PW	22.0	18.0	5.1
40% MSW + 60% wet E&PW	37.2	27.1	4.6
20% MSW + 80% E&PW	21.4	17.7	7.6
20% MSW + 80% wet E&PW	34.6	25.7	8.3
As-received E&PW	18.9	15.9	11.5
Wet E&PW	35.8	26.3	13.2

*MSW= Municipal Solid Waste
**E&PW= Exploration and production waste

Table 3.3. Summary of hydraulic conductivity tests on fresh municipal solid waste, including method, specimen composition, vertical stress, dry unit weight, void ratio, saturated hydraulic conductivity, and description.

Source	Method	Specimen	Vertical stress (kPa)	Dry unit weight (kN/m^3)	Void ratio	Hydraulic conductivity (m/s)	Description
Reddy et al. 2009b	Rigid-wall permeameter, Constant head	Shredded fresh MSW	0 - 276	4.06 -13.43	-	1.8×10^{-3} -4.9×10^{-5}	D[a]= 300 mm
Machado et al. 2010	Triaxial cell	Fresh MSW: paper, cardboard, plastic, rubber, metal, wood, glass, ceramic materials, stone, textile, and paste fraction.	10 - 300	-	-	3.4×10^{-5} -4.1×10^{-8}	D= 400 mm; 50% of particles were smaller than 30 mm
Feng et al. 2016	Rigid-wall	5% metal and glass; 19% plastic; 23% paper, wood, and fiber; 22% organic matter; 31% waste residue	-	3.08 - 4.84	-	8.0×10^{-3} - 5.5×10^{-5}	D= 400mm; samples from 4-m depth, 0.3 yr old; Use leachate as a permeant
Zhang et al. 2018	Constant head	Fresh synthetic shredded MSW	0 - 300	3 - 5.9	-	1.9×10^{-4} - 8.0×10^{-7}	D= 150 mm
Breitmeyer et al. 2019	Rigid wall permeameter, Falling head	Fresh MSW from working face of landfill, shredded	0 - 400	6.4 – 10.1	1.04 - 0.3	1.1×10^{-3} - 4.6×10^{-7}	D= 150 mm; Specimen compacted using Standard Proctor[b]
				7.9 - 11	0.66 - 0.19	4.5×10^{-5} – 3.0×10^{-7}	D= 150 mm; Specimen compacted using modified Proctor[c]
	Rigid wall permeameter, Constant head	Fresh MSW from working face of landfill	-	5.2 - 8.8	1.53 - 0.49	7.7×10^{-1} - 6.8×10^{-4}	D= 305 mm
Karimi 2021, (Current study)	Consolidation-mold permeameter	Fresh MSW	0 - 400	3.3 – 6.1	2.7 - 1.04	4.4×10^{-3} - 6.6×10^{-5}	D= 305 mm

a: D= Diameter of specimen
b & c: ASTM D698 and ASTM D1557

Fig. 3.1. Photograph of (a) Oil and gas Exploration and Production waste (E&PW) obtained from a landfill (b) E&PW mixed with water to a water content that E&PW passes the paint filter test.

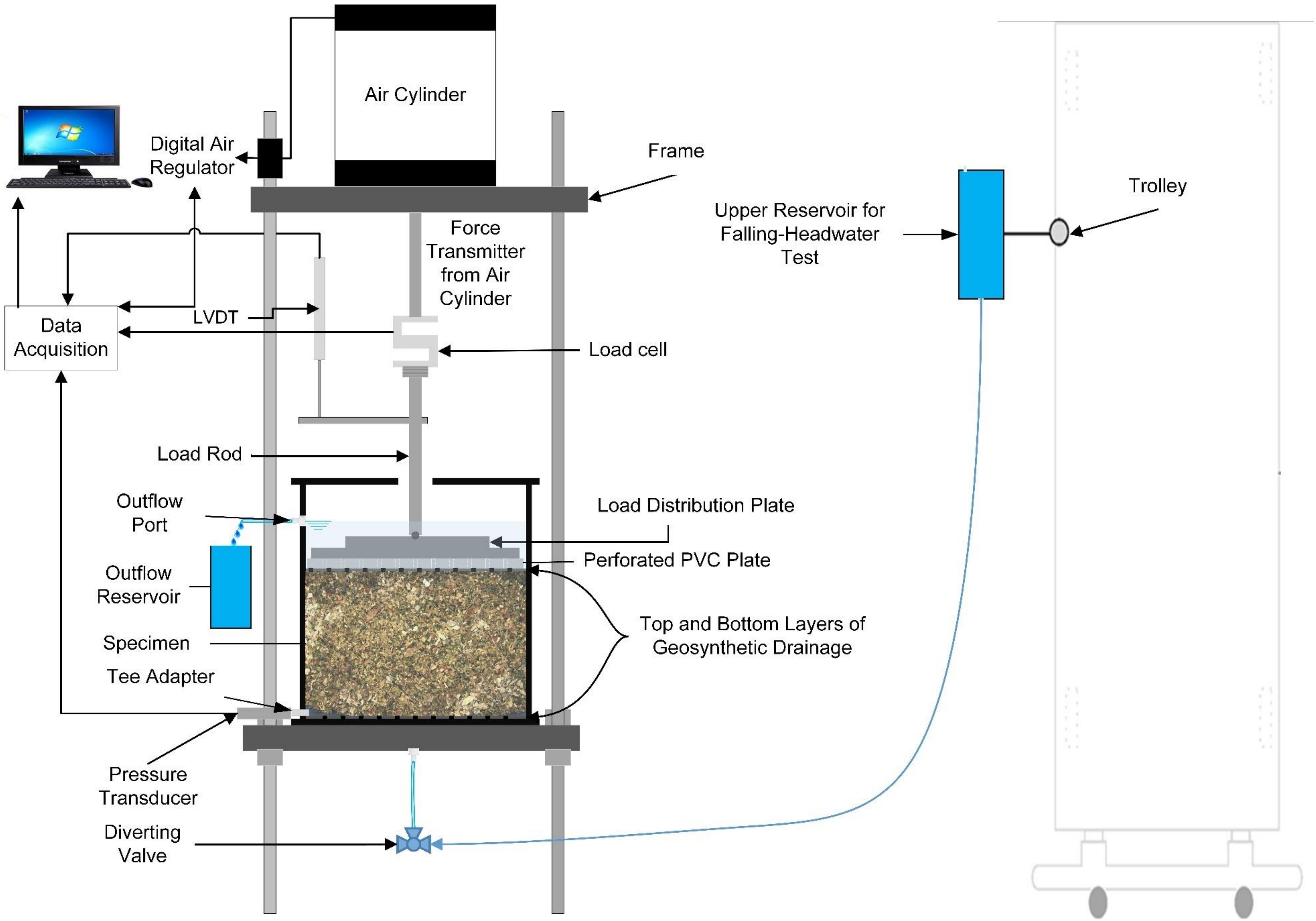

Fig. 3.2. Schematics of 305-mm-diameter compaction-mold permeameter used in this study.

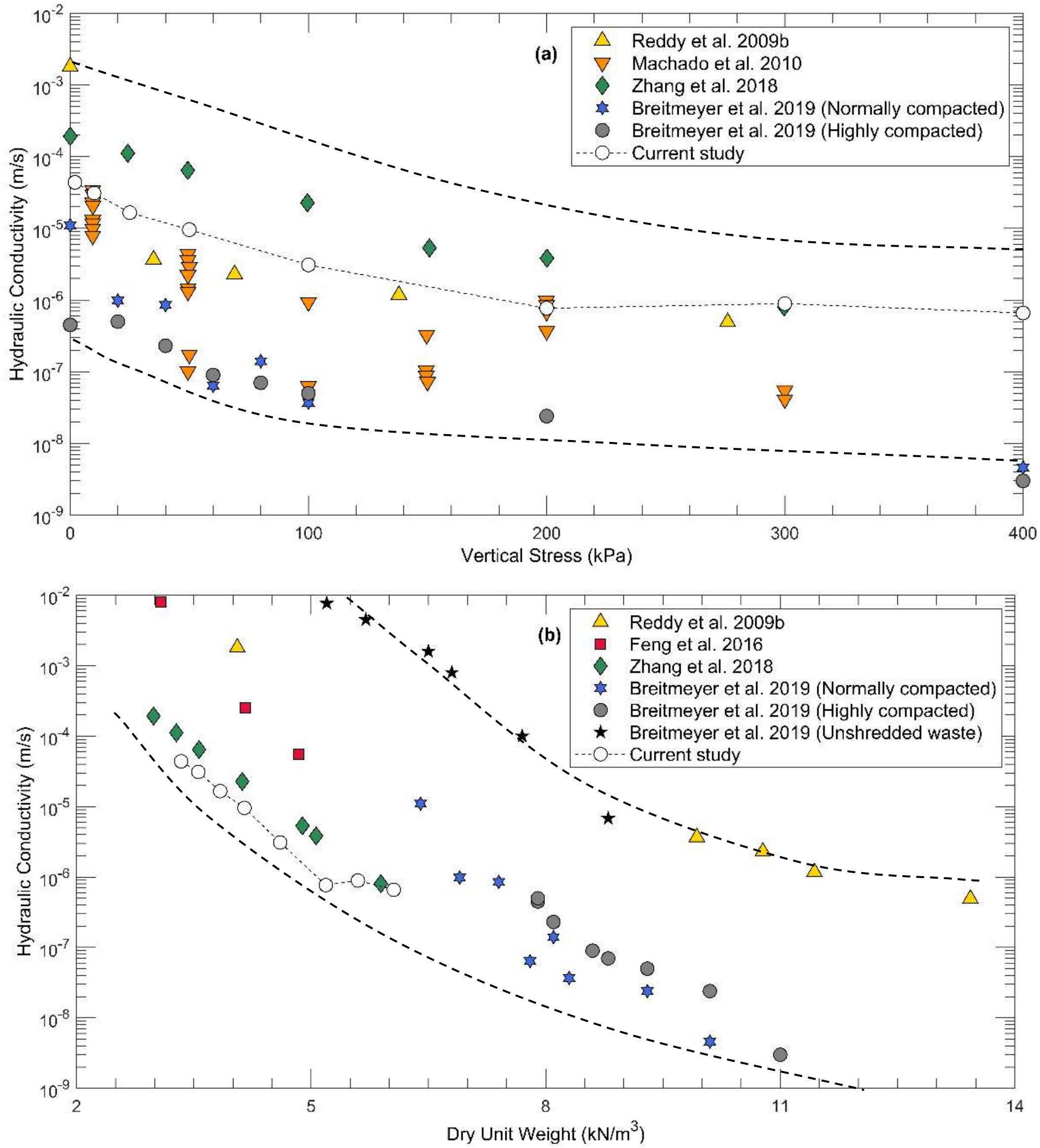

Fig. 3.3. A summary of studies regarding the effect of increasing (a) vertical stress and (b) dry unit weight on saturated hydraulic conductivity of fresh municipal solid waste (MSW)

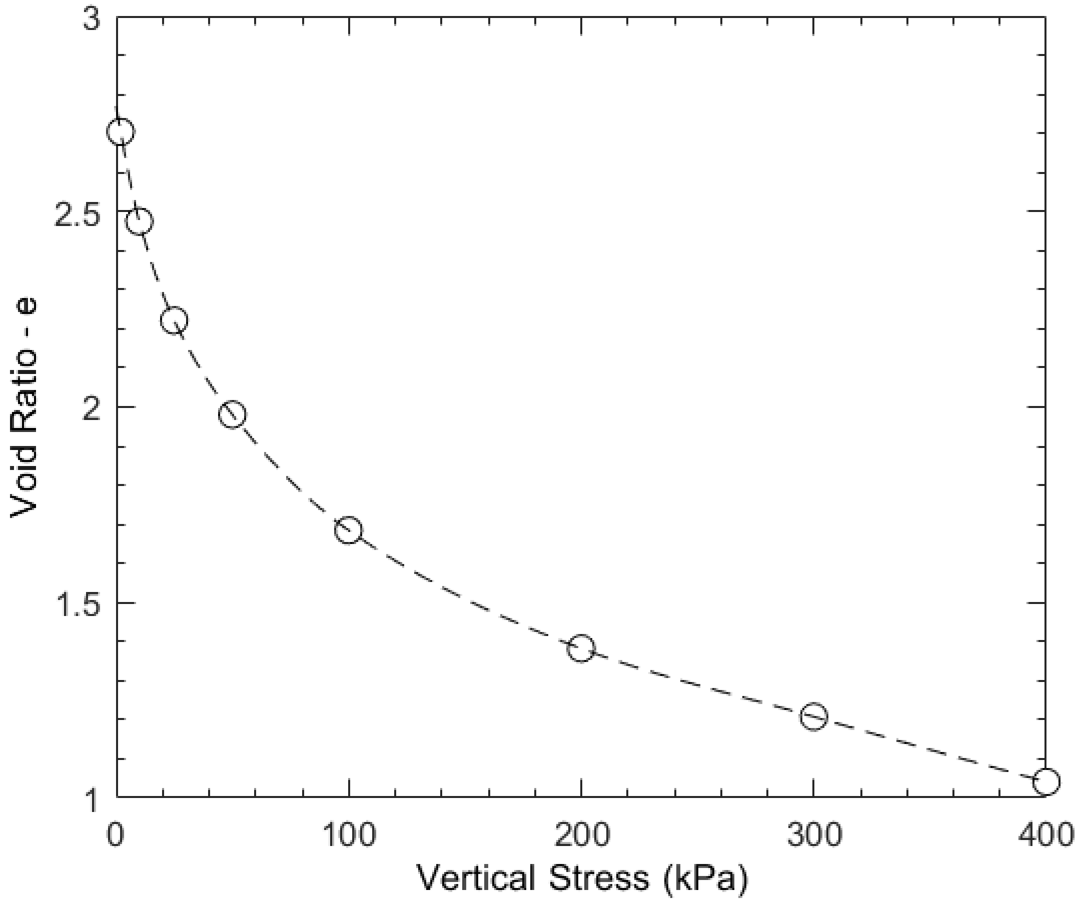

Fig. 3.4. Relationship of vertical stress versus void ratio for fresh municipal solid waste.

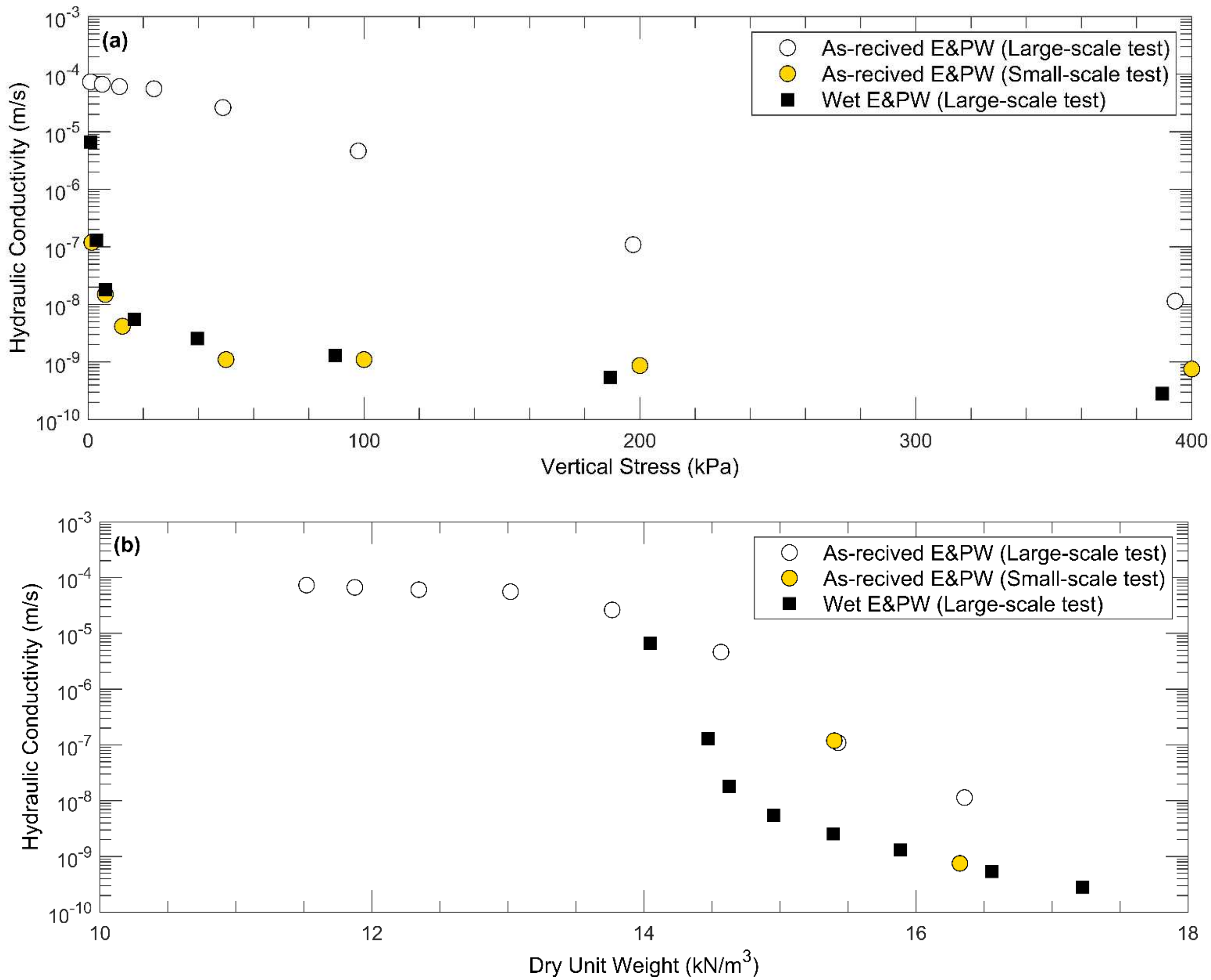

Fig. 3.5. Hydraulic conductivity versus (a) verticals stress and (b) dry unit weight for Exploration and Production waste (E&PW) in as-received and wet condition. As-received E&PW hydraulic conductivity tests were conducted in 102-mm-diameter (small-scale) and 305-mm-diameter (large-scale) permeameters.

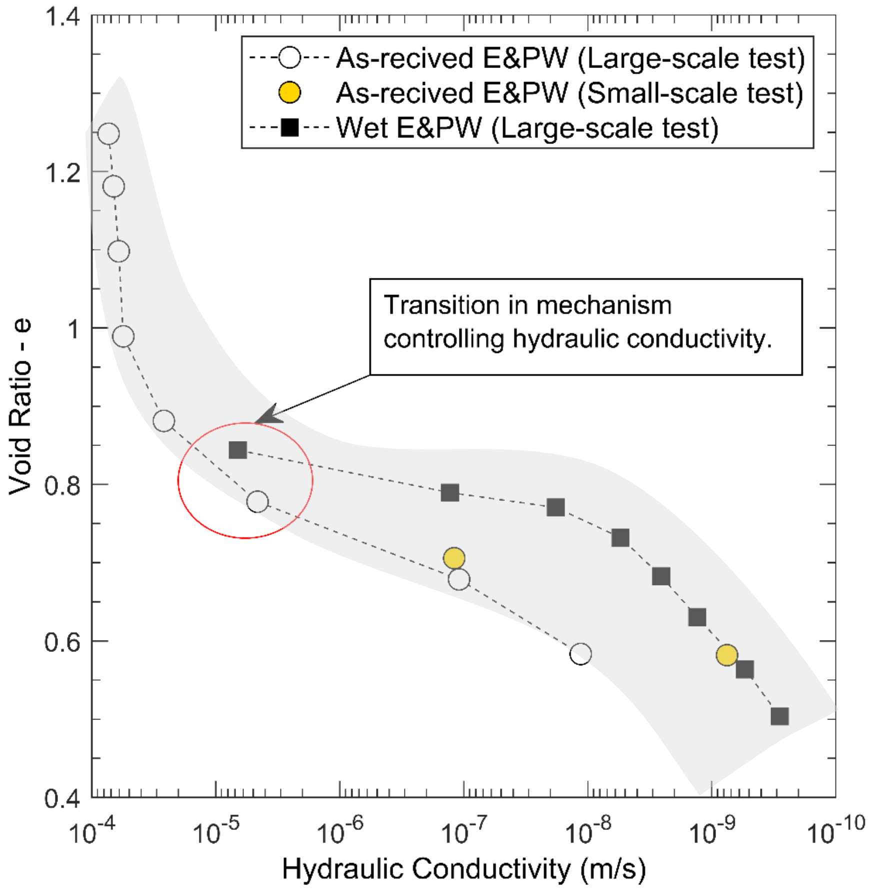

Fig. 3.6. Hydraulic conductivity versus void ratio for the as-received and wet Exploration and Production waste (E&PW) measured in large-scale test. Shaded area represents the changes in hydraulic conductivity with void ratio.

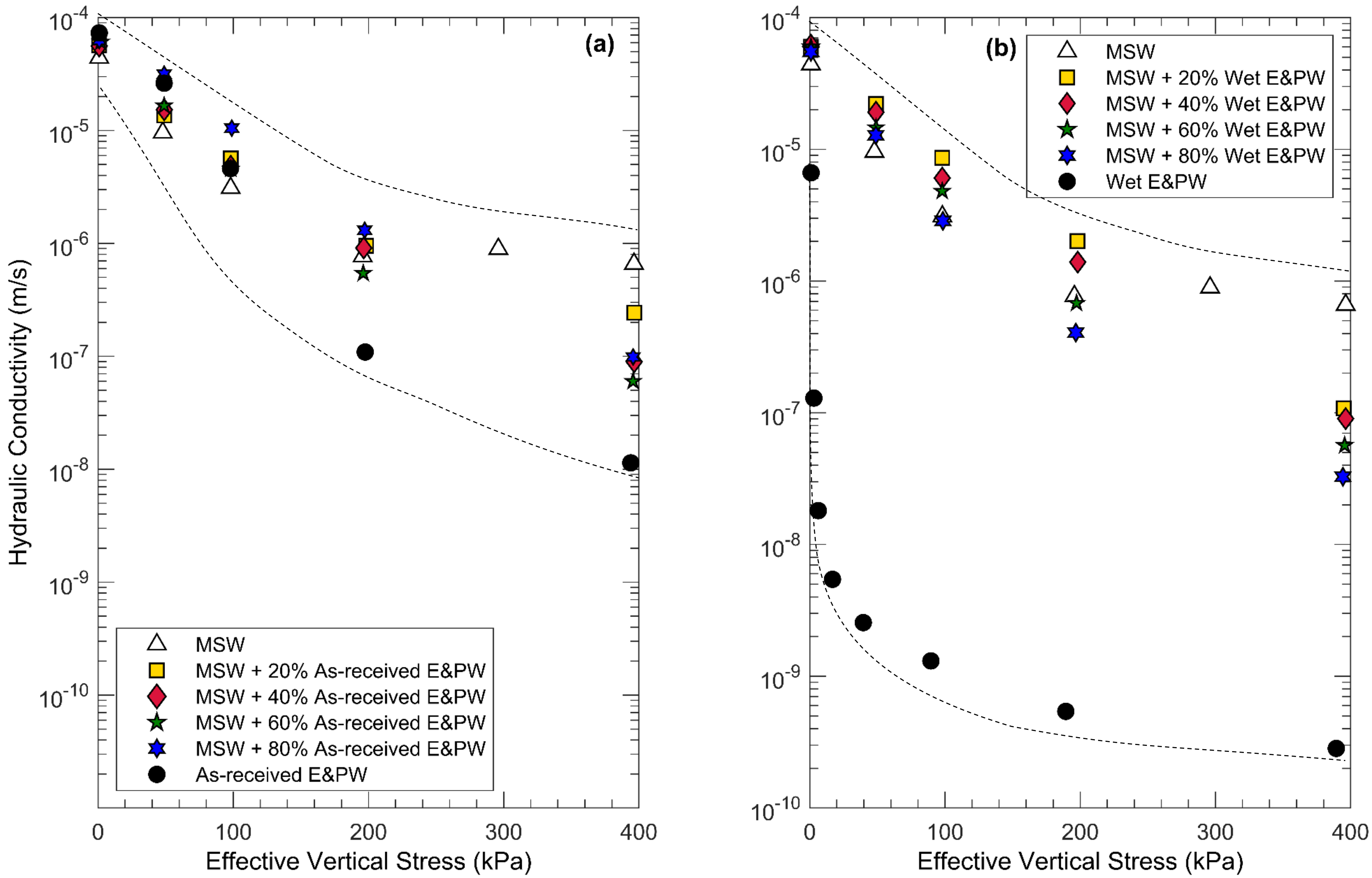

Fig. 3.7. Hydraulic conductivity versus effective vertical stress for the mixtures of MSW and as-received E&PW or MSW and wet E&PW under 1 kPa, 50 kPa, 100 kPa, 200 kPa, and 400 kPa effective vertical stress.

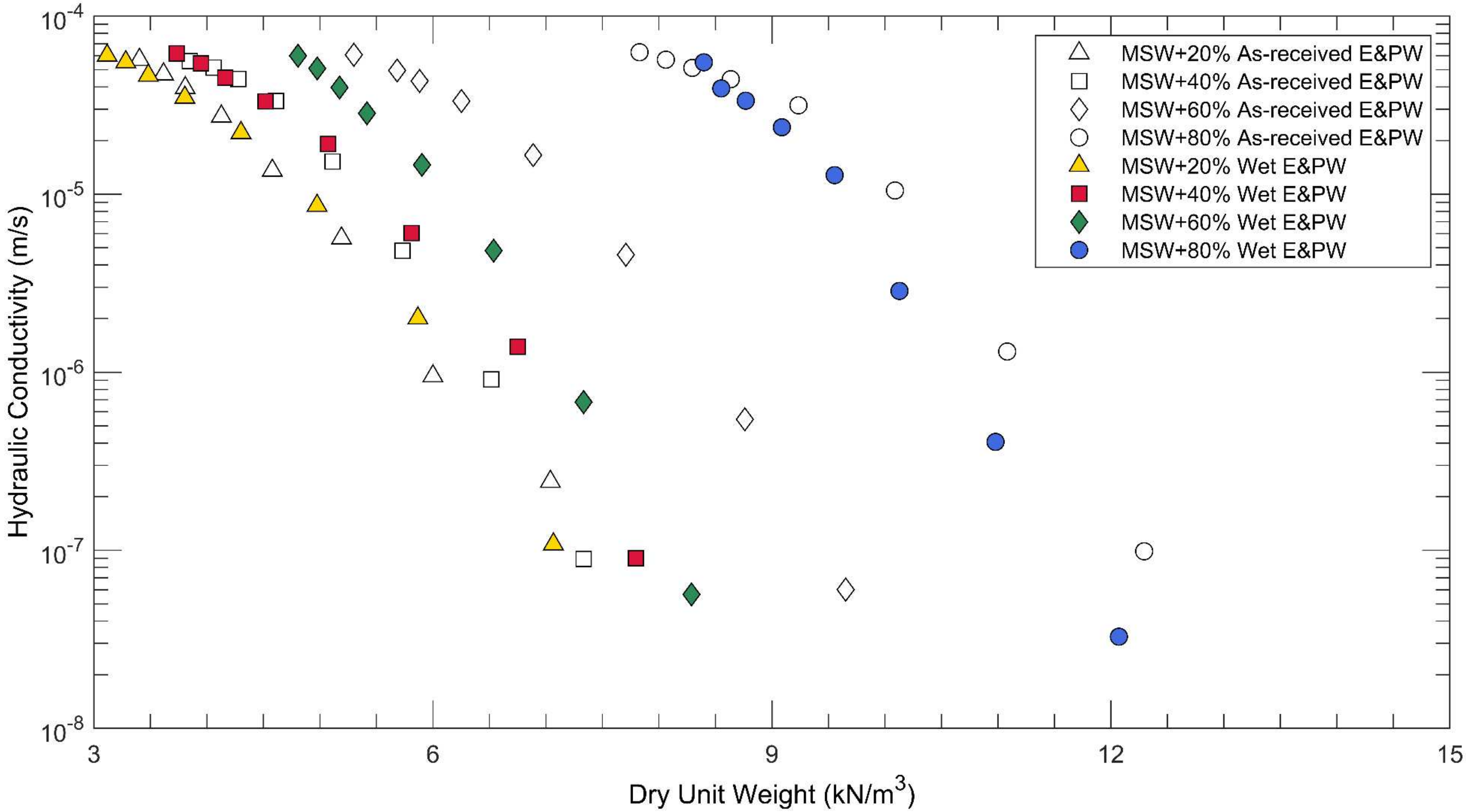

Fig. 3.8. Hydraulic conductivity versus dry unit weight for the mixtures of MSW and as-received E&PW and the mixtures of MSW and wet E&PW

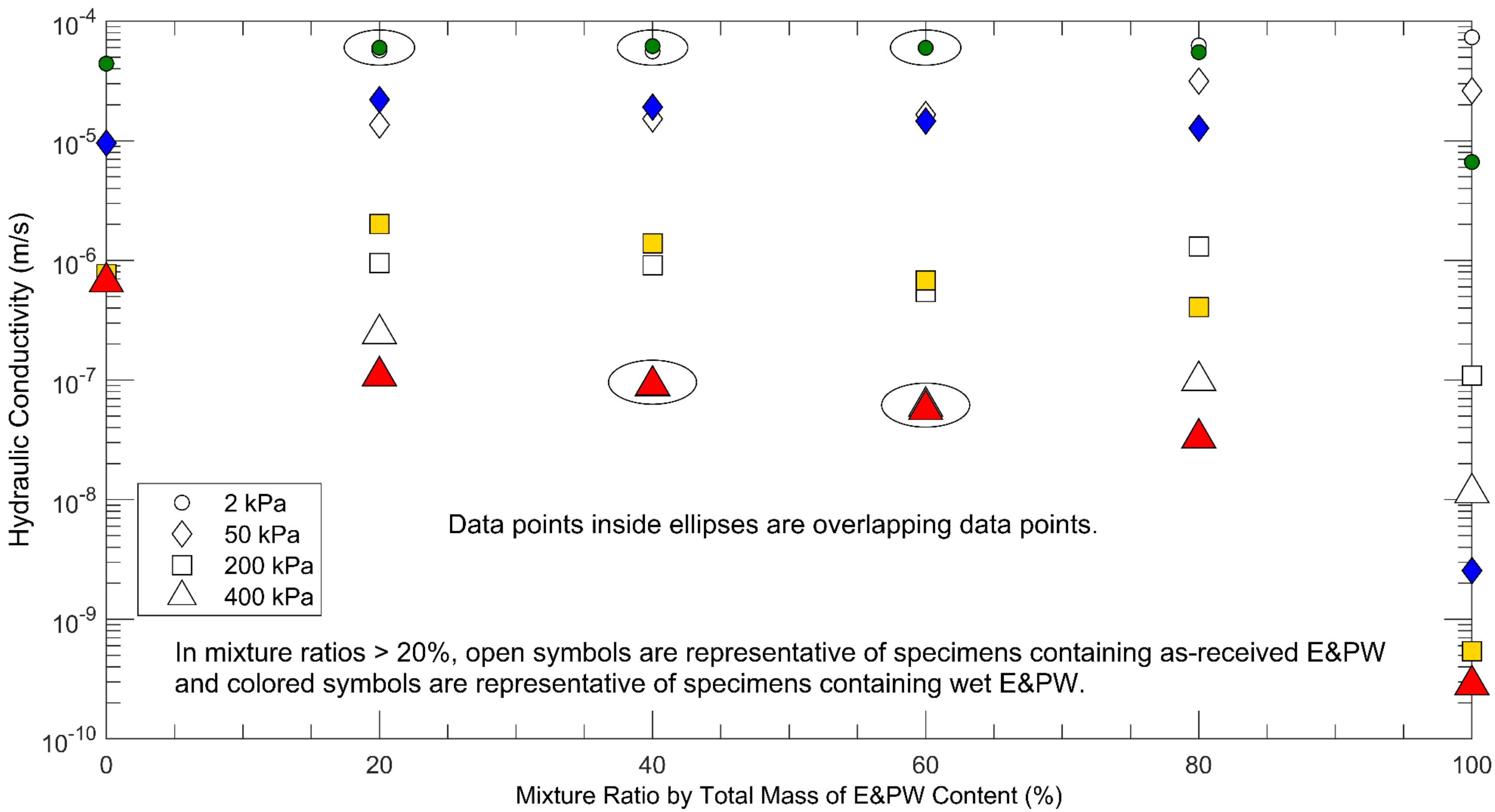

Fig. 3.9. Hydraulic conductivity versus as-received and wet Exploration and Production waste (E&PW) content under 1 kPa, 50 kPa, 200kPa, and 400 kPa effective vertical stress.

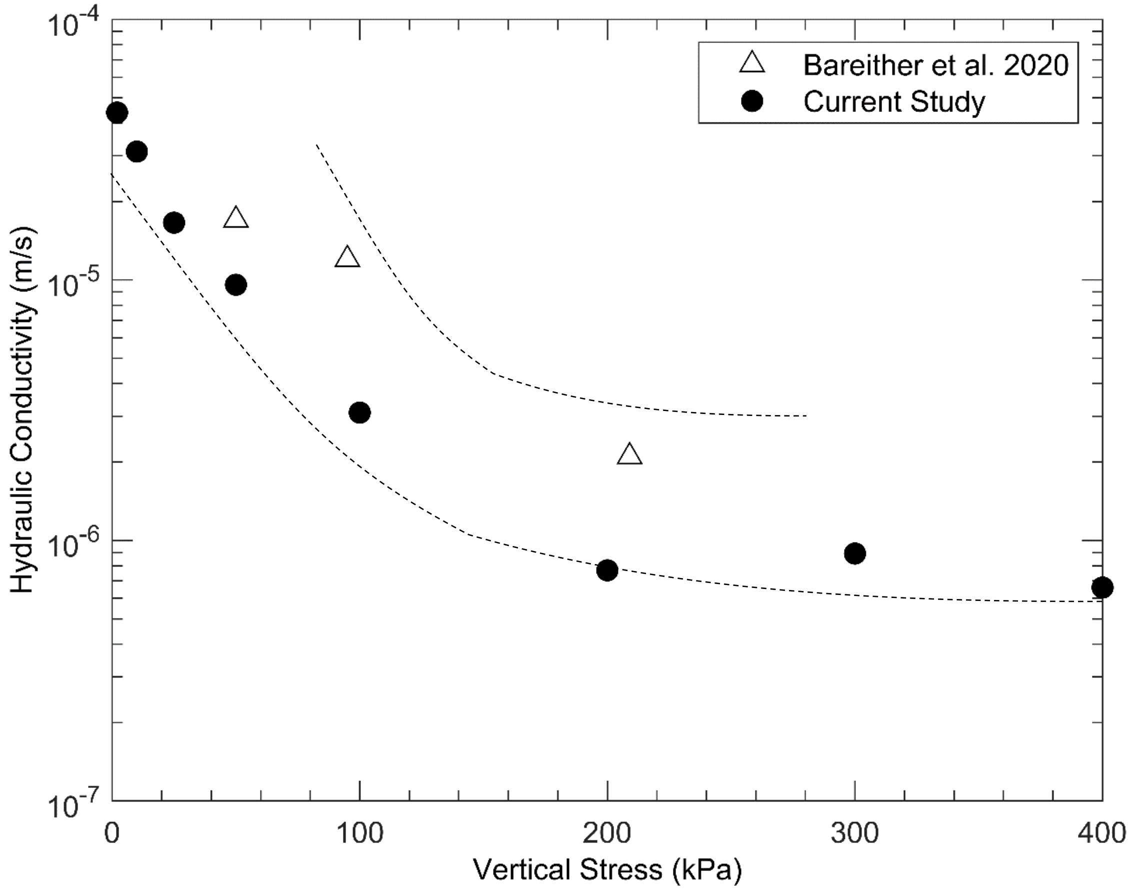

Fig. 3.10. Hydraulic conductivity versus vertical stress for MSW specimen prepared in the current study and Bareither et al. (2020).

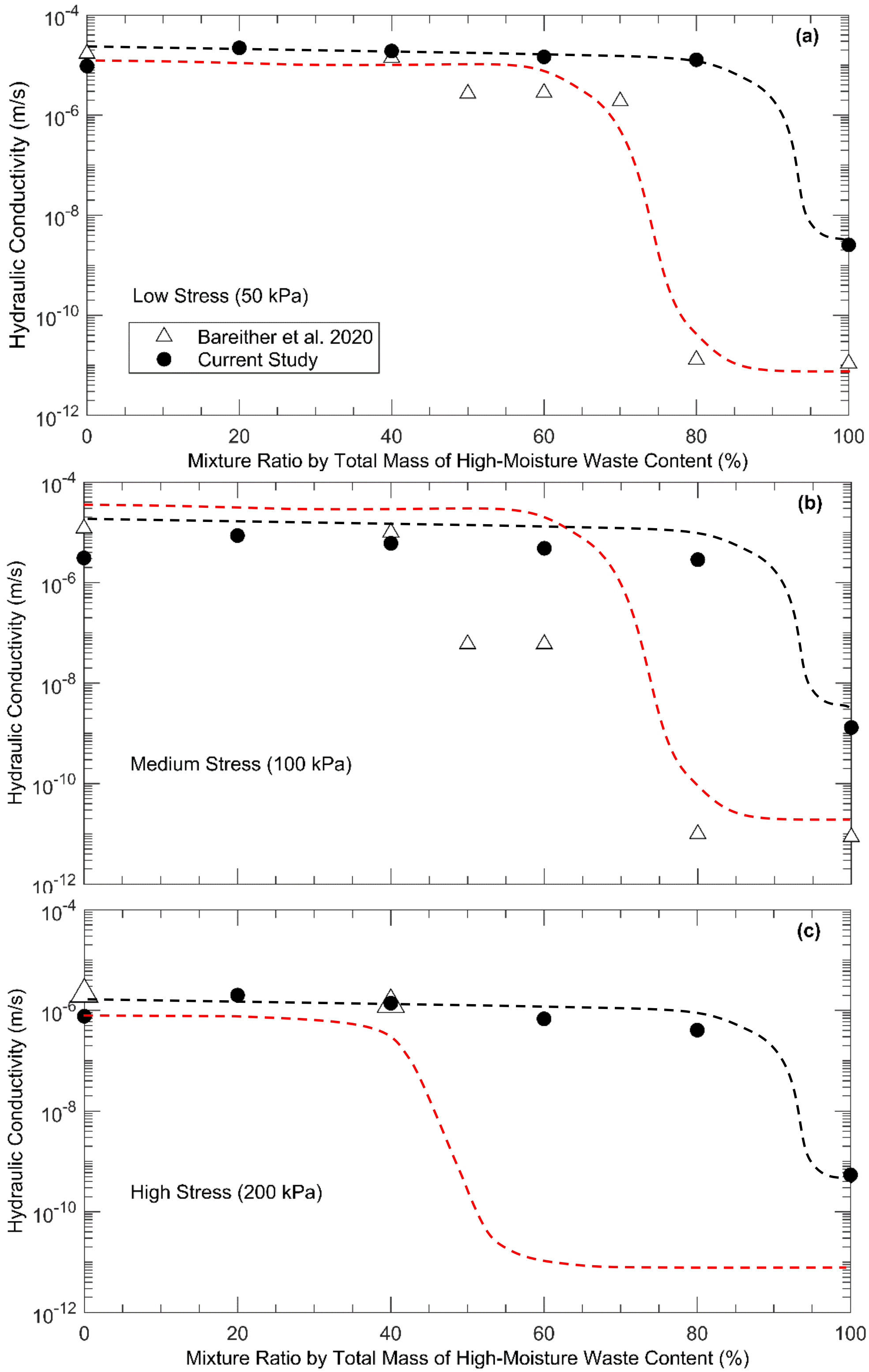

Fig. 3.11. Hydraulic conductivity versus mixtures of MSW and wet Exploration and Production waste (E&PW) or MSW and high-moisture waste (a) under 50 kPa, (b) 100 kPa, (c) 200 kPa vertical stress

3.5. References

ASTM. (2012). Standard Test Methods for Laboratory Compaction Characteristics of Soil Using Standard Effort. *ASTM International*, 1–13. https://doi.org/10.1520/D0698-12E01.1

ASTM. (2015). D5856-15 -Standard Test Method for Measurement of Hydraulic Conductivity of Porous Material Using a Rigid-Wall, Compaction-Mold Permeameter. *ASTM International,* West Conshohocken, PA, 1–9. https://doi.org/10.1520/D5856-15.2

ASTM. (2000). D854 - Standard Test Methods for Specific Gravity of Soil Solids by Water Pycnometer. *Astm D854*, 2458000(C), 1–7. https://doi.org/10.1520/D0854-10.2

ASTM. (2004). SW-846 Test Method 9095B: Paint Filter Liquids Test. *ASTM*, November, 55. http://eprints.uanl.mx/5481/1/1020149995.PDF

ASTM International. (2003). Standard Test Methods for Laboratory Compaction Characteristics of Soil Using Modified Effort. *ASTM Standard Guide*, 3, 1–10. https://doi.org/10.1520/D1557-12.1

Bareither, C. A., Benson, C. H., Rohlf, E. M., & Scalia, J. (2020). Hydraulic and mechanical behavior of municipal solid waste and high-moisture waste mixtures. *Waste Management*, 105, 540–549. https://doi.org/10.1016/j.wasman.2020.02.030

Benson, C. H., & Dniel, D. E. (1991). Influence of clods on hydraulic conductivity of compacted clay. *Manager*, 116(8), 1231–1248.

Breitmeyer, R. J., Benson, C. H., & Edil, T. B. (2019). Effects of Compression and Decomposition on Saturated Hydraulic Conductivity of Municipal Solid Waste in Bioreactor Landfills. *Journal of Geotechnical and Geoenvironmental Engineering*, 145(4), 1–15. https://doi.org/10.1061/(ASCE)GT.1943-5606.0002026

Chiado, E. D. (2014). The impact of shale gas/oil waste on MSW landfill composition and operations. *Shale Energy Engineering 2014: Technical Challenges, Environmental Issues, and Public Policy - Proceedings of the 2014 Shale Energy Engineering Conference*, 412–420. https://doi.org/10.1061/9780784413654.044

Daniel, D. E., Stp, A., Daniel, D. E., Trautwein, S. J., & Art, D. O. N. S. (1994). *STATE-OF-THE-ART Laboratory Hydraulic Conductivity Tests For Saturated Soils, Hydraulic Conductivity And Waste Contaminant Transport In Soil.* 30–78.

de Abreu, R. C., & Fourrier, J. E. (2019). Landfilling of oil and gas exploration and production wastes: Geotechnical and environmental considerations. In *Environmental Science and Engineering*. Springer Singapore. https://doi.org/10.1007/978-981-13-2224-2_22

Feng, S., Gao, K., Chen, Y., Li, Y., Zhang, L. M., & Chen, H. X. (2016). Geotechnical properties of municipal solid waste at Laogang Landfill , China. *Waste Management*. https://doi.org/10.1016/j.wasman.2016.09.016

Hanson, J. L., Yesiller, N., Von Stockhausen, S. a., & Wong, W. W. (2010). Compaction Characteristics of Municipal Solid Waste. *Journal of Geotechnical and Geoenvironmental Engineering*, 136(8), 1095–1102. https://doi.org/10.1061/(ASCE)GT.1943-5606.0000324

Hendron, D. M., Fernandez, G., Prommer, P. J., Giroud, J. P., & Orozco, L. F. (1999). INVESTIGATION OF THE CAUSE OF THE 27 SEPTEMBER 1997 SLOPE FAILURE AT THE DONA JUANA LANDFILL. *Proceeding Sardiana 99, Seventh International Waste Management and Landfill Symposium*, October.

Hossain, M. S., Penmethsa, K. K., & Hoyos, L. (2008). Permeability of municipal solid waste in bioreactor landfill with degradation. *Geotechnical and Geological Engineering*, 27(1), 43–51. https://doi.org/10.1007/s10706-008-9210-7

Karimi, S., & Bareither, C. A. (2021). The influence of moisture enhancement on solid waste biodegradation. *Waste Management*, 123, 131–141. https://doi.org/10.1016/j.wasman.2021.01.022

Koenig, A., Kay, J. N., & Wan, I. M. (1996). Physical properties of dewatered wastewater sludge for landfilling. *Water Science and Technology*, 34(3-4–4 pt 2), 533–540. https://doi.org/10.1016/0273-1223(96)00621-X

Koerner, R. M. H., Soong, T.-Y., Robert M. Koernerl-Hon, & Soong, T.-Y. (2000). Stability Assessment of Ten Large Landfill Failures. *Geo-Denver; Advances in Transportation and Geoenvironmental Systems Using Geosynthetics*. https://doi.org/10.1061/40515(291)1

Machado, S. L., Karimpour-Fard, M., Shariatmadari, N., Carvalho, M. F., & Nascimento, J. C. F. d. (2010). Evaluation of the geotechnical properties of MSW in two Brazilian landfills. *Waste Management*, 30(12), 2579–2591. https://doi.org/10.1016/j.wasman.2010.07.019

O'kelly, B. C. (2005). Sewage sludge to landfill: Some pertinent engineering properties. *Journal of the Air and Waste Management Association*, 55(6), 765–771. https://doi.org/10.1080/10473289.2005.10464670

Reddy, K. R., Hettiarachchi, H., Parakalla, N. S., Gangathulasi, J., & Bogner, J. E. (2009). Geotechnical properties of fresh municipal solid waste at Orchard Hills Landfill, USA. *Waste Management*, 29(2), 952–959. https://doi.org/10.1016/j.wasman.2008.05.011

Rohlf, E. M., Karimi, S., & Bareither, C. A. (2021). Implications of municipal solid waste co-disposal experiments on biodegradation and biochemical compatibility. *Waste Management*, 129, 62–75. https://doi.org/10.1016/j.wasman.2021.05.009

Suthagaran, V., Arulrajah, A., & Bo, M. W. (2010). Geotechnical laboratory testing of biosolids. *International Journal of Geotechnical Engineering*, 4(3), 407–415. https://doi.org/10.3328/IJGE.2010.04.03.407-415

The Environmental Research and Education Foundation. (2018). *Disposal of Aqueous Wastes in MSW Landfills Utilization and Effectiveness of Bulking & Stabilization Strategies*. October.

Tolaymat, T., Kim, H., Jain, P., Powell, J., & Townsend, T. (2013). Moisture Addition Requirements for Bioreactor Landfills. *Journal of Hazardous, Toxic, and Radioactive Waste*, 17(4), 360–364. https://doi.org/10.1061/(ASCE)HZ.2153-5515.0000184

U.S. EPA. (1991). Solid Waste Disposal Facility Criteria; Final Rule. Federal Register, 40CFR Part 258.

US EPA. (2002). Exemption of Oil and Gas Exploration and Production Wastes from Federal Hazardous Waste Regulations. 41.

Wong, W. W. Y. (2009). Investigation of the Geotechnical Properties of Municipal Solid (Issue September). California Polytechnic State University.

Yesiller, N., Hanson, J. L., Cox, J. T., & Noce, D. E. (2014). Determination of specific gravity of municipal solid waste. *Waste Management*, 34(5), 848–858. https://doi.org/10.1016/j.wasman.2014.02.002

Zhan, L., Chen, Y., & Bouazza, A. (2019). *Correction to: Proceedings of the 8th International Congress on Environmental Geotechnics Volume 3* (Vol. 2). https://doi.org/10.1007/978-981-13-2227-3_70

Zhang, Z., Wang, Y., Xu, H., Fang, Y., & Wu, D. (2018). Influence of effective stress and dry density on the permeability of municipal solid waste. *Waste Management and Research*. https://doi.org/10.1177/0734242X18763520

CHAPTER 4: PRACTICAL IMPLICATION

4.1. Practical implication

Landfill practitioners require hydraulic conductivity of MSW to determine landfill slope stability, design leachate collection and recirculation systems, and gas extraction systems. Hydraulic conductivity of MSW varies in landfills, and making a reliable prediction or measurement of hydraulic conductivity aids in landfill design and operation. Co-disposal of HMWs in MSW landfills can affect the hydraulic conductivity of MSW, which requires additional testing to measure MSW-HMW hydraulic conductivity. The hydraulic behavior of MSW-HMW mixtures depends on the composition of the waste as well as the response to changes in vertical stress and unit weight. Hence, each HMW and MSW-HMW mixtures need to be evaluated individually. Moreover, the hydraulic responses of MSW-HMW mixtures varies based on mixture ratio and vertical stress which can change throughout a landfill depth. Thus, it is important to consider a range for hydraulic conductivity for MSW and MSW-HMW mixtures as it reduces the risks associated with engineering design.

Determining an appropriate mixture ratio for co-disposing HMW with MSW requires an assessment of hydraulic and mechanical behavior. According to current regulations regarding disposal of HMW in MSW landfills, passing the paint filter test is the only criterion required to allow MSW landfills to accept and dispose HMWs. Although the paint filter test is a straightforward and inexpensive test that can be performed in the field by landfill operators, the results of paint filter test do not provide reliable data to make informed decisions regarding co-disposal. Additional assessments of hydraulic and mechanical behavior are important to predict the impacts of HMW addition on the operation and physical stability of MSW landfills.

Methods of landfilling E&PW in MSW landfills can result in significantly different outcomes. Findings from this study indicate that if E&PW is mixed with MSW, addition of E&PW did not change the hydraulic behavior of MSW. Mixing E&PW with MSW creates a waste matrix such that hydraulic behavior still is controlled by MSW materials. It is important to mention that the

E&PW that was tested in this study was similar to soil-like materials. Only if vertical stress exceeds 50 kPa, mixtures of MSW + 80% and above E&PW content may create a low permeable layer (i.e., $k_s < 1\times10^{-9}$ m/s) (Fig. 3.9). However, suppose the E&PW is disposed in discrete layers in concentrated zone in landfill without mixing with MSW. In that case, due to the relationship between E&PW hydraulic conductivity and dry unit weight, increasing vertical stress may substantially reduce the E&PW hydraulic conductivity and make perched zones in landfill.

Hydraulic response of HMW to stress or dry unit weight increase can be varied. If the hydraulic conductivity of HMW is influenced by the increase in dry unit weight or stress, the HMW must not be landfilled in zones that will be under higher overburden pressure (i.e., cells located in the lower part of landfill). Increasing the height of a landfilled waste mass increases the vertical stress on low permeable HMW materials and may lead to the creation of perched zones, which can lead to excess pore pressure development and potentially reduce landfill stability. The development of saturated zones can affect biogas collection and leachate recirculation systems in a landfill (Fig. 3.1), and furthermore, placement of HMW and low permeability wastes adjacent to the landfill slopes can potentially lead to leachate seeps and reduce slope stability.

Mixing waste in the working face of a landfill can be challenging, especially if the waste has high moisture content and low stability. Disposal of this waste in concentrated zones in landfill can bog down heavy landfill compactors and make trouble for landfill operators. HMW can be disposed in thin layers (i.e., 6 in) on top of an MSW layer. Then, a layer of MSW is placed on top of the HMW layer, and afterward, both layers, including the top MSW layer and HMW layer will be compacted. This method provides a condition that HMW is sandwiched between two MSW layers (i.e., similar to layered cake) and HMW can mix with the top MSW layer and infiltrate to the lower MSW layer. Further, MSW particles absorb the liberated moisture from HMW, which softens the MSW particles and improves the compaction efficiency. Moreover, there is no contact between the compactor's wheels and the HMW, as HMW can stick on the wheels.

Solid waste decomposes with time. Degradation of waste particles results in breaking down the particle size and changing the geometry of waste particles and flow paths. MSW degradation rates vary based on the waste composition and landfill operation. Therefore, further studies are needed to simultaneously evaluate the influence of stress and degradation on MSW permeability. The influence of MSW decomposition on MSW hydraulic conductivity was discussed in detail in the second chapter.

4.2. Summary and Conclusion

This study was conducted to evaluate the impacts of the addition of oil and gas exploration and production waste (E&PW) on the hydraulic conductivity of MSW. Hydraulic conductivity tests were conducted on MSW, E&PW, and mixtures of MSW and E&PW, and at vertical stress ranging from 2 kPa to 400 kPa to assess the influence of stress and dry unit weight on hydraulic conductivity. The MSW-E&PW mixtures were prepared to four mixture ratios that included MSW + 20%, 40%, 60%, and 80% E&PW content based on the total mass. The E&PW was mixed with MSW in two conditions: (i) as-received, which represented the moisture content of the bulk E&PW received at an MSW landfill; and (ii) wet E&PW, which represented the E&PW prepared to the maximum potential moisture content that met landfill disposal requirements

- The results of hydraulic conductivity tests on MSW-E&PW mixtures indicated that the hydraulic behavior of MSW was relatively consistent by increasing the mixture ratio to 60% E&PW content. The k_s reduced one order of magnitude for MSW-E&PW mixtures with more than 60% E&PW content and under vertical stress above 400 kPa.
- Findings from the k_s test on mixtures of MSW-E&PW suggested the addition of E&PW did not change the flow mechanism in solid waste. This means the flow still permeate through the interconnected void spaces between MSW particles.

- The addition of E&PW did not impact the available flow path, even though adding E&PW to MSW reduced the void spaces. This indicated that the waste matrix is capable of accepting E&PW while keeping the flow structure within the waste matrix.
- The k_s of E&PW reduced substantially when dry unit weight surpassed 14 kN/m^3 and void ratio exceeded 0.8. The k_s of E&PW at dry unit weight of 15.5 kN/m^3 was between 1×10^{-7} m/s to 1×10^{-9} m/s.
- Disposal of E&PW in discrete layers can potentially create a low permeable layer and, based on the area of a low permeable layer, can form perched water lenses and cause water accumulation in landfills.

APPENDIX A[1]:

1. Introduction

Solid waste landfills are an integral part of solid waste management in the U.S. and throughout the world. In 2017, more than 50% of the municipal solid waste (MSW) generated in the U.S. was disposed in landfills (US EPA 2017). Although landfilling has evolved during the past decades and environmental regulations have reduced negative impacts associated with landfills, there remain challenges associated with leachate leakage into groundwater, air pollution, odors, settlement, greenhouse gases emissions, and long-term post-closure care (e.g., Berge et al. 2009; Morris et al. 2012; Loureiro et al. 2013; Bareither and Kwak 2015; Pantini et al. 2015; Townsend et al. 2015; O'Donnell et al. 2018). Bioreactor landfills address some of the aforementioned challenges related to solid waste landfills. The primary objective of a bioreactor landfill is to promote in situ waste decomposition, which most commonly is achieved via enhancing anaerobic conditions that are beneficial to increasing the rate of organic waste decomposition (Benson et al. 2007; Bareither et al. 2010; Barlaz et al. 2010; Abichou et al. 2013a,b; Clarke et al. 2016; Bareither et al. 2017; Zhan et al. 2017a,b).

The most common strategy to improve in situ anaerobic biodegradation in landfills is moisture enhancement, which can include leachate addition and recirculation as well as liquid waste addition and solidification (e.g., Pommier et al. 2006; Tolaymat et al. 2010; Townsend et al. 2015; Bareither et al. 2017). Methods to add liquids (e.g., liquid waste and leachate) to landfills include direct disposal at the working face, vertical wells, horizontal trenches, and permeable

[1] Karimi, S., & Bareither, C. A. (2021). The influence of moisture enhancement on solid waste biodegradation. *Waste Management*, 123, 131–141. https://doi.org/10.1016/j.wasman.2021.01.022

blankets. Bareither et al. (2010) evaluated leachate recirculation operations for five full-scale bioreactor landfills and reported that operations included broad ranges of dose volumes and frequencies. Bareither et al. (2017) reported that landfills operating with a U.S. EPA Research Development and Demonstration (RD&D) Permit indicated that direct disposal of liquid waste in solid waste landfills was attractive due to revenue from waste tipping fees and progression towards organic stability. Nwaokorie et al. (2018) assessed moisture enhancement strategies at a full-scale landfill and reported that early, aggressive leachate recirculation combined with continuous leachate recirculation and liquid waste addition resulted in enhanced biogas generation.

Although the objective of moisture enhancement is to increase the rate and extent of in situ anaerobic biodegradation, there is limited guidance on dose rates and frequencies of liquid addition / leachate recirculation that are most beneficial to gas generation and organic waste stabilization. Field-scale operations for moisture addition are generally ad hoc and controlling the amount of liquid added and frequency of dosing is challenging as operations depend on multiple factors, such as moisture availability (e.g., leachate to recirculate, liquid waste, etc.), landfill infrastructure, and landfill personnel. However, controlling the frequency and amount of moisture addition to MSW can be achieved at laboratory scale to provide an assessment of moisture enhancement techniques that can provide guidance for full-scale bioreactor landfills.

The overall objective of this research was to assess the influence of moisture enhancement strategies on biodegradation of MSW in laboratory-scale reactors. Moisture enhancement strategies were varied with respect to dose volume and dose frequency. Biodegradation was evaluated based on methane (CH_4) generation to identify relevant and practical moisture enhancement strategies that can (i) reduce the lag-time between waste disposal and onset of CH_4 generation and (ii) increase the first-order decay rate for CH_4 generation.

2. Materials and Methods

2.1 Experiment Overview

Laboratory reactors were operated in a temperature-controlled room at 37 °C, which is near the optimal temperature for mesophilic waste decomposition (e.g., Barlaz et al. 1989). A collection of photographs documenting the setup and operation of the laboratory reactors are included in Fig. S1 (supplemental content). The main variable of the experiment was moisture addition, which included leachate dose / recirculation rates of 40, 80, 160, and 320 L/Mg-MSW (wet weight) that were applied at frequencies of every ½ week, 1 week, 2 weeks, and 4 weeks. The possible dose rate and frequency combinations yielded 16 reactors with varying moisture addition strategies; an additional control reactor was operated without any liquid added. The dose rates and frequencies used in this study were selected to represent relevant moisture enhancement strategies observed in full-scale landfills (e.g., Bareither et al. 2010; Abichou et al. 2013a; Bareither et al. 2017; Nwaokorie et al. 2018).

2.2. Reactor Design

A schematic of a laboratory-scale reactor used in this study is shown in Fig. 1. Each reactor was filled with 2.4 kg of shredded MSW representative of the U.S. average composition (Staley and Barlaz 2009; US EPA 2015). Reactors were equipped with capabilities of leachate and gas management. Leachate was distributed to the surface of the MSW via a perforated pipe placed within a gravel layer, and was collected in inert plastic bags below the reactors. Biogas generated during organic waste decomposition was collected in gas bags.

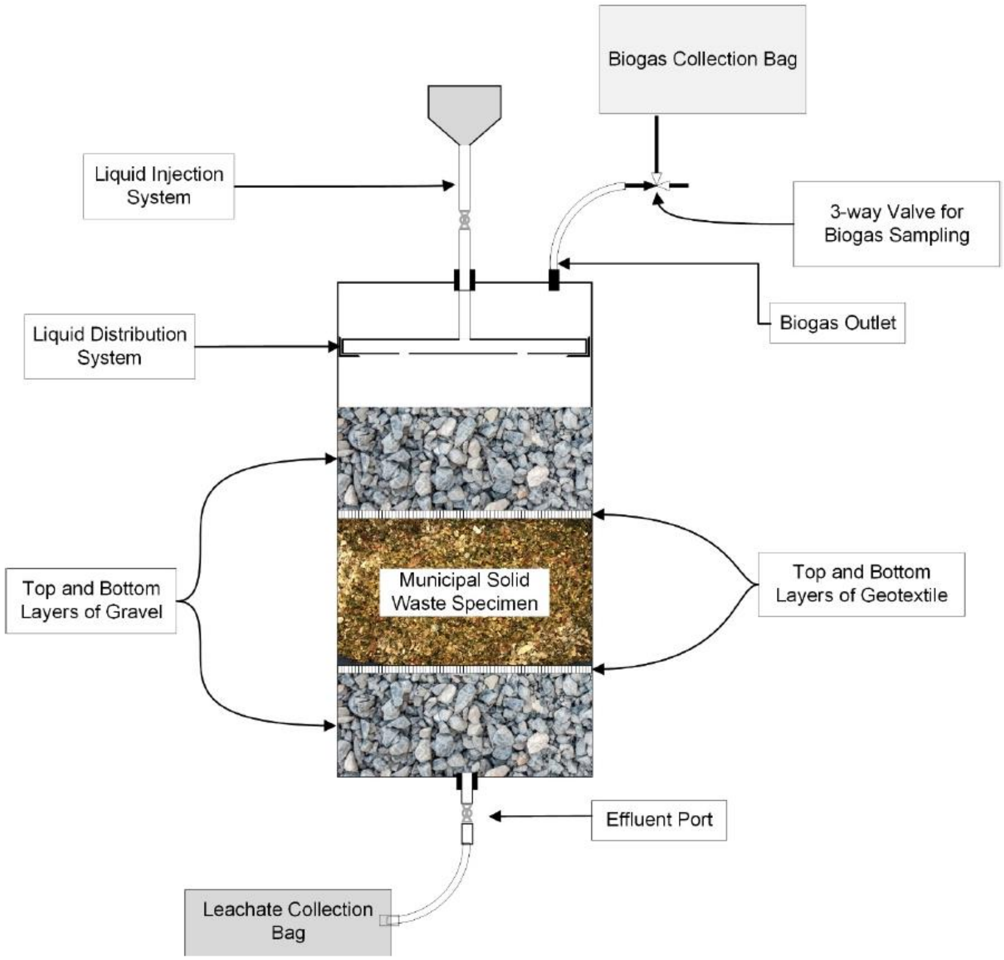

Fig. A1. Schematic of a laboratory-scale reactor.

The reactors consisted of polycarbonate cylinders with a height of 457 mm and an inside diameter of 203 mm. The MSW specimens were compacted between two layers of nonwoven geotextile and washed gravel. The bottom gravel layer (50-mm thick) was for leachate collection and the top gravel layer (140-mm thick) was for liquid/leachate distribution as well as to apply a 2-kPa vertical stress that represented interim landfill cover. Liquid/leachate distribution was conducted via a funnel external to the reactor cell that connected to a perforated PVC pipe network inside the upper gravel layer via a flexible tube (Fig. A1). The system included a ball valve below the funnel to limit ingress of atmospheric air into the reactor. Leachate was collected in an inert plastic bag connected to the effluent port at the bottom of reactor.

Biogas generated from MSW biodegradation was collected in 10-L, 25-L, or 40-L Flexfoil gas bags (SKC Inc., Eight Four, PA) depending on the flow rate. A three-way valve was included within the flexible tube that connected the head-space of the reactor to the gas bag. These valves facilitated gas sampling and disconnecting of the gas bag during gas volume measurement.

2. 3. Municipal Solid Waste

Municipal solid waste was collected during disposal at the working face of Larimer County Landfill in Fort Collins, Colorado, USA. Waste was hand-sorted into relevant categories (e.g., paper, plastic, metal, etc.), air-dried, and stored in sealed barrels. All waste materials used in the laboratory reactors were shredded with a slow-speed, high-torque shredder to a maximum particle size of approximately 20 mm (i.e., approximately one-tenth the reactor diameter). Food waste for this study was collected as pulped, pre-consumer food waste from Colorado State University.

A summary of the MSW composition used in the laboratory reactors is in Table S1 (supplemental content), which was reflective of the U.S. national average (Staley and Barlaz 2009; US EPA 2015). Each reactor was filled with 2.4 kg of shredded MSW that was moisture equilibrated via addition of food waste and left overnight in sealed buckets prior to specimen preparation. Waste specimens were compacted via hand tamping in four layers of equal thickness to an average total thickness of 200 mm, which corresponded to an average total unit weight of 3.58 kN/m^3 and average dry unit weight of 2.65 kN/m^3. Sub-samples of the MSW reactor specimens were oven-dried at 105 °C for 24 h to determine water content and subsequently combusted at 550 °C for 2 h to determine volatile solids. The average initial wet-weight water of the MSW specimens was 26% (dry-weight water content ≈ 34%) and average initial volatile solids was 72%.

Specific gravity of the MSW was estimated based on recommendations in (Yesiller et al. 2014):

$$G_s = \frac{\left(\sum_{i=1}^{n} M_{si}\right)}{\left[\sum_{i=1}^{n} \frac{M_{si}}{G_{si} \cdot \rho_w}\right] \cdot \rho_w} \tag{1}$$

where M_{si} is the initial mass of an individual component, G_{si} is the specific gravity of individual components (Table S1), and ρ_w is the density of water (1 g/cm^3). This approach yield G_s = 1.29 of the MSW, which was used to estimate an initial porosity (0.79), void ratio (3.8), and degree of saturation (12%) for the as-prepared MSW specimens in the reactor experiments.

2.4. Liquid management

Liquid dosing initiated in all reactors with centrifuged and diluted anaerobic digester sludge (ADS) (i.e., inoculum). The ADS was obtained from the Water Reclamation Facility in Fort Collins, Colorado, USA to provide a source of anaerobic microorganisms to the MSW during initial dosing. The ADS was centrifuged to remove solid particles and then diluted with de-ionized water (DIW) to approximate a chemical oxygen demand (COD) concentration representative of landfill leachate (≈ 2000 mg-O_2/L) (Kjeldsen et al. 2002). Fresh inoculum was added to all reactors until leachate was generated, whereupon leachate was recirculated with additional fresh inoculum added (as needed) to achieve the target dose volumes. Excess effluent that exceeded the target dose volumes was stored in plastic containers with minimal headspace at 4 °C until required for subsequent recirculation.

Leachate samples were collected on a weekly basis and evaluated for pH, electrical conductivity (EC), oxidation-reduction potential (ORP), and COD. Samples were collected from all reactors prior to recirculating the leachate. An additional leachate sample for the reactors with a 4-week dose frequency was collected one week after recirculation to generate additional leachate chemistry data for analysis. pH, EC, and ORP were measured on 10-mL samples using a multi-parameter hand-held meter (Hach Sension+MM150). The 10-mL samples were subsequently acidified with H_2SO_4 and stored at 4 °C for COD analysis. Chemical oxygen demand was measured with commercially-available test kits. A Hach DRB200 heating block and Hach DR3900 spectrometer were used in the COD analysis.

2.5. Gas management

2.5.1. Biogas Measurement and Composition

The volume of biogas collected in the gas bags was measured via water displacement. Gas bags were removed from the temperature-controlled reactor room and allowed to equilibrate to ambient laboratory temperature (≈ 20 °C) prior to measuring the volume. Biogas was evacuated from the gas bags using a vacuum pump and discharged into an inverted 10-L graduated cylinder that was submerged in water acidified with hydrochloric acid (pH ≈ 3) to prevent dissolution of CO_2. Gas volume measurements (± 10 mL) were made after the displaced cylinder equilibrated with atmospheric pressure.

Biogas samples for composition analysis were collected from each reactor and injected into evacuated 80-mL glass bottles with Butyl Rubber Stoppers. Composition of the biogas was measured with a HP6990 Gas Chromatograph (GC) (Hewlett-Packard, Palo Alto, CA) to determine the relative composition of carbon dioxide (CO_2) and methane (CH_4). The GC was equipped with a thermal conductivity detector (TCD) and RT-Q-Bond column (Restek Corporation, Bellefonte, PA). A small sample of biogas was extracted from the glass bottles and injected into the GC using a 50-µL gas tight syringe. OpenLab chromatography software (Agilent Technologies, Santa Clara, CA) was used to analyze the GC data. Operating parameters for the TCD method included a 30 °C inlet and oven temperature, 200 °C thermal conductivity detector temperature, 50 cm/s linear column velocity, and 40:1 split flow. Hydrogen was used as the carrier gas. Calibration curves were created from pure CO_2 and CH_4 gases (Airgas, Radnor, PA) to determine percentages of CO_2 and CH_4 in the biogas samples.

2.5.2. Decay Rate and Lag-Time

Methane generated data from the reactors was modeled using the U.S. EPA LandGEM to determine the first-order decay rate (US EPA 2005). The LandGEM model applied to the reactor data in this study was integrated to a simplified form that represented cumulative CH_4 generation (Barlaz et al. 2010):

$$V = L_0 M\left(1 - e^{-k \cdot t}\right) \tag{2}$$

where V is cumulative CH_4 collected during the experiment (m^3) and M is the initial total mass of solid waste (Mg). Eq. (1) can be rearranged as shown in Eq. (2), where the numerator on the right-hand side of the equation is the remaining CH_4 potential at time t.

$$-k \cdot t = \ln\left(\frac{L_0 - V/M}{L_0}\right) \tag{3}$$

The decay rate in Eq. 2 was determined via linear regression of the cumulative CH_4 volume versus time relationship with an assumed L_0 and measured V. The L_0 was assumed equal to 129 m^3-CH_4/Mg-MSW (dry mass), which was based on the maximum CH_4 yield among the reactors operated in this study. An upper-bound L_0 = 146 m^3-CH_4/Mg-MSW (dry mass) was computed assuming complete degradation and conversion of all paper, yard waste, and food waste to gaseous end-products (Tchobanoglous and Kreith 2002). Thus, L_0 was set equal to the maximum CH_4 yield measured in this study considering (i) the measured L_0 agreed with the theoretical L_0 and was expectedly lower due to a lack of complete biodegradation and (iii) all reactors included MSW from the same source and prepared to the same composition. The use of a single L_0 was advantageous to isolate the influence of dose volume and frequency (i.e., moisture enhancement) on the decay rate.

The amount of potential CH_4 generated from the inoculum added to the reactors was evaluated for the reactor with the largest amount of inoculum added. Potential CH_4 generated from the inoculum was calculated via the measured CH_4 potential of the inoculum (1.34 mL-

CH_4/mL) multiplied by the total volume of fresh inoculum added. The total potential CH_4 generated due to fresh inoculum was negligible (i.e., < 1.8% of total CH_4 collected from the reactor with the highest cumulative inoculum added); thus, corrections were not applied to CH_4 generation data from the reactors.

3. Results

3.1. Reactor Operation and Data Processing

A summary of the 17 laboratory reactors (R1 – R17) conducted for this study is in Table 1. The summary includes dose volume, dose frequency, total liquid added per MSW mass, total CH_4 yield, peak CH_4 flow rate, ratio of CH_4 yield per MSW mass to CH_4 potential, lag-time between onset of liquid dosing and CH_4 generation, and the modeled decay rate based on Eq. 2. Reactors were operated for 220 d, and inoculum dosing in all reactors started on Day 22.

Temporal trends of data collected during reactor operation are shown for R14 in Fig. A2. Reactor operation data for R14 are representative of data collected for all reactors in which leachate recirculation was implemented (i.e., R1 through R16). This reactor (R14) was operated with a dose volume of 320 L/Mg-MSW and a dose frequency of 1 week, which meant that 320 L/Mg-MSW (i.e., 768 mL based on initial mass of the MSW specimen) of leachate and additional fresh inoculum (as needed) was added to the reactor each week. The ratio of effluent leachate volume to influent dose volume rapidly approached unity (Fig. A2a) due to the large dose volume and high frequency, and the wet-weight water content increased and remained at approximately 67% for the duration of the experiment (Fig. A2b). Water content was calculated based on the present mass of water and solid in a given reactor. Mass loss due to biodegradation was determined via stoichiometric calculations that incorporated biogas production (Tchobanoglous and Kreith 2002).

Temporal trends of leachate pH, EC, ORP, and COD shown in Fig. A2 depict anticipated trends for anaerobic biodegradation of MSW (e.g., Barlaz et al. 1989; Pholand and Kim 1999; Bareither et al. 2013; Fei and Zekkos 2018; Gu et al. 2020). pH initially decreased to approximately 5 on Day 50 and concurrently COD reached a maximum of nearly 35,000 mg-O_2/L, which reflected hydrolysis and acidogenesis. During the subsequent 50 days (~ Day 50 to Day 100), ORP reduced to less than -200 mV reflecting the onset of methanogenic conditions, pH increased and stabilized above neutral, and COD decreased to less than 10,000 mg-O_2/L. These leachate chemistry trends support the onset of CH_4 generation observed in R14 during this same time period (Fig. A2).

Biogas generation in R14 initiated quickly after initial inoculum dosing (Fig. A2j) and increased rapidly with subsequent leachate recirculation. The ratio of CH_4:CO_2 and CH_4 flow rate increased from Day 22 and both peaked approximately on Day 80. At the end of the experiment, R14 generated 351 L of biogas, of which 173 L were CH_4.

Reactors that were operated with higher dose volumes and, in particular, higher dose frequencies, yielded a greater potential to collect and analyze leachate chemistry. However, limited leachate chemistry data were obtained for R3 and R8, and no leachate chemistry data were obtained for R4. These reactors had low dose volumes and dose frequencies of either 2 or 4 weeks (Table 1), which limited potential leachate generation. Although leachate never generated from R4 and only limited leachate generated from R3 and R8, all reactors produced biogas and achieved methanogenesis.

Table A1. Summary of reactor experiments, including dose volume, dose frequency, total liquid added per MSW mass, cumulative methane yield, peak methane flow rate, ratio of methane yield to methane potential, lag-time between onset of liquid dosing and methane generation, and first-order decay rate.

Reactor	Dose Volume (L/Mg-MSW) [a]	Dose Frequency (week)	Total Liquid Added / Total MSW Mass (L/Mg-MSW)	Cumulative CH_4 (m^3/Mg-MSW) [b]	Peak CH_4 Flow Rate (m^3/Mg-MSW/d) [b]	Cumulative CH_4 / L_0 [d]	Lag-Time (d) [e]	Decay Rate (1/yr)
R1	40 (96)	0.5	2,160	97	1.29	0.75	14	1.90
R2		1	1,120	74	0.59	0.57	20	1.22
R3		2	560	43	0.56	0.33	32	0.73
R4		4	280	25	0.27	0.19	48	0.40
R5	80 (192)	0.5	4,320	101	2.02	0.78	14	2.10
R6		1	2,240	100	1.81	0.78	19	1.96
R7		2	1,120	88	1.05	0.68	22	1.67
R8		4	560	48	0.56	0.37	35	0.81
R9	160 (384)	0.5	8,690	107	1.96	0.83	11	2.24
R10		1	4,500	103	1.95	0.80	13	2.08
R11		2	2,250	103	2.04	0.80	22	2.15
R12		4	1,130	90	1.13	0.70	27	1.75
R13	320 (768)	0.5	17,280	123	1.89	0.96	7	2.75
R14		1	8,960	100	1.96	0.78	7	1.89
R15		2	4,480	129	1.97	1	7	2.79
R16		4	2,240	101	1.48	0.79	7	1.84
R17	—	—	—		—			-

[a] Volume of actual dose in mL provided in parentheses.
[b] Cumulative CH_4 and peak CH_4 flow rate are calculated based on dry mass of MSW.
[c] Methane potential is based on wet mass of MSW.
[d] L_0 assumed (129) m^3/Mg-MSW (dry mass).
[e] Lag-times is a time between the initiation of liquid addition and onset of methane generation.

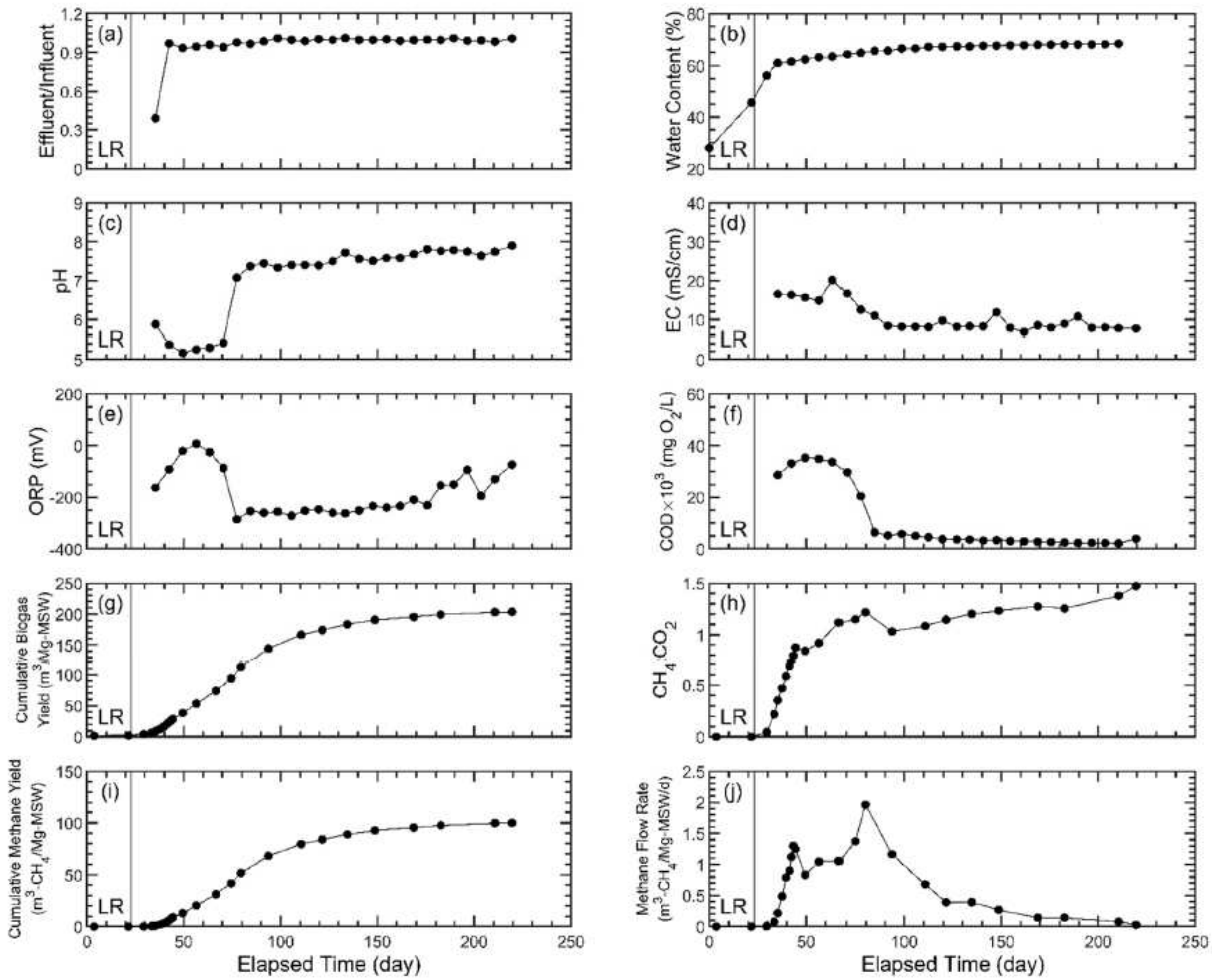

Fig. A2. Temporal trends of operational data collected for Reactor 14: (a) ratio of influent to effluent volumes; (b) wet weight water content; (c) leachate pH; (d) leachate electrical conductivity; (e) leachate oxidation-reduction potential; (f) leachate chemical oxygen demand; (g) cumulative biogas yield; (h) ratio of methane to carbon dioxide; (i) cumulative methane yield; and (j) methane generation rate. Note: LR = leachate recirculation, and the vertical line identifies the start of inoculum addition and leachate recirculation on Day 22.

Methane generation data for each reactor were evaluated to determine two key parameters: (i) lag-time between the onset of inoculum dosing and CH_4 generation (i.e., lag-time); and (ii) first-order decay coefficient (i.e., decay rate or *k*) (Table 1). Cumulative CH_4 generation data from R14 are linearized in Fig. S2 (supplemental content) and fitted with Eq. 2 to provide an example of the method used to determine the lag-time and decay rate. The x-axis in Fig. S2 is elapsed time from onset of liquid dosing and the y-axis is linearized CH_4 production. Eq. 2 was fit to the data using an L_0 = 129 m^3-CH_4/Mg-MSW and decay rate was taken as the slope of the linear regression. This L_0 was adopted based on the maximum CH_4 produced among the 16 reactors (i.e., R15), and was used in the evaluation of all reactors. The variables M and V in Eq. 2 were reactor specific, which were the mass of solid waste (Mg) and cumulative CH_4 generated (m^3), respectively. Lag-time was identified as the intercept of the linear regression (Fig. S2), which represented the time after onset of inoculum addition that CH_4 production began.

3.2. Moisture Response

Temporal trends of the ratio of leachate effluent to dose influent volume and wet-weight water content for reactors grouped by dose volume are shown in Fig. A3. Each plot in Fig. A3 includes the four reactors operated with the same dose volume, but with dose frequencies of ½, 1, 2, and 4 weeks. Reactors with a dose volume of 40 L/Mg-MSW (Fig. A3a,b) exhibited the broadest range of effluent / influent ratios and water contents during reactor operation. This broad range in moisture response was attributed to the low dose volume. For example, R4 had the least amount of liquid added (40 L/Mg-MSW added every 4 weeks), which resulted in zero leachate generation during the experiment. The amount of leachate theoretically consumed via microorganisms to produce biogas was approximately 1.6% of total leachate that was added to R4. Thus, zero leachate generation in R4 primarily was due to the moisture holding capacity of the MSW combined with the low dose volume and dose frequency. Each of the reactors operated with a dose volume of 40 L/Mg-MSW achieved a different water content at the end of operation, whereby the water content increased with more frequent dosing.

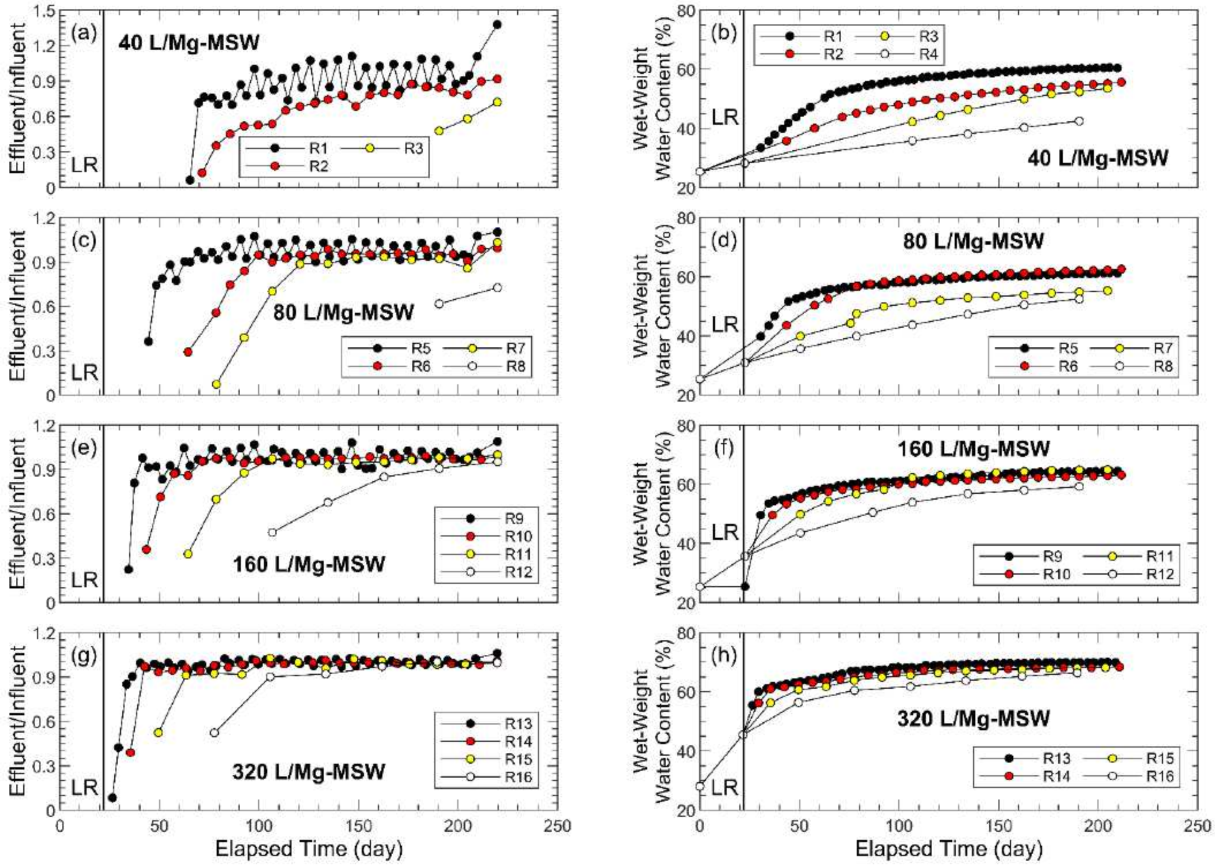

Fig. A3. Temporal trends of the ratio of effluent to influent volume and wet-weight water content for reactors grouped based on different dose volumes: (a and b) 40 L/Mg-MSW; (c and d) 80 L/Mg-MSW; (e and f) 160 L/Mg-MSW; and (g and h) 320 L/Mg-MSW. The duration between doses for given dose volume increases with reactor number (e.g., for 40 L/Mg-MSW, R1 = ½ week, R2 = 1 week, R3 = 2 weeks, and R4 = 4 weeks.

Liquid dosing at volumes of 80, 160, and 320 L/Mg-MSW exhibited similar trends in the moisture response. The effluent / influent ratio and moisture contents for dosing conducted at a frequency of ½ week (i.e., R5, R9, and R13) increased rapidly and leveled off at what represented hydraulic equilibrium. The majority of the reactors generated leachate after reaching wet-weight water contents of 50-52% (dry-weight water contents = 98-107%), and subsequently the ratio of leachate effluent to influent volume increased and leveled off at approximately 90-100%. A decrease in the frequency of dosing for each of the dose volumes (i.e., from ½ week to 1, 2, and 4 weeks) corresponded with a delay in leachate generation observed as the effluent / influent ratio required more time to reach 90-100% and stabilize. However, as the dose volume increased from 80 L/Mg-MSW to 160 L/Mg-MSW and ultimately to 320 L/Mg-MSW, the elapsed time required to generate leachate and achieve hydraulic equilibrium decreased.

The least amount of variability in the equilibrated and final moisture contents was observed in those reactors operated with a dose volume of 320 L/Mg-MSW (Fig. A3h), which was the largest dose volume used in this study. Wet-weight water contents for all reactors that generated leachate ultimately stabilized between approximately 60% and 65% (Fig. A3). This range of water contents is at the upper end of the range observed in full-scale landfills (e.g., Bareither et al. 2010, 2017; Feng et al. 2017). The higher range of wet-weight water contents observed in the laboratory reactors was attributed to more aggressive moisture enhancement strategies combined with small volumes of shredded MSW used in the laboratory.

3.3. Leachate Chemistry

Temporal trends of leachate pH and COD for reactors grouped by dose volume are shown in Fig. A4. pH and COD were selected as representative parameters to assess leachate chemistry for comparison among the moisture enhancement scenarios to decreasing the amount of data plotted in Fig. A4. Electrical conductivity of the leachate closely replicated the COD response (e.g., Figs. 2e and 2f) and ORP trends predominantly documented a decrease to below -200 mV for active methanogenic conditions with subsequent increase as COD reduced. Thus, effective and efficient comparison between leachate chemistry data from the reactors is possible via evaluating pH and COD.

The leachate pH and COD trends observed in the reactors were dependent on the dose volume and dose frequency. The only reactor operated with a dose volume of 40 L/Mg-MSW that exhibited the dynamic nature of increasing pH and decreasing COD was R1, which was operated with a dose frequency of ½ week. The higher rate of dosing for R1 generated sufficient leachate to capture the dynamic changes in leachate chemistry, whereas R2 and R3 with dose frequencies of 1 and 2 weeks, respectively, only exhibited pH > 7 and low COD concentration when leachate was first generated (Figs. 4a,b). Thus, these low dose frequencies at a dose volume of 40 L/Mg-MSW appear to have allowed hydrolysis, acidogenesis, and methanogenesis to develop within the reactor prior to sufficient inoculum added to generate leachate. Leachate was not generated from R4 and no leachate chemistry data were measured for that reactor.

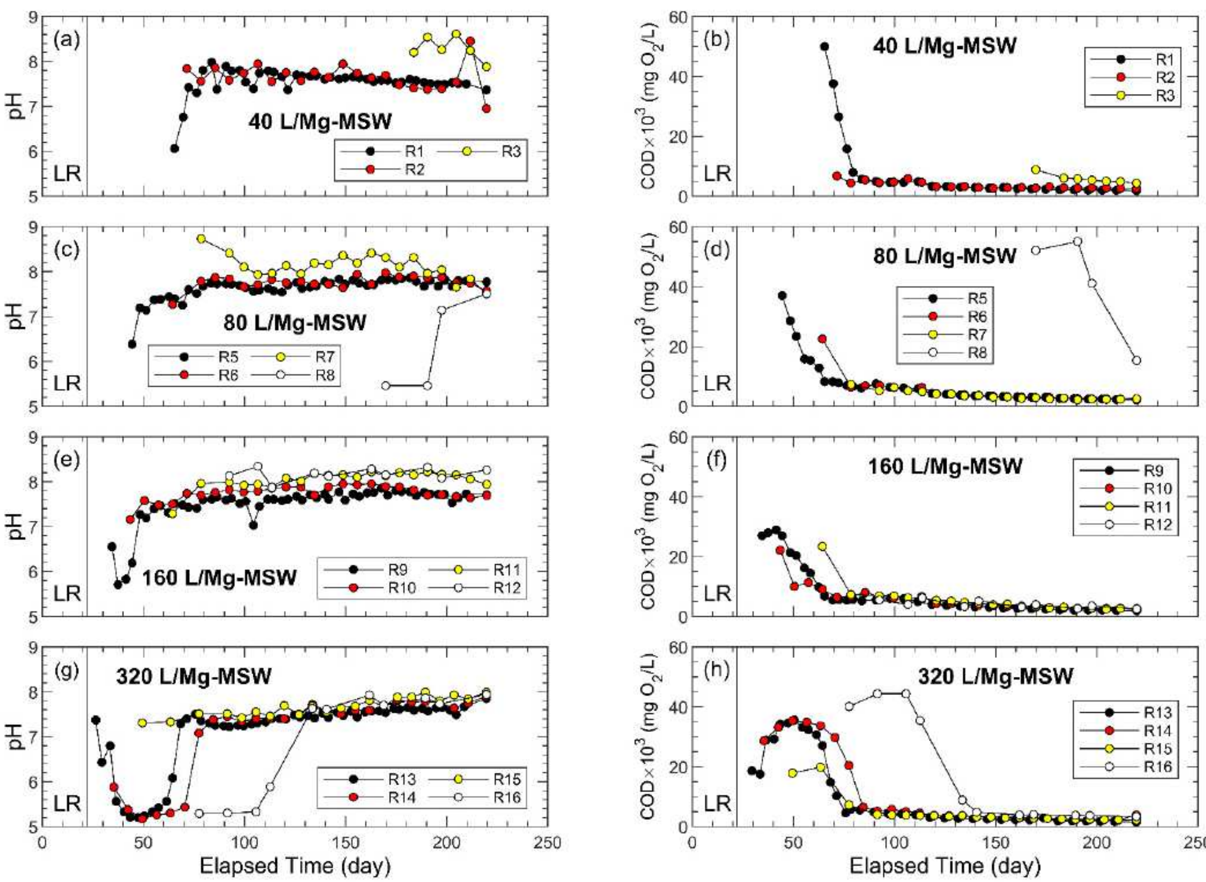

Fig. A4. Temporal trends of leachate pH and chemical oxygen demand (COD) for reactors groups based on dose volume: (a and b) 40 L/Mg-MSW; (c and d) 80 L/Mg-MSW; (e and f) 160 L/Mg-MSW; and (g and h) 320 L/Mg-MSW. The duration between doses for given dose volume increases with reactor number (e.g., for 40 L/Mg-MSW, R1 = ½ week, R2 = 1 week, R3 = 2 weeks, and R4 = 4 weeks.

An increase in dose volume from 40 L/Mg-MSW to 80 L/Mg-MSW did not considerably change the leachate chemistry trends observed as a function of dose frequency. The most dynamic behavior observed in leachate pH and COD for the 80 L/Mg-MSW reactors was for R5, which was operated with a dose frequency of ½ week. However, modest increasing pH and decreasing COD trends were also observed in R6 that was operated with a dose frequency of 1 week. Thus, the increase in dose volume from 40 to 80 L/Mg-MSW allowed for more rapid leachate generation at a dose frequency of 1 week such that the dynamic changes in leachate chemistry were captured. The main difference observed in reactors with a dose volume of 80 L/Mg-MSW was pH < 6 measured for R8 upon initial leachate generation on Day 170 (Fig. A4c). Although leachate pH for R8 was considerably acidic upon initial generation, the reactor was generating CH_4 (described subsequently). The third and final leachate chemistry measurement for R8 indicated that pH increased above neutral. The low initial pH measured for R8 may have been due to accumulation of organic acids near the bottom of the waste mass due to gravity-induced seepage within the waste specimen prior to leachate generation. Staley et al. (2011) observed active methanogenesis in laboratory MSW reactors with leachate chemistry representative of below neutral pH. Thus, there could have been an active community of low-pH tolerant methanogens in R8 as postulated by Staley et al. (2011) or the presence of pH-neutral pockets within the reactor that promoted CH_4 generation.

Leachate chemistry data for reactors operated with dose volumes of 160 and 320 L/Mg-MSW exhibited the most dynamic responses as a function of time due to the larger volumes of liquid added and recirculated. Reactors R9, R13, and R14 all exhibited a complete leachate chemistry signature for MSW experiencing hydrolysis, acidogenesis, and methanogenesis. Leachate chemistry from these reactors exhibited a decrease in pH concurrently with peak in COD as hydrolysis and acidogenesis were the dominant microbiological process. Subsequently, pH increased above neutral while COD decreased, which reflected consumption of readily-available soluble organic compounds in the leachate (e.g., acetate) as methanogenesis was established and began to flourish (e.g., Barlaz et al. 1989; Pohland and Kim 1999). Interestingly, R16 that was operated with a dose volume of 320 L/Mg-MSW and a dose frequency of 4 weeks also showed these characteristic trends in leachate chemistry; however, the elapsed time at which the trends developed was delayed relative to reactors operated with dosing conducted at higher frequencies (i.e., R13 and R14).

3.4. Methane Generation

Temporal trends of cumulative CH_4 yield and CH_4 flow rate for reactors grouped based on dose volume are shown in Fig. A5. A consistent increase in CH_4 yield and flow rate was observed with an increase in dose frequency from 4 weeks to ½ week for reactors operated with a dose volume of 40 L/Mg-MSW (Fig. A5a,b). The peak CH_4 flow rate increased from 0.27 to 1.29 m^3/Mg-MSW/d from R4 to R1 as the dose frequency increased from every 4 weeks to every ½ week (Table 1). In addition, only R1 exhibited a sharp peak in CH_4 flow rate; the other three reactors with a dose volume of 40 L/Mg-MSW yielded low CH_4 flow rates that did not exhibit pronounced dynamic changes (Fig. A5b). Cumulative CH_4 yields from these four reactors were compared to the highest CH_4 yield measured for the entire set of reactors (i.e., R13, Table 1) to compute a percent CH_4 yield. The increase in dose frequency from R4 to R1 corresponded to an increase in percent CH_4 yield from 19% to 75% (Table 1). Thus, the increase in dose frequency at the lowest dose volume of 40 L/Mg-MSW considerably increased CH_4 yield and flow rate. This enhanced CH_4 generation was attributed to an increase in moisture availability within the reactors.

A similar increase in CH_4 yield and CH_4 flow rate was observed with increasing dose frequency from 4 weeks (R8) to ½ week (R5) for reactors operated with a dose volume of 80 L/Mg-MSW. Peak CH_4 flow rate increased from 0.56 to 2.02 m^3/Mg-MSW/d (Table 1). However, the cumulative CH_4 yield for reactors R5 and R6 that were operated with dose frequencies of ½ week and 1 week, respectively, were essentially the same (Fig. A5c). The prolonged acidic conditions of R8 (Fig. A5c), discussed previously, likely reduced the cumulative CH_4 yield and CH_4 flow rate for this reactor. However, CH_4 generation was ongoing concurrently while leachate pH was less than 6 (i.e., between 170-190 d). A small peak in CH_4 flow rate for R8 towards the end of the experiment coincided with an increase in leachate pH to above neutral conditions.

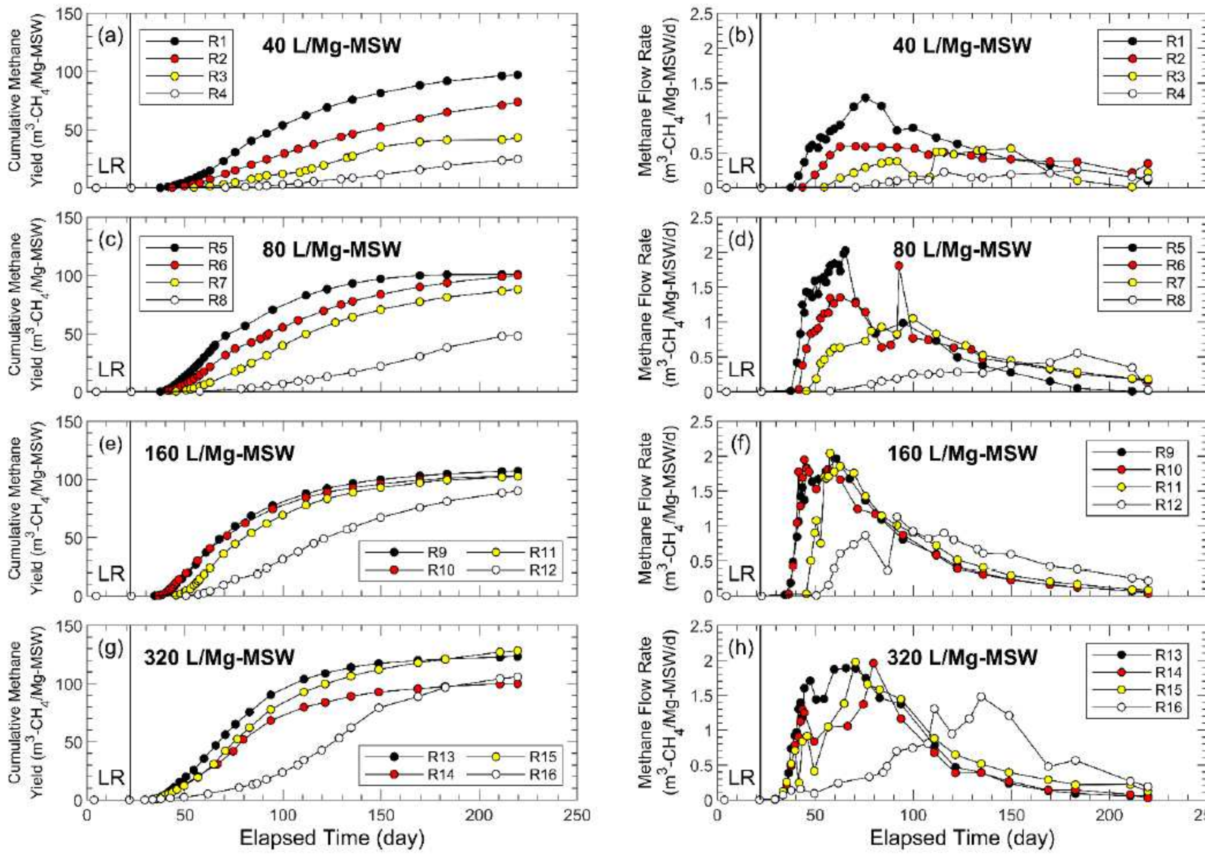

Fig. A5. Temporal trends of cumulative methane yield and methane flow rate normalized to MSW mass for reactors groups based on dose volume: (a and b) 40 L/Mg-MSW; (c and d) 80 L/Mg-MSW; (e and f) 160 L/Mg-MSW; and (g and h) 320 L/Mg-MSW. The duration between doses for given dose volume increases with reactor number (e.g., for 40 L/Mg-MSW, R1 = ½ week, R2 = 1 week, R3 = 2 weeks, and R4 = 4 weeks.

The temporal trends of cumulative CH_4 yield and CH_4 flow rate were nearly identical for reactors R9, R10, and R11 (Figs. 5e,f), which were operated with a dose volume of 160 L/Mg-MSW and dose frequencies of ½, 1, and 2 weeks, respectively. A decrease in dose frequency to 2 weeks resulted in a short lag-time for the increase in CH_4 flow rate compared to the reactors with dose frequencies of ½ and 1 week. Regardless, the cumulative CH_4 yield for reactors R9, R10, and R11 ranged between 103 and 107 m^3/Mg-MSW and peak CH_4 flow rate ranged between 1.95 and 2.04 m^3/Mg-MSW/d (Table 1). The reduced dose frequency to 4 weeks for R12 did yield a lower CH_4 yield (90 m^3/Mg-MSW) and substantially lower peak CH_4 flow rate (1.13 m^3/Mg-MSW/d). Regardless of the difference in CH_4 generation for R12, there were negligible differences in CH_4 yield and flow rate considering dose frequencies of ½, 1, and 2 weeks for reactors operated with a dose volume of 160 L/Mg-MSW.

An increase in dose volume from 160 to 320 L/Mg-MSW had limited influence on the trends in CH_4 generation for the four dose frequencies evaluated. The two reactors operated with dose frequencies of ½ and 2 weeks and a dose volume of 320 L/Mg-MSW (R13 and R15) yielded very comparable CH_4 yield and flow rate (Figs. 5g,h and Table 1). The peak CH_4 flow rate and general trend in CH_4 flow rate as a function of time for R14, which was operated with a dose frequency of 1 week, were also similar to R13 and R15. A lower cumulative CH_4 yield for R14 (100 m^3/Mg-MSW) was measured relative to R13 and R15 (123-129 m^3/Mg-MSW); however, this difference likely was attributed more to variability in the MSW source material than actual reactor operation. Reactor R16, which was operated with a dose frequency of 4 weeks and dose volume of 320 L/Mg-MSW, yielded the same amount of total CH_4 as R14. The main differences with R16 were that peak CH_4 flow rate prolonged in development (i.e., occurred on Day 140 compared to Day 80 for R14) and was slightly lower. The prolonged development of the peak CH_4 flow rate in R16 corresponded to the prolonged establishment of neutral pH and reduced COD observed in the leachate chemistry (Figs. 4g,h). Regardless of the minor variability observed among the four reactors operated with a dose volume of 320 L/Mg-MSW, the cumulative CH_4 yields were comparable at the end of the experiment.

3.5. First-Order Decay Rate and Lag-Time

The relationship between decay rate and dose volume is shown in Fig. A6a, which includes all reactors grouped with respect to similar dose frequency. In general, the decay rate increased with an increase in dose volume for all four dose frequencies evaluated. The only reactor that did not fit the general trend was R14, which was operated with a dose volume of 320 L/Mg-MSW and dose frequency of 1 week. The most pronounced difference in decay rate as a function of dose frequency was observed for a dose volume of 40 L/Mg-MSW. An increase in dose frequency from 4 weeks to ½ week increased the decay rate from 0.4 1/yr to 1.9 1/yr (Table 1), which was more than a four-fold increase in the rate of CH_4 generation. In addition, for reactors operated with a dose frequency of ½ week, the decay rate increased 50%, from 1.9 to 2.75 1/yr, with an increase dose volume from 40 L/Mg-MSW to 320 L/Mg-MSW. The highest decay rates determined for the reactors operated in this study were 2.75 and 2.79 1/yr, which were for R13 and R15 (Table 1). These two reactors were operated with a dose volume of 320 L/Mg-MSW and dose frequencies of ½ and 2 weeks, respectively. These reactors also generated the largest CH_4 yields among the 16 reactors (Table 1).

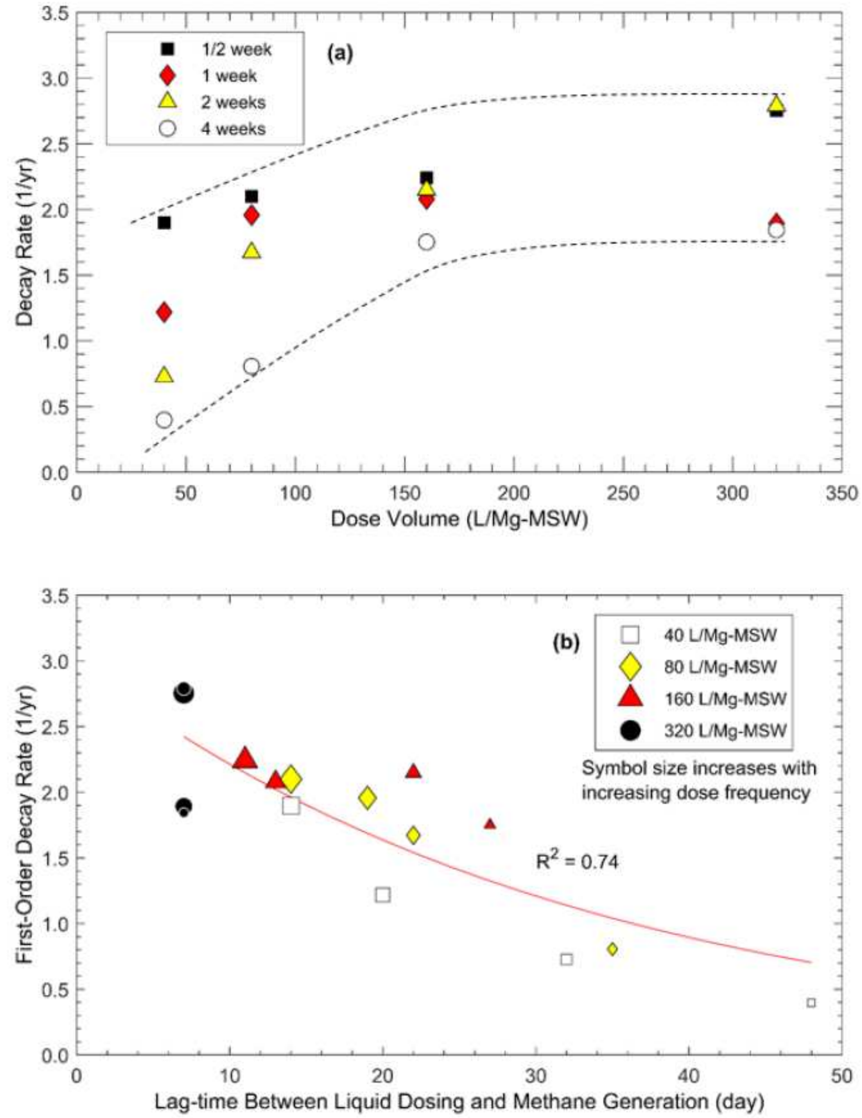

Fig. A6. First-order decay rate for methane generation versus (a) dose volume for reactors grouped based on dose frequency (½ week, 1 week, 2 weeks, and 4 weeks, and (b) lag-time between the start of liquid dosing and onset of biogas generation for reactors grouped based on dose volume (40, 80, 160, and 320 L/Mg-MSW).

The relationship between decay rate and lag-time between liquid dosing and the onset of CH_4 generation is shown in Fig. A6b. Data for all reactors are included in Fig. A6b and grouped with respect to dose volume. The range of dose frequencies is included in each dose volume group, whereby an increase in symbol size corresponds to an increase in dose frequency (i.e., symbol size increases from 4 weeks to ½ week). Reactors that were operated with dose volumes of 40, 80, and 160 L/Mg-MSW all individually support the trend of increased decay rate and reduced lag-time with an increase in dose frequency. However, reactors that were operated with a dose volume of 320 L/Mg-MSW all yielded a lag time of 7 d. The absence of any trend in lag-time for reactors operated with the largest dose volume was attributed to sufficient moisture availability with the initial inoculum addition to start CH_4 generation. In contrast, trends between decay rate and lag-time for the lower three dose volumes suggest that more rapid dosing (i.e., increasing the dose frequency from every 4 weeks to every ½ week) was advantageous to initiating CH_4 generation sooner after the first inoculum dose was added.

A composite analysis of the reactor data was conducted via evaluating the decay rate and lag-time based on the amount of liquid added to each reactor per month. A month time equivalent was used as a method to normalize the data set considering that a month (i.e., 4 weeks) was the longest duration between any two subsequent doses. The relationship between decay rate and lag-time is shown in Fig. A7 with individual plots created for cumulative liquid addition ranging from 40 L/Mg-MSW/month (i.e., R4 = 40 L/Mg-MSW added every 4 weeks) to 2560 L/Mg-MSW/Month (i.e., R13 = 320 L/Mg-MSW added every ½ week). The general trend in the composite data set is a shift to higher decay rates and lower lag-times with an increase in monthly dose volume. Thus, reactors with more aggressive moisture enhancement strategies (higher monthly dosing) attained elevated CH_4 generation (higher decay rate) that initiated in a shorter amount of time following the onset of dosing (reduced lag-time). Fei et al. (2016) report a similar finding in that methods to enhance MSW biodegradation (e.g., moisture availability) had the most pronounced impact on increasing *k* and decreasing lag time, which was based on their evaluation of 49 laboratory experiments and 57 full-scale landfill studies.

The reactors operated with the lowest dose volumes (40 and 80 L/Mg-MSW) that were added only once every 4 weeks lacked sufficient moisture availability, which prolonged the onset of CH_4 generation and reduced CH_4 yield relative to the other reactors. Reactors that were operated such that they received a cumulative monthly liquid addition ≥ 320 L/Mg-MSW achieved decay rates approximately ≥ 2.0 1/yr and lag-times ≤ 22 d. The two highest decay rates of approximately 2.8 1/yr were determined for reactors operated with a dose volume of 320 L/Mg-MSW added on a ½-week and 2-week frequency. If these two reactors are not considered in the composite data set, there was limited change in the decay rate and lag-time as the monthly dose volume increased above 320 L/Mg-MSW. In other words, the influence of additional moisture added to a reactor beyond 320 L/Mg-MSW/month as a means to increase the decay rate and/or decrease the lag-time was not pronounced. There was more value of increasing the moisture enhancement strategy from 40 L/Mg-MSW/month to 320 L/Mg-MSW/month as a means to increase the decay rate and decrease the lag-time for CH_4 generation.

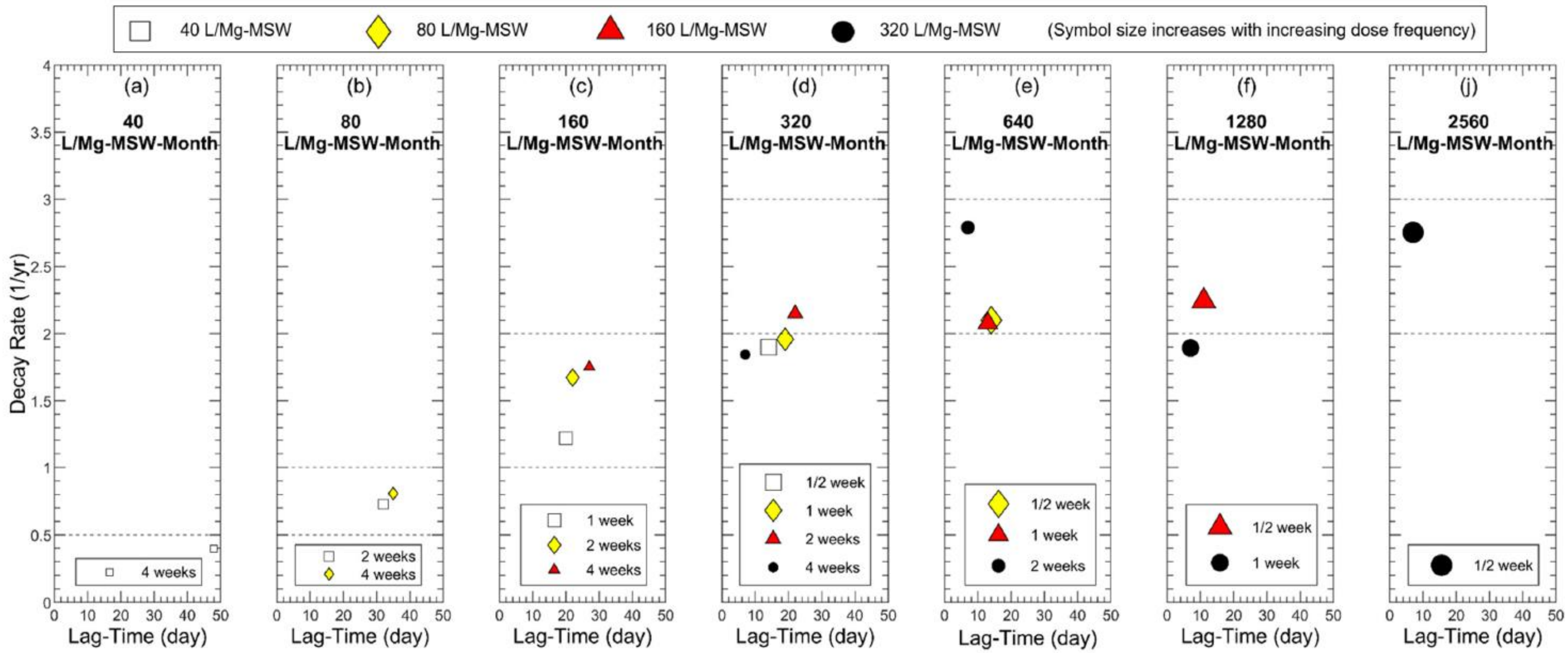

Fig. A7. First-order decay rate for methane generation versus lag-time between the start of liquid dosing and onset of biogas generation for the following monthly dose considerations: (a) 40 L/Mg-MSW/month; (b) 80 L/Mg-MSW/month; (c) 160 L/Mg-MSW/month; (d) 320 L/Mg-MSW/month; (e) 640 L/Mg-MSW/month; (f) 1280 L/Mg-MSW/month; (g) 2560 L/Mg-MSW/month.

4. Practical implications

In general, laboratory reactors operated with higher dose frequencies or dose volumes had shorter lag-times and started CH_4 generation earlier than other reactors. This was attributed to the reactors having sufficient moisture for a suitable microbial environment to accelerate the hydrolysis, fermentation, and acetogenesis phases. The use of centrifuged and diluted anaerobic digester sludge provided the necessary microorganisms for these initial stages of biodegradation, while also providing the necessary methanogenic microorganisms to help transition the reactors to states of active methanogenesis. Cook (2018) indicated that using landfill leachate and liquid waste did not consistently lead to methanogenic conditions in MSW laboratory reactors. However, using anaerobic digester sludge, even in diluted form, was advantageous to anaerobic biodegradation of MSW to generate CH_4.

Select studies have reported moisture enhancement analyses pertaining to the amount of liquid added per mass of waste in full-scale landfills (e.g., Bareither et al. 2010; Abichou et al. 2013a; Nwaokorie et al. 2018). Total liquid added per mass of waste in these studies ranged from approximately 30 to 420 L/Mg-MSW, at the time the studies were conducted. The total duration of liquid addition ranged from less than 1 year to more than 10 years, with average duration between doses ranging on the order of days to months. Thus, considerable variability exists among the moisture enhancement strategies employed in full-scale landfills. Furthermore, Bareither et al. (2013) reported order of magnitude differences between first-order decay rates and elapsed time for the onset of biodegradation between laboratory- and full-scale studies. Considering the variability in moisture enhancement strategies implemented in full-scale landfills and differences that exist in CH_4 generation parameters between laboratory- and full-scale processes (Bareither et al. 2013; Fei et al. 2016), there is no direct methodology for applying laboratory reactor results to predict landfill behavior. However, laboratory studies can provide anecdotal guidance for full-scale landfill operations.

There is an abundance of literature (including most cited in this study) that support enhanced biodegradation and CH_4 generation in landfills practicing liquid addition / leachate recirculation compared to conventional landfills. Nwaokorie et al. (2018) reported full-scale landfill data that show early, aggressive leachate recirculation to approximately 120 L/Mg-MSW during the first 4 yr led to enhanced CH_4 generation, whereas low amounts of leachate added to MSW (< 27 L/Mg-MSW) did not beneficially increase CH_4 generation. In addition, landfill operators and engineers have reported issues with watering out of gas wells, leachate seeps, and excessive leachate generation for aggressive moisture enhancement strategies that may include liquid waste addition and/or leachate recirculation (Bareither et al. 2017). These observations from full-scale landfills, combined with the data compiled from the reactors operated in this study, suggest that there is an optimal range of liquid addition / leachate recirculation that enhances CH_4 generation without leading to issues when excessive liquid is present within the waste mass.

Observations from this study, combined with observations from the state-of-practice, were used to develop guidance for moisture enhancement. If the goal is to increase CH_4 generation and MSW biodegradation, an aggressive moisture enhancement strategy (e.g., larger doses added more frequently) will be more advantageous. An upper-bound cumulative moisture addition (Fig. A7) should be considered, which may help avoid watering-out of gas wells, leachate seeps, and/or additional operational requirements to support leachate management. In addition, sufficient gas collection infrastructure should be in place to aid in removing biogas to amplify recovery and avoid gas pressure buildup. In contrast, if the goal is to reduce leachate treatment, a less aggressive moisture enhancement strategy is more advantageous, whereby liquid may be dispersed throughout the landfill to leverage the moisture holding capacity of the MSW.

5. Summary and conclusions

A laboratory reactor study was conducted to evaluate the influence of moisture enhancement strategies on the biodegradation of MSW. Moisture enhancement strategies implemented in the reactors included four dose volumes (40, 80, 160, and 320 L/Mg-MSW) that were applied in four dose frequencies (½, 1, 2, and 4 weeks). Data were collected to assess moisture response (influent / effluent ratio and moisture content), leachate chemistry (pH, EC, ORP, and COD), and CH_4 generation (CH_4 yield and CH_4 flow rate). Methane generation data were evaluated to determine the first-order decay rate and lag-time between the start of liquid dosing and onset of CH_4 generation.

The majority of reactors generated leachate after reaching wet-weight water contents of 50-52%. The wet-weight water contents stabilized near 60% to 65% for reactors that reached hydraulic equilibrium (i.e., effluent / influent ratio ≈ 90-100%). Biodegradation processes of hydrolysis, acidogenesis, and methanogenesis developed within select reactors prior to leachate generation (e.g., dose volume = 40 L/Mg-MSW and frequencies = 2 and 4 weeks) based initial effluent leachate showing neutral pH and low COD coupled with active CH_4 generation.

The first-order decay rate increased from 0.4 to 1.9 1/yr for reactors operated with a dose volume of 40 L/Mg-MSW as the dose frequency increased from every 4 weeks to every ½ week. The highest decay rates (≈ 2.8 1/yr) and CH_4 yields (≈ 125 m^3/Mg-MSW) were measured in reactors operated with dose frequencies of ½ and 2 weeks and a dose volume of 320 L/Mg-MSW (R13 and R15). In general, the first-order decay rate for CH_4 generation increased with an increase in dose volume for all four dose frequencies. In addition, trends of increased decay rate and reduced lag-time with an increase in dose frequency were observed for reactors operated with dose volumes of 40, 80, and 160 L/Mg-MSW.

An assessment of liquid dosing / leachate recirculation per month indicated that there was a more pronounced impact on increasing decay rate and decreasing lag-time with an increase from 40 L/Mg-MSW/month to 320 L/Mg-MSW/month as compared to the impact from subsequent moisture addition above 320 L/Mg-MSW/month. Reactors with more aggressive moisture enhancement (i.e., higher monthly dosing) attained elevated CH_4 generation (higher decay rate) that initiated at shorter elapsed times following the onset of dosing (reduced lag-time).

6. References

Abichou, T. Barlaz, M.A., Green, R., and Hater, G. (2013a). Liquid balance monitoring inside conventional, Retrofit, and bio-reactor landfill cells. *Waste Management*, 33, 2006-2014. DOI: 10.1016/j.wasman.2013.05.023.

Abichou, T. Barlaz, M.A., Green, R., and Hater, G. (2013b). The Outer Loop bioreactor: A case study of settlement monitoring and solids decomposition. *Waste Management*, 33, 2035-2047. DOI: 10.1016/j.wasman.2013.02.005.

Bareither, C., Benson, C., Barlaz, M., Edil, T., and Tolaymat, T. (2010). Performance of North American bioreactor landfills. I: Leachate hydrology and waste settlement. *Journal of Environmental Engineering,* 136(8), 824-838. DOI: 10.1061/(ASCE)EE.1943-7870.0000219.

Bareither, C., Benson, C., and Edil, T. (2013). Compression of municipal solid waste in bioreactor landfills: Mechanical creep and biocompression. *Journal of Geotechnical and Geoenvironmental Engineering*, 139(7), 1007-1021. DOI: 10.1061/(ASCE)GT.1943-5606.0000835.

Bareither, C.A. and Kwak, S. (2015). Assessment of municipal solid waste settlement models based on field-scale data analysis. *Waste Management*, *42*, 101–117. DOI: 10.1016/j.wasman.2015.04.011.

Bareither, C., Barlaz, M., Doran, M., and Benson, C. (2017). Retrospective analysis of Wisconsin's landfill organic stability rule. *Journal of Environmental Engineering,* 143(5). DOI: 10.1061/(ASCE)EE.1943-7870.0001192.

Barlaz, M.A., Schaefer, D.M., and Ham, R.K. (1989). Bacterial population development and chemical characteristics of refuse decomposition in a simulated sanitary landfill. *Applied and Environmental Microbiology*, *55*(1), 55–65.

Barlaz, M., Chanton, J., and Green, R. (2009). Controls on landfill gas collection efficiency: Instantaneous and lifetime performance. *Journal of the Air & Waste Management Association,* 59, 1399-1404. DOI: 10.3155/1047-3289.59.12.1399

Barlaz, M., Bareither, C., Hossain, A., Saquing, J., Mezzari, I., Benson, C., Tolaymat, T., and Yazdani, R. (2010). Performance of North American bioreactor landfills. II: Chemical and biological characteristics. *Journal of Environmental Engineering,* 136(8), 839-853. DOI: 10.1061/(ASCE)EE.1943-7870.0000220.

Benson, C., Barlaz, M., Lane, D., and Rawe, J. (2007). Practice review of five bioreactor/recirculation landfills. *Waste Management,* 27, 13-29. DOI: 10.1016/j.wasman.2006.04.005

Berge, N.D., Reinhart, D.B., Batarseh, E.S. (2009). An assessment of bioreactor landfill costs and benefits. *Waste Managemet*, 29, 1558-1567. DOI: 10.1016/j.wasman.2008.12.010.

Clarke, W.P., Xie, S., and Patel, M. (2016). Rapid digestion of shredded MSW by sequentially flooding and draining small landfill cells. *Waste Management*, 55, 12-21. DOI: 10.1016/j.wasman.2015.11.050.

Fei, X., Zekkos, D., and Raskin, L. (2016). Quantification of parameters influencing methane generation due to biodegradation of municipal solid waste in landfills and laboratory experiments. *Waste Management*, 55, 276-287. DOI: 10.1016/j.wasman.2015.10.015.

Fei, X. and Zekkos, D. (2018). Coupled experimental assessment of physico-biochemical characteristics of municipal solid waste undergoing enhanced biodegradation. *Géotechnique*, 68(12), 1031-1043. DOI: 10.1680/jgeot.16.P.253.

Feng, S.J., Gao, K.W., Chen, Y.X., Li, Y., Zhang, L.M., and Chen, H.X. (2017). Geotechnical properties of municipal solid waste at Laogang Landfill, China. *Waste Management*, 64, 354-365. DOI: 10.1016/j.wasman.2016.09.016.

Gu, Z., Chen, W., Wang, F., and Li, Q. (2020). A pilot-scale comparative study of bioreactor landfills for leachate decontamination and municipal solid waste stabilization. *Waste Management*, 103, 113-121. DOI: 10.1016/j.wasman.2019.12.023.

Kjeldsen, P., Barlaz, M., Rooker, A., Baun, A., Ledin, A., and Christensen, T. (2002). Present and long-term composition of MSW landfill leachate: A review. *Environmental Science and Technology,* 32(4), 297-336. DOI: 10.1080/10643380290813462.

Loureiro, S.M., Rovere, E.L.L., and Mahler, C.F. (2013). Analysis of potential for reducing emissions of greenhouse gases in municipal solid waste in Brazil, in the state and city of Rio de Janeiro. *Waste Management*, *33*(5), 1302–1312. DOI: 10.1016/j.wasman.2013.01.024.

Morris, J. W. F., Crest, M., Barlaz, M. A., Spokas, K. A., Åkerman, A., & Yuan, L. (2012). Improved methodology to assess modification and completion of landfill gas management in the aftercare period. *Waste Management*, *32*(12), 2364–2373. DOI: 10.1016/j.wasman.2012.07.017

Nwaokorie, K.J., Bareither, C.A., Mantell, S.C., Leclaire, D.J., 2018. The influence of moisture enhancement on landfill gas generation in a full-scale landfill. *Waste Management*, 79, 647-657. DOI: 10.1016/j.wasman.2018.08.036.

O'Donnell, S.T., Caldwell, M.D., Barlaz, M.A., Morris, J.W.F. (2018). Case study comparison of functional vs. organic stability approaches for assessing threat potential at closed landfills in the USA. *Waste Management*, 75, 415-426. DOI: 10.1016/j.wasman.2018.02.001.

Pantini, S., Verginelli, I., & Lombardi, F. (2015). Analysis and modeling of metals release from MBT wastes through batch and up-flow column tests. *Waste Management*, *38*(1), 22–32.

Pohland, F.G. and Kim, J.C., (1999). In situ anaerobic treatment of leachate in landfill bioreactors. *Water Science & Technology*, 40 (8), 203–210. DOI: 10.2166/wst.1999.0422.

Pommier, S., Chenu, D., Quintard, M., and Lefebvre, X. (2007). A logistic model for the prediction of the influence of water on the solid waste methanization in landfills. *Biotechnology and Bioengineering*, 97 (3), 473–482. DOI: https://doi.org/https://doi.org/10.1002/bit.21241

Staley, B., and Barlaz, M. (2009). Composition of municipal solid waste in the united states and implications for carbon sequestration and methane yield. *Journal of Environmental Engineering*, 135(10), 901-909. DOI: 10.1061/(ASCE)EE.1943-7870.0000032.

Staley, B., de los Reyes III, S., and Barlaz, M. (2011). Effect of special differences in microbial activity, pH, and substrate levels on methanogenesis initiation in refuse. *Applied and Environmental Microbiology,* 77(7), 2381-2391. DOI: 10.1128/AEM.02349-10.

Tolaymat, T. M., Green, R. B., Hater, G. R., Barlaz, M. A., Black, P., Bronson, D., and Powell, J. (2010). Evaluation of landfill gas decay constant for municipal solid waste landfills operated as bioreactors. *Journal of the Air and Waste Management Association*, 60(1), 91–97. https://doi.org/10.3155/1047-3289.60.1.91

Tchobanoglous, G., & Kreith, F. (2002). *Handbook of Solid Waste Management*, 2nd Ed. The McGraw-Hill Companies, Inc, New York, USA. DOI: 10.1036/0071356231.

Townsend T.G., Powell J., Jain P., Xu Q., Tolaymat T., and Reinhart D. (2015) *Sustainable Practices for Landfill Design and Operation.* Springer, New York, NY. DOI: 10.1007/978-1-4939-2662-6.

US EPA (2005). Landfill gas emissions model (LandGEM) version 3.02 user's guide. EPA/600/R-05/047, United Stated Environmental Protection Agency, Research Triangle Park, NC 2005.

US EPA (2017). *Advancing Sustainable Materials Management: 2017 Fact Sheet*. EPA 530-F-19-007, United Stated Environmental Protection Agency, Office of Land and Emergency Management (5306P), Washington, DC.

Wong, W.W., 2009. *Investigation of Geotechnical Properties of Municipal Solid Waste*. M.S. Thesis, California Polytechnic State University, San Luis Obispo, California.

Yesiller, N., Hanson, J. L., Cox, J. T., and Noce, D. E. (2014). Determination of specific gravity of municipal solid waste. *Waste Management*, 34(5), 848–858. https://doi.org/10.1016/j.wasman.2014.02.002

Zhan, L.T., Xu, H., Chen, Y.M., Lü, F., Lan, J.W., Shao, L.M., Lin, W.A., and He, P.J. (2017a). Biochemical, hydrological and mechanical behaviors of high food waste content MSW landfill: Preliminary findings from a large-scale experiment. *Waste Management*, 63, 27-40. DOI: 10.1016/j.wasman.2017.03.008.

Zhan, L.T., Xu, H., Chen, Y.M., Lan, J.W., Lin, W.A., Xu, X.B., and He, P.J. (2017b). Biochemical, hydrological and mechanical behaviors of high food waste content MSW landfill: Liquid-gas interactions observed from a large-scale experiment. *Waste Management*, 68, 307-318. DOI: 10.1016/j.wasman.2017.06.023.

APPENDIX B:

Table B1. Summary of hydraulic conductivity experiments that assessed the impacts of vertical stress and dry unit weight on hydraulic conductivity of MSW.

Source	Method	Specimen	Vertical stress (kPa)	Dry unit weight (kN/m^3)	Hydraulic conductivity (m/s)	Description
Fungaroli and Steiner 1979	Laboratory-scale mini-lysimeter, constant head	Milled fresh MSW		0.4 – 3	10^{-4} – 3.2×10^{-5}	D[a] =18.3 mm
Korfiatis et al. 1984	Laboratory column, constant head	Shredded 2-months-old landfilled MSW: paper, cans, glass, some soil, plastic containers, etc.		6.0	1.3×10^{-4} –8.0×10^{-5}	D=565 mm Simulate rainfall
Ettala 1987[b]	Modified double cylinder infiltrometer and pumping tests, Jacob method	Highly compacted			5.9×10^{-9} – 2.5×10^{-8}	Finland
		Lightly Compacted			2.0×10^{-7} – 2.5×10^{-7}	
Oweis et al. 1990	Pump test, Jacob straight-line method	Landfilled MSW			1.6×10^{-5} – 2.5×10^{-5}	New Jersey, U.S.
	In-situ falling head			6.3 – 14.1*	1.5×10^{-6}	
	Test pit infiltration test			6.3 – 9.4*	1.1×10^{-5}	
Bleiker et al. 1993	Falling head	Shredded 10-yrs old landfilled MSW: large pieces of wood such as plywood, plastic, corroded metal, glass, and paper (bundled several sheets thick)	0 – 1200	5.9 – 11.8	1.6×10^{-8} – 1.0×10^{-10}	D=63 mm
Brandle 1994[c]		Fresh MSW		9 – 17	2.0×10^{-5} – 3.0×10^{-8}	

Source	Method	Specimen	Vertical stress (kPa)	Dry unit weight (kN/m3)	Hydraulic conductivity (m/s)	Description
Beaven and Powrie 1995	Large-scale compression cell	Crude domestic refuse	0	3.5	1.7×10^{-4}	D=2 m, W_d^{**} at the start of compression=112%
		Processed refuse smaller than 150 mm	0 – 600	2.5 – 5.9	2.0×10^{-4} – 3.5×10^{-9}	D=2 m, W_d=141%
			600	5.6	1.0×10^{-9}	D=2 m, W_d=40%
		Crude domestic refuse	40 – 600	3.8 – 7.0	3.5×10^{5} – 1.0×10^{-7}	D=2 m, W_d=102%
Zeiss and Uguccioni 1995	Unsaturated hydraulic conductivity, Laboratory-scale	Fresh residential waste from tipping face of landfill+ 75 mm cover soil	4		6.1×10^{-7} – 6.1×10^{-8}	D=570 mm
Chen and Chynoweth 1995	Plexiglas column, constant head	RDF[e] (paper & plastic and yard waste) RDF and yard waste Paper		1.6 – 4.7	8.1×10^{-4} –3.7×10^{-7} 1.3×10^{-3} – 3.4×10^{-6} 3.4×10^{-4} –5.7×10^{-5}	D=370 mm, particles less than 100 mm, hydraulic gradient (i)=2, 2.8, and 4
Townsend et al. 1995	Infiltration ponds, Zaslasky wetting front test	2- to 3-yrs old landfilled MSW		6.2 – 7.8*	4.0×10^{-6} – 3.1×10^{-6}	
Gabr and Valero 1995	Constant and falling head	15- to 30-yrs old landfilled MSW: paper products 2%; plastic, rubber, and textiles 13%; wood 23%; metal products 9%; ceramics ash 10%; rock 10%; soil 33%		7.3 – 8.0	1×10^{-5} – 1×10^{-7}	D=70 mm, Pioneer Crossing landfill, Exeter Township, Berks County, Pennsylvania, U.S.

Source	Method	Specimen	Vertical stress (kPa)	Dry unit weight (kN/m3)	Hydraulic conductivity (m/s)	Description
Landva et al. 1998	Constant head, Consolidometer	Old landfilled MSW: high amount of fabric, plastic bags, wood wastes, paper, trace glass, trace styrofoam, dirty gravel	20 – 200		$3.7\times10^{-5} – 2.9\times10^{-7}$	D=447 mm, Kingston, Ontario, Canada
		Landfilled MSW: wood wastes, plastic, paper, metal waste, fabric, trace glass, moist	20 – 400		$7.0\times10^{-5} – 1.2\times10^{-6}$	D=447 mm, Ottawa old landfill
		Landfilled MSW: wood/wood waste, plastic, paper, metal waste, trace of glass, dirty gravel, moist.	80 – 200		$2.3\times10^{-5} – 9.8\times10^{-8}$	D=447 mm, Edmonton, Canada
		Fresh MSW: high amount of plastic and textiles, paper, wood waste, trace metal waste, trace glass, dirty gravel, damp to moist	90 – 200		$1.9\times10^{-6} – 6.0\times10^{-9}$	
			54 – 300		$1.4\times10^{-5} – 1.1\times10^{-6}$	
Landva et al. 1998	Constant head, Consolidometer	Landfilled MSW: paper, plastic, trace of wood, trace glass, trace metal, trace food waste, dirty gravel	54 – 330		$1.2\times10^{-6} – 2.0\times10^{-8}$	D=447 mm
			54 – 300		$1.4\times10^{-5} – 1.1\times10^{-6}$	
		Artificial MSW: fine paper, plastic, wood and rubber, trace of gravel, trace of metal.	54 – 313		$3.3\times10^{-5} – 2.7\times10^{-6}$	
Powrie and Beaven 1999	Large compression cell, constant head	Crude waste[d]: unprocessed and undegraded, household waste obtained direct from the tipping face of a landfill	34 – 463	3.8 – 7.1	$1.5\times10^{-4} – 3.7\times10^{-8}$	D=2 m
Beaven 2000	Large compression cell, constant head	20-yrs old landfilled waste. material excavated had the appearance of old household waste, with newspapers from 1964 being recovered, contained a large proportion of soil-like material.	36 – 458	6.3 – 9.3	$4.6\times10^{-4} – 1.1\times10^{-7}$	D=2 m, waste contained about 34% fines materials (by weight) which passed through a 10 mm sieve. Essex. England

Source	Method	Specimen	Vertical stress (kPa)	Dry unit weight (kN/m^3)	Hydraulic conductivity (m/s)	Description
Hudson et al. 2001	Large compression cell, constant head	Fresh processed waste	30 – 500	3.9 – 7.2	4.6×10^{-4} –1.4×10^{-8}	D=2 m, Finland
Jang et al. 2002	Constant head	Landfilled MSW and cover soil, paper and cardboard 15%, Plastic and resins 20%, glass 5%, wood 5%, soil and concrete 30%, the rest 25%		7.8 – 1.8	2.95×10^{-4} –2.9×10^{-5}	D=72 mm, Korea
Durmusoglu et al. 2006	Small-scale cells, falling head	10-yrs old landfilled MSW: cloth, paper, glass, and metal and other unidentifiable materials	123 – 369		1.2×10^{-4} – 2.4×10^{-6}	D=63.5 mm, particles were less than 5 mm, Texas, U.S.
	Large-scale consolidometer mold, falling head				1.0×10^{-5} – 4.7×10^{-6}	D=711 mm, particles were less than 20 mm, Texas, U.S.
Olivier and Gourc 2007	A rigid square cell (1 m ×0.98 m), raising/falling head, immersion/drawdown	Degraded reconstituted household waste, fresh to decomposed waste, 55% degradable waste and 45% deformable or inert waste	130		1.0×10^{-4} – 5.0×10^{-6}	Particles less than 150 mm, constituents larger than 150 mm in size, as well as vegetables and raw meat, were shredded
Olivier et al. 2007	A rigid square cell (1 m × 0.98 m), constant head	Pretreated fresh shredded household waste	0 – 130	5.1 – 7.6	1×10^{-6} – 1.2×10^{-7}	
Reddy et al. 2009a	Rigid-wall permeameter, constant head	Shredded fresh MSW from tipping face of landfill, 29% inert (non-biodegradable) waste	0	3.4	1.2×10^{-4} – 4.5×10^{-5}	D=64 mm, Orchard Hills landfill, Illinois, U.S.
	Flexi-wall tri-axial, Constant head		67 – 275	2.9 – 6.1	8.2×10^{-6} – 1.3×10^{-8}	D=70 mm, Orchard Hills landfill, Illinois, U.S.

Source	Method	Specimen	Vertical stress (kPa)	Dry unit weight (kN/m^3)	Hydraulic conductivity (m/s)	Description
Staub et al. 2009	Rigid Polymethyl Methacrylate cylindrical, falling head, used deionized water as a permeant	Landfilled MSW		3.8 – 4.7	$7.7\times10^{-5} – 4.1\times10^{-5}$	D=200 mm, maximum particle size 700 mm, France
				3.7 – 5.2	$7.6\times10^{-5} – 1.3\times10^{-5}$	D=200 mm, maximum particle size 400 mm, France
Olivier et al. 2009	Field pumping tests, Theis and Cooper-Jacob	5- to 7-yrs old landfilled MSW	80 – 150		2.8×10^{-6}	France
Reddy et al. 2009b	Small-scale rigid-wall permeameter, constant head	Fresh MSW from working face (sieved), approximately 70% MSW, 17% construction and demolition waste, 11% soils, and 2% other types of waste	69 – 276	3.9 – 5.1	$2.8\times10^{-5} – 1.2\times10^{-4}$	D=63 mm, the fresh MSW samples had approximately 53%, 16%, and 11% (by wet weight) of the MSW retained on 100-, 50-, and 20-mm sieves, respectively, and 20% (by wet weight) finer than 20 mm
		15- and 19-months-old landfilled MSW exhumed from a borehole in landfill after 1.5-yr leachate recirculation, (sieved)		4.5 – 5.5	$6.3\times10^{-6} – 3.3\times10^{-4}$	D=63 mm, approximately 40%, 12%, and 13% of MSW (by wet weight) retained on 100-, 50-, and 20-mm sieves, respectively
	Large-scale rigid-wall permeameter, constant head	Shredded fresh MSW	0 – 276	4.1 – 13.4	$1.8\times10^{-3} – 4.9\times10^{-5}$	D=300 mm
		Shredded landfilled MSW, 15 and 19 months old		3.2 – 9.6	$2\times10^{-3} – 7.9\times10^{-5}$	
	Small-scale triaxial, constant head	Fresh MSW	69 – 276	6.2 – 6.	$1.4\times10^{-6} – 2.4\times10^{-9}$	D=50 mm
		Landfilled MSW		5.7 – 6.5	$1.6\times10^{-6} –1.4\times10^{-9}$	

Source	Method	Specimen	Vertical stress (kPa)	Dry unit weight (kN/m^3)	Hydraulic conductivity (m/s)	Description
Stoltz et al. 2010	Large-scale oedopermeameter, Constant head	Household and nonhazardous industrial wastes: paper/cardboard, plastic, textiles, glass, metal, garden/food waste, wood, miscellaneous	0 – 200	3.5 – 5.9	1.6×10^{-2} – 4.9×10^{-5}	D=270 mm, particles were less than 70 mm, France
	Large-scale oedopermeameter, Falling head with backpressure		100 – 200	4.8 – 5.9	1×10^{-3} – 1.1×10^{-4}	
Machado et al. 2010	Infiltration test in landfill, Borehole	Landfilled MSW from depth of 1.9 m to 27.2 m	12 – 302		2.6×10^{-5} – 3.8×10^{-8}	65%, 73% and 85% of the particles were smaller than 30 mm for 1-, 4- and 15-yrs old landfilled MSW, respectively. Bandeirantes Landfill, São Paulo, Brazil
	Large triaxial cell	Fresh MSW, paper/cardboard, plastic, rubber, metal, wood, glass, ceramic materials/stone, textile, and paste fraction.	10 – 300		3.4×10^{-5} – 4.1×10^{-8}	D= 400 mm, 50% of particles were smaller than 30 mm, Metropolitan Center landfill,Salvador.
Han et al. 2011	Rigid wall, Forchheimer equation	Crumpled newspaper	30 – 45	1.3 – 2.6*	1.9×10^{-2} – 2.2×10^{-4}	D= 290 mm, particles sizes=50 mm and 100 mm
Jie et al. 2013		The perishable organic components had decayed into organic soil. the remaining non-perishable organic materials included: plastic bags, foam, rubber, cloth, wood, paper, packing boxes, fast food boxes, and disposable plastic tableware; plastic bags were the most common component		9.8 – 15.4	1.8×10^{-5} – 3.1×10^{-10}	China, D=101 mm, the degradation process of MSW at this site was incomplete.

Source	Method	Specimen	Vertical stress (kPa)	Dry unit weight (kN/m^3)	Hydraulic conductivity (m/s)	Description
Zhan et al. 2014	Constant head		20 – 260	6.8 – 9.2	1.4×10^{-7} – 5.5×10^{-6}	D=100 mm, China
Zhang et al. 2016[g]		Fresh MSW		2.4	7.6×10^{-6}	D= 300 mm
Feng et al. 2016	Large-scale rigid-wall, use leachate as a permeant	5.3% metal and glass, 18.6% plastic, 22.9% paper, wood, and fiber, 21.9% organic matter, 31.3% waste residue		3.1 – 4.8	8.0×10^{-3} – 5.5×10^{-5}	D= 400mm, Pudong District of Shanghai, it is China's largest landfill, Samples from 4 m depth, 0.3 yr age
Feng et al. 2016	Large-scale rigid-wall, used leachate as a permeant	2-yrs old landfilled MSW, Samples from 11 m depth, 5.3% Metal and Glass - 18.6% Plastic - 22.9% Paper, Wood, and Fiber - 21.9% Organic matter - 31.3% Waste residue		4 – 6.6	3.2×10^{-3} – 1.1×10^{-4}	D= 400mm, Shanghai, China. It is China's largest landfill,
Feng et al. 2016		4 yrs-old landfilled MSW, samples from 16 m depth, 5.7% metal and glass, 14.7% plastic, 16.5% paper, wood, and fiber, 16% organic matter, 47.1% waste residue		4 – 7.4	5.9×10^{-3} – 9.3×10^{-6}	
Zhang et al. 2018	Constant head	Fresh synthetic shredded MSW	0 – 300	3 – 5.9	1.9×10^{-2} – 8.0×10^{-5}	D= 150 mm, Used different gradient,
Choi et al. 2019	Falling head test	13-yrs old landfilled MSW from 2001 to 2013, extracted from 15 m depth of landfill, 81.8% was biodegradable and 18.2% was non-biodegradable		3.9 – 10.8 * Bulk density	6.3×10^{-6} –4.4×10^{-6}	Sudokwon landfill, Incheon, Republic of Korea

Source	Method	Specimen	Vertical stress (kPa)	Dry unit weight (kN/m^3)	Hydraulic conductivity (m/s)	Description
Bareither et al. 2020	Falling head, consolidation cell	Landfilled MSW extracted from 10 m and 30 m depth, 54% MSW, 20% municipal sewage sludge, 13% special residual waste	50 – 209	11.7 – 16.7	1.7×10^{-5} – 2.1×10^{-6}	D = 305 mm, maximum particle size was 50 mm

* Bulk density (Wet density)
** Dry weight water content
a) D=Diameter of specimen
b) Extracted from Bleiker et al. 1993
c) Powrie et al. 2005
c) Extracted Zhang et al. 2018
d) Crude waste= unprocessed and undegraded, household waste obtained directly from the tipping face of a landfill
e) RDF= Refuse derived fuel
g) Zhang et al. 2018

Table B2. A summary of studies reporting hydraulic conductivity of MSW

Source	Method	Specimen	Hydraulic conductivity (m/s)	Description
Zeiss and Major 1992	Unsaturated hydraulic conductivity in landfill	Residential waste, paper, cardboard, plastic, organics, cans, food waste, grass, small organics, sand, dirt and small plastics	2.1×10^{-4} – 1.2×10^{-5}**	Vertical stress = 4 kPa, Unit weight ranged between 1.6 to 3 kN/m^3, Simulate rainfall, D = 570 mm, West Edmonton landfill, Canada
Shank 1993[b]	Unsaturated hydraulic conductivity in landfill; Bouwer and Rice slug test analysis method	20-yrs old landfilled MSW	6.7×10^{-7} – 9.8×10^{-6} **	Southwest of Gainesville, Florida. US
Hentges et al. 1993[c]	In-situ slug tests	Landfill	2.0×10^{-7} – 2.5×10^{-6}	Iowa Metropolitan Park East Sanitary Landfill, Hamilton County, Iowa, US
Moore et al. 1997	Empirical method	Permeability in test cell with leachate recirculation	3.9×10^{-6}	Yolo county landfill, California, US
Burrows et al. 1997	Pumping test	18-yrs old commercial, industrial, domestic waste and co-disposed materials. At depth of 10 m to 35 m	1.5×10^{-5} – 3.9×10^{-7}	Buckinghamshire, England. The waste was compacted in lifts of up to 2 m in height. The waste was covered daily with an average of 150 mm of low permeability weathered Oxford Clay. Capped with 1 m of engineered Oxford Clay.
		18-yrs old domestic and commercial waste; poorly compacted. At depth of 10 m to 15 m	1.4×10^{-5} – 6.7×10^{-5}	Cambridgeshire, England.
Wysocki et al. 2003[d]	Pumping Test		1.2×10^{-7} – 6.3×10^{-6}	
Jain et al. 2006	Borehole Permeameter Test	MSW; Relatively new and undegraded waste	6.1×10^{-7} – 5.4×10^{-8}	3 m to 6 m depth of borehole
			2.3×10^{-7} to 5.6×10^{-8}	6 m to12 m depth of borehole
			1.9×10^{-7} to 7.4×10^{-8}	12 m to 18 m depth of borehole

Source	Method	Specimen	Hydraulic conductivity (m/s)	Description
Machado et al. 2010	Infiltration tests in boreholes in landfill; Constant head	Fresh MSW; paper/cardboard, plastic, rubber, metal, wood, glass, ceramic materials/stone, textile, and paste fraction	7.8×10^{-5} to 3.3×10^{-5}	Waste at depth of 1.9 m to 27.2 m. To compare field and triaxial lab results at rest pressure K_0 was assumed equal to 0.4. 65%, 73%, and 85% of the elements were smaller than 30 mm for 1-, 4- and 15-yrs old MSW, respectively. Bandeirantes Landfill, São Paulo, Brazil
Bareither et al. 2012	Field-scale experiment conducted in a drainage lysimeter	Landfilled MSW	4.1×10^{-5} to 4.0×10^{-6}	D=2.4 m, Hydraulic conductivities measured after 800 to 1040 days after onset of experiment.
Wu et al. 2012	Injection in landfill; Model proposed by Zangar (1953)	5- to 12-yrs old Waste; primarily residential waste and some commercial waste	$6.6\times10^{-6} – 7.2\times10^{-6}$	Shallow layer (1 to 4 m deep); 40 km south of Beijing, China,
			$1.6\times10^{-6} – 1.6\times10^{-6}$	Middle layer (11 to 14 m deep); 40 km south of Beijing, China
			$5.9\times10^{-7} – 6.7\times10^{-7}$	Deep layer (22 to 25 m deep); 40 km south of Beijing, China.
Zhan et al. 2014	Pumping test		$2.4\times10^{-6} – 5.5\times10^{-6}$	15.5 m to 17.5 m depth; China
Gao et al. 2015	Triaxial permeability tests	Undisturbed Landfilled MSW specimen, 55% kitchen waste, 12% plastics. Cut from integral, undisturbed MSWs.	$3.9\times10^{-6} – 3.6\times10^{-8}$	Specimens from depths of 4.2 m to 29.2 m, D [e]=100 mm, China
	Pumping tests	MSW	4.0×10^{-6}	At depth of 16.6 m, China
Zhang et al. 2016[f]		Fresh MSW	7.6×10^{-6}	D= 300 mm

** Unsaturated hydraulic conductivity

a) From Jain et al. 2006
b) From Penmethsa 2007
c) From Bleiker et al. 1995
d) From Jain et al. 2006
e) Diameter of specimen
f) From Zhang et al. 2018

Table B3. Summary of laboratory tests based on impacts of degree of decomposition on hydraulic conductivity of MSW

Source	Method	Decomposition phase	Vertical stress (kPa)	Dry unit weight (kN/m^3)	Hydraulic conductivity (m/s)	Description
Korman et al. 1987[a]	Rigid wall	Fresh MSW, Hollow stem auger and reconstituted samples to the same density			$2.0\times10^{-7} - 3.0\times10^{-9}$	
	Shelby tubes, Flexible wall	Approximately 1- to 15-yrs old waste, undisturbed specimen, waste from paper mills			$2.0\times10^{-8} - 4.0\times10^{-9}$	Samples from 8.07 m to 8.2 m and 12.65 m depth
Olivier et al. 2007	A rigid square cell (1 m × 0.98 m), Constant head	Fresh shredded pretreated household waste, 60% biodegradable	0 – 130	5.13 – 7.60	$10^{-6} - 1.2\times10^{-7}$	
		Two-yrs old MSW, 35% of MSW was decomposed after two years	130			The waste specimen had become impervious. Thus, the hydraulic conductivity could not be assessed.
Hossain et al. 2009	Constant head	Aerobic		6.47 – 9.32	$1.1 - 2.8\times10^{-1}$	Refuse representative of various decomposition stages, generated in the laboratory. D[b]=152.4 mm, particle size larger than 76 mm were shredded.
		Anaerobic		6.45 – 9.17	$5.6\times10^{-1} - 1.9\times10^{-1}$	
		Accelerated methane production		6.38 – 9.12	$2.6\times10^{-1} - 1.6\times10^{-1}$	
		Decelerated methane production		6.65* – 9.14*	$1.3\times10^{-1} - 7.2\times10^{-2}$	
Reddy et al. 2011	Rigid wall permeameter, constant and falling head, used deionized water as permeant	Fresh MSW	0 – 276	6.3 – 8.4	$5.1\times10^{-6} - 8.5\times10^{-10}$	Fresh synthetic shredded MSW prepared in the laboratory, D=50 mm, Typical composition of MSW generated in the U.S., 60% biodegradable fractions and 40% non-biodegradable fractions on wet mass basis
		Anaerobic		8.3 – 11.1	$1.6\times10^{-7} - 5.7\times10^{-10}$	
	Falling head, used deionized water as permeant	Accelerated methane production		11 – 11.9	$1.0\times10^{-9} - 9\times10^{-11}$	Flexible wall permeameter, D=50 mm, Synthetic MSW decomposed in laboratory
		Decelerated methane production		10.2 – 11.4	$1.2\times10^{-7} - 5.5\times10^{-10}$	
		Methane stabilization		12.1 – 12.4	$1.7\times10^{-9} - 2.3\times10^{-10}$	

Source	Method	Decomposition phase	Vertical stress (kPa)	Dry unit weight (kN/m3)	Hydraulic conductivity (m/s)	Description
Ke et al. 2017	Triaxial flexible wall, Upward flow	Synthetic MSW after 3 months Degradation	38 – 285		$2.5\times10^{-6} - 3.0\times10^{-8}$	Triaxial permeameter, D=100 mm, Particle size larger than 30 mm were shredded. Void ratio=3
					$9.0\times10^{-6} - 7.0\times10^{-8}$	Void ratio=4
					$4.0\times10^{-5} - 9.0\times10^{-8}$	Void ratio=5
		Synthetic MSW after 6 months Degradation	38 – 280		$1.4\times10^{-6} - 4.9\times10^{-8}$	Void ratio=2.6
					$6.0\times10^{-6} - 7.0\times10^{-8}$	Void ratio=3.6
					$6.0\times10^{-6} - 8.0\times10^{-8}$	Void ratio=4.6
		Synthetic MSW after 9 months Degradation	38 – 287		$1.0\times10^{-6} - 3.5\times10^{-8}$	Void ratio=2.2
					$4.2\times10^{-5} - 6.0\times10^{-8}$	Void ratio=3.2
					$1.8\times10^{-5} - 8.0\times10^{-8}$	Void ratio=4.2
Miguel et al. 2018	Large-scale rigid wall, Constant	92 days degradation experiments45.5% organic matter, 12.9%paper and cardboard, 15.3% hard and soft plastics.		7.1* 6.2*	$9.0\times10^{-5} - 7.4\times10^{-6}$ $1.3\times10^{-4} - 2.3\times10^{-5}$	D= 300 mm
		42.9% organic matter, 12.8%paper and cardboard, 12.8% hard and soft plastics.		7.2*	$3.0\times10^{-3} - 6.0\times10^{-5}$	196 days acid-stuck condition after about 90 days, Remain in anaerobic acid phase
				4.9*	$1.0\times10^{-2} - 6.0\times10^{-3}$	89 days, Acid-stuck condition
Breitmeyer et al. 2019	Falling head	Initial MSW	0-400	5.5 – 11	$2\times10^{-3} - 3\times10^{-7}$	Small-scale rigid wall permeameter, D=150 mm, shredded MSW
		Low degradation		6.2 – 9.2	$2.4\times10^{-2} - 4.1\times10^{-4}$	
		Medium degradation		5.2 – 10.2	$10 - 7.7\times10^{-3}$	
		High degradation		5.2 – 9.2	$9.3 - 5.8\times10^{-2}$	
	Constant head	Initial MSW		5.2 – 8.8	$7.7\times10^{-1} - 6.8\times10^{-4}$	Large-scale rigid wall permeameter, D=305 mm, unshredded MSW
		Final (Decomposed) MSW		5.2 – 8.8	$3.4 - 3.1\times10^{-2}$	

* Bulk density (Total unit weight)
a) From Penmethsa 2007
D=Diameter of specimen

APPENDIX C:

Table C1. Summary of geotechnical laboratory tests on HMW

Source	Waste type	Water content (%)[a]	Compaction method	Optimum water content (%)	Maximum dry unit weight (kN/m^3)	Liquid limit (%)	Plasticity index (%)	Specific gravity	Hydraulic conductivity (m/s)	Description
Belfiore et al. 1990	Industrial Sludges	-	-	100	9.6	160	106	-	10^{-10}-10^{-7}	Vertical stress for k[b] test: 150 kPa
Koenig et al. 1996	Dewatered wastewater wludge	-	-	-	-	-	-	-	1.36×10^{-12}-26.6×10^{-12}	-
Lo et al. (2002)	Dewatered sewage sludge	180 and 43	Standard Proctor	40	6.47	-	-	1.55	5×10^{-9}-6×10^{-11}	Range of vertical stress for k test 24-196 kPa
O'Kelly (2006)	Municipal sewage sludge	720	Standard Proctor	85	5.49	315	260	1.55	10^{-9}	-
Suthagaran et al. (2010)	Biosolids	46.8-58.6	Standard Proctor	48- 56	8.14-8.53	100-110	21-27	1.75-1.79	1.24×10^{-7}-1.60×10^{-7}	-
Chiado 2014	Exploration and Production waste	5-110	-	-	-	44	16	2.15-2.85	2×10^{-7} to 1×10^{-11}	
Bareither et al. (2020)	High-moisture waste	125 - 155	-	-	-	-	-	-	1.1×10^{-11} and 8.7×10^{-12}	Vertical stress for k test 49 kPa - 100 kPa

a) Mass of water per mass of solids
b) k=Hydraulic conductivity

Table C2. Recommended maximum hydraulic gradient for hydraulic conductivity test according to ASTM D5856

Range of Hydraulic Conductivity (m/s)	Recommended Maximum Hydraulic Gradient
1×10^{-5} to 1×10^{-6}	2
1×10^{-6} to 1×10^{-7}	5
1×10^{-7} to 1×10^{-8}	10
1×10^{-8} to 1×10^{-9}	20
$< 1\times10^{-9}$	30

Fig. C1. Photograph of (a) recyclable municipal solid waste, (b) yard waste, (c) food waste

Fig. C2. Photograph of (a) shredded wood mulch, (b) shredding food waste, (c) squeezing food waste to reduce moisture content.

Fig. C3. Photograph of well-mixed MSW representing average municipal solid waste generated in the US

Fig. C4. Photograph of (a) Oil and gas Exploration and Production waste (E&PW) obtained from a landfill and stored in 5-gallons buckets, (b) sample of E&PW, (c) mixing E&PW to prepare a homogenous waste

Fig. C5. Photograph of paint filter test

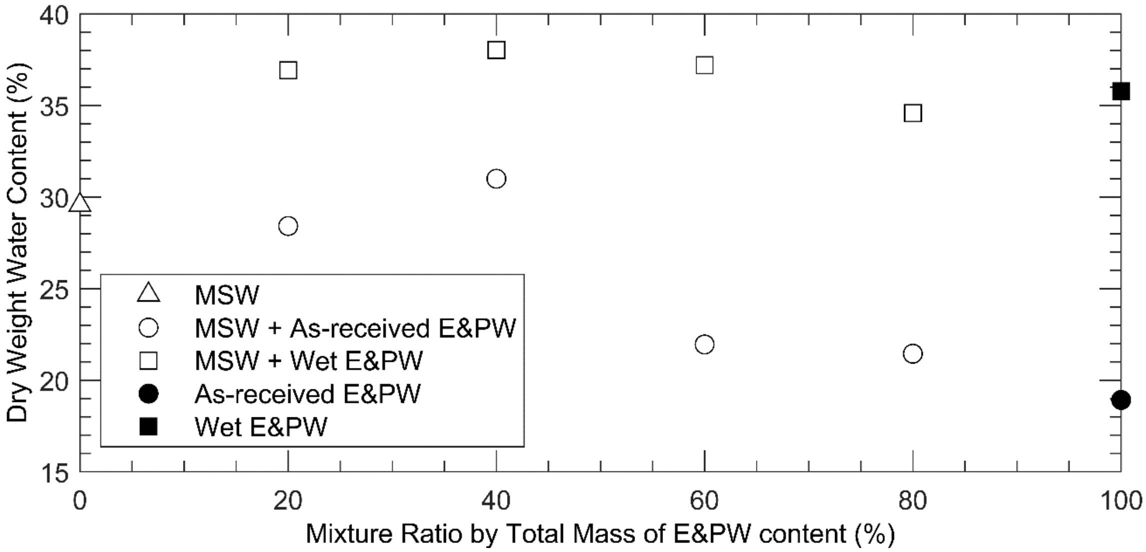

Fig. C6. Relationship between dry weight water content and MSW-E&PW mixture ratios

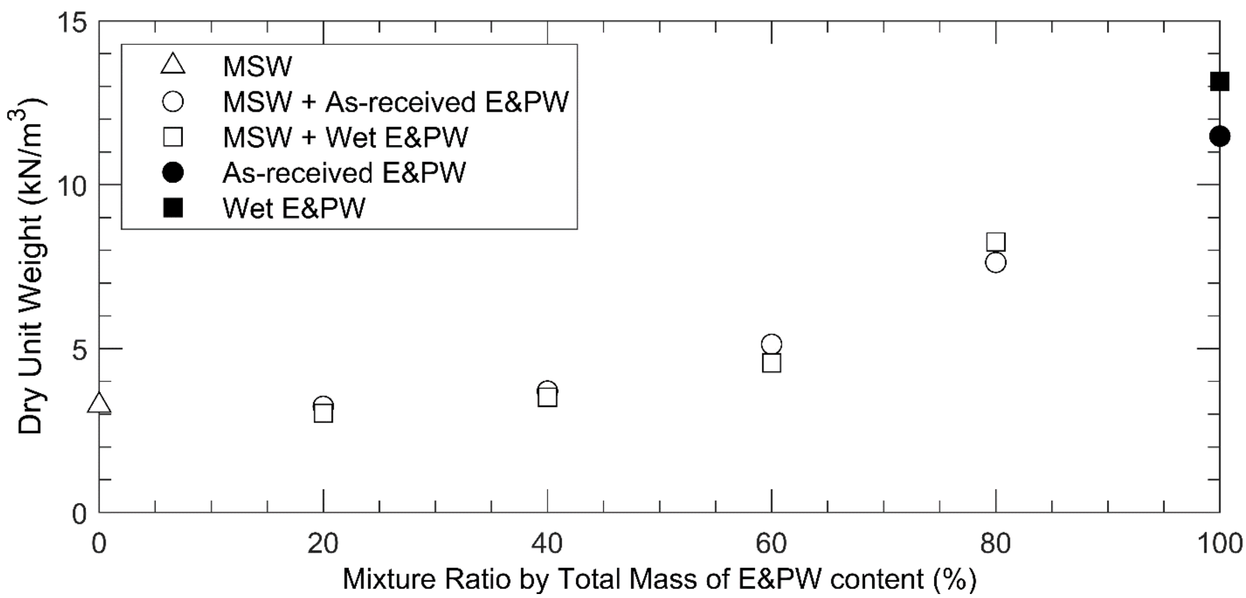

Fig. C7. Relationship between dry unit weight and MSW-E&PW mixture ratios

APPENDIX D:

Compaction tests:

Compaction tests were conducted according to the modified Proctor compaction test (ASTM D1557-Method C) as the author believes the results of modified Proctor compaction tests can be used as target unit weights for creating specimens for hydraulic conductivity tests. In general, compacting MSW using laboratory equipment is arduous work, and it is not feasible to obtain high dry unit weight, especially for the fresh waste that does not contain soil or soil-like materials. Modified Proctor compaction tests are doable and feasible to perform in the laboratory. A 152-mm diameter mold was used to compact waste materials. The maximum dimensions of waste particles were less than 20 mm, and waste constituents were passed a sieve with 20-mm openings. The range of dry weight water content of MSW specimens was between 33% to 127% to reflect the compaction behavior of relatively dry and wet waste. A pre-determined amount of water required to reach the target water contents for each specimen was added to MSW. After that, each specimen was kept in a sealed bucket to allow them to hydrate for 24 h prior to the compaction test.

The results of modified Proctor tests on MSW are shown in Fig. D1. The optimum dry weight water content was 116%, and the maximum dry unit weight ($\gamma_{d\ max}$) was 4.33 kN/m^3. The results of modified Proctor compaction tests by Hanson et al. 2010 were shown in Fig. D1 to compare with the current study. The optimum water content and $\gamma_{d\ max}$ were determined 65% and 5.2 kN/m^3. The differences in results are attributed to the waste constituent, initial waste content, and using an automatic compactor. Hanson et al. 2010 used waste particles that initially had some moisture content, and this could affect the physical behavior of waste. Although in both experiments MSW specimens were hydrated for approximately 24 hr (i.e., 16 hr to 24 hr), in the current study initially wastes were in dry condition, and they adsorb the moisture only when they were mixed with food waste or mixed with added water for specimens with higher water content.

Thus, they only had 24 hr to hydrate. However, some of the waste constituents utilized in Hanson et al. (2010) study were initially contained 11% natural moisture content (Wong 2009). Further, using an automatic compactor can reduce human errors during the compaction process.

Compaction tests were conducted for the mixtures of as-received E&PW and MSW to determine a target dry unit weight corresponding to each mixture ratio for specimen preparation. The water content of the compacted materials for the Proctor test was relatively similar to the specimens were prepared for the hydraulic conductivity tests.

For E&PW, compaction tests were performed initially on waste with as-received water content. Then, a pre-determined about of water was added to E&PW and mixed it thoroughly. To capture the dry behavior of E&PW (i.e., water content less than 18%), E&PW was air-dried for three days and then utilized to run the Proctor test. A pre-determined amount of water was added to air-dried E&PW for the first two data points.

The results of dry unit weights from modified Proctor compaction tests and compaction of specimens were prepared for hydraulic conductivity tests are shown in Fig. D2. For pure MSW, the specimen was compacted according to the target density obtained from the Proctor compaction test. However, for 20% mixture ratio, the specimen compacted to the 76% of target density, and the ratio of "specimen dry unit weight to modified Proctor dry unit weigh" reduced to 64% on average for the 40% 60%, and 80% mixture ratios. This reduction is due to addition of E&PW which are less compressible than MSW materials and reduce the moisture content of specimen which reduce the compressibility of the waste materials. The results of modified Proctor tests on E&PW are shown in Fig. D3. The optimum dry weight water content was 10%, and the maximum dry unit weight was 18.24 kN/m^3.

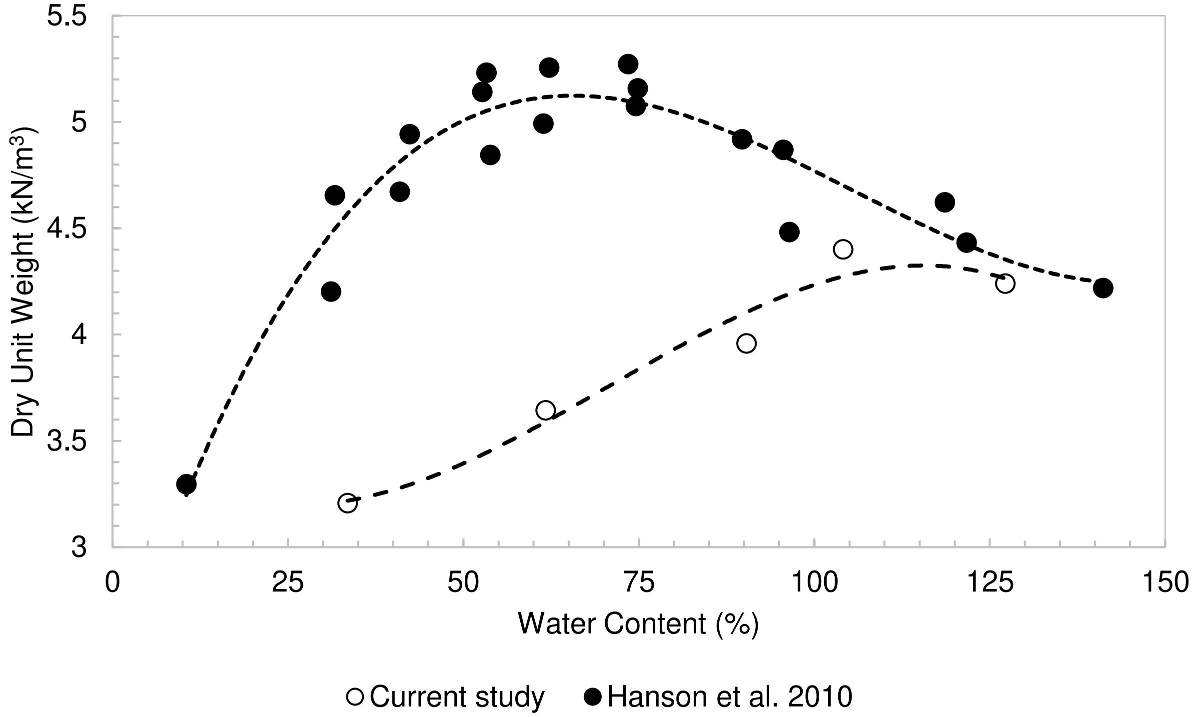

Fig. D1. Laboratory modified Proctor compaction data on municipal solid waste

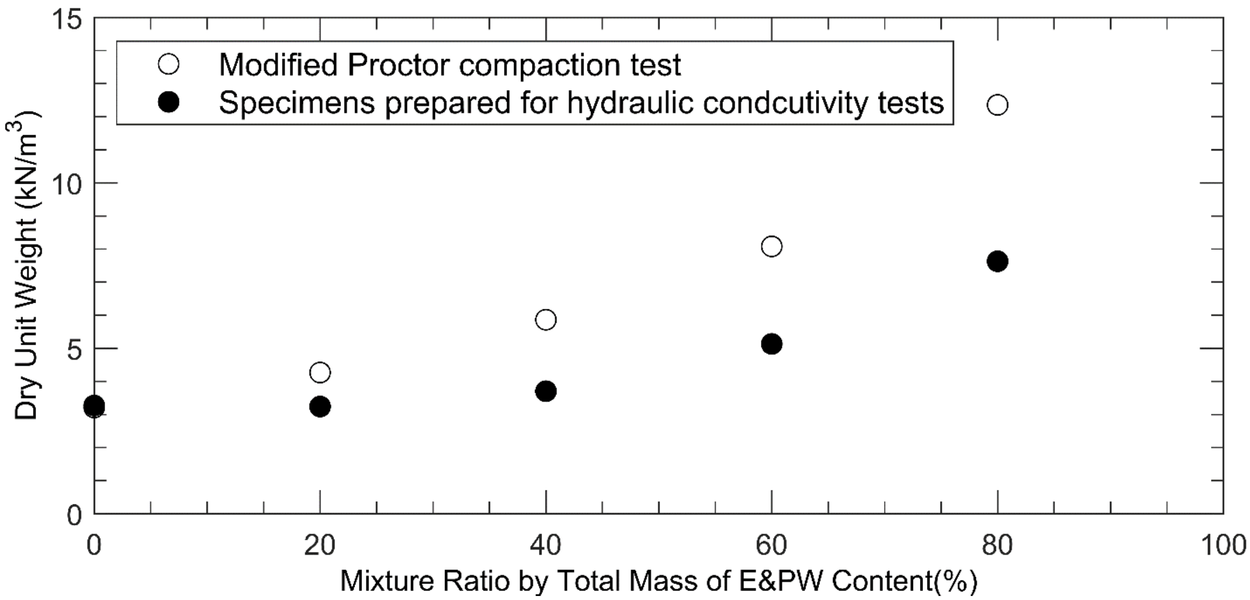

Fig. D2. Dry unit weight data from modified Proctor compaction tests and hydraulic conductivity tests specimens for MSW and mixtures of MSW and as-received E&PW

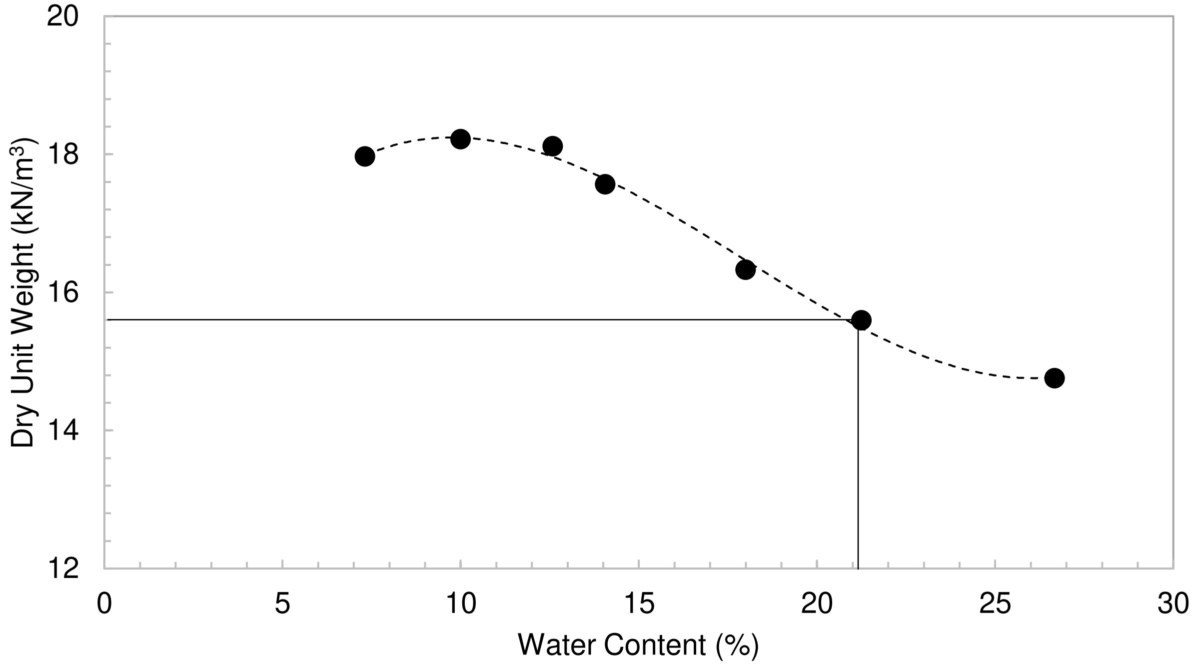

Fig. D3. Laboratory modified Proctor compaction on oil and gas exploration and production waste (E&PW)

APPENDIX E:

Table E1. Summary of saturated hydraulic conductivity tests on municipal solid waste (MSW).

Method	Dry Unit Weight (kN/m^3)	Effective Vertical Stress (kPa)	Void Ratio	Hydraulic Conductivity (m/s)
Constant-Head	3.34	1	2.70	4.4×10^{-5}
	3.56	9	2.47	3.1×10^{-5}
	3.84	24	2.22	1.7×10^{-5}
	4.15	48	1.98	9.6×10^{-6}
	4.60	98	1.68	3.1×10^{-6}
	5.19	196	1.38	7.7×10^{-7}
	5.60	296	1.21	8.9×10^{-7}
	6.06	396	1.04	6.6×10^{-7}

Table E2. Summary of saturated hydraulic conductivity tests on oil and gas exploration and production waste (E&PW) at as-received condition.

Method	Dry Unit Weight (kN/m^3)	Effective Vertical Stress (kPa)	Void Ratio	Hydraulic Conductivity (m/s)
Constant-Head	11.52	1	1.25	7.3×10^{-5}
	11.87	5	1.18	6.7×10^{-5}
	12.34	11	1.10	6.1×10^{-5}
	13.02	24	0.99	5.6×10^{-5}
	13.77	49	0.88	2.6×10^{-5}
	14.57	98	0.78	4.6×10^{-6}
Falling-Head	15.43	198	0.68	1.1×10^{-7}
	16.36	394	0.58	1.1×10^{-8}

Table E3. Summary of saturated hydraulic conductivity tests in 102-mm rigid-wall permeameter on E&PW at as-received condition.

Method	Effective Vertical Stress (kPa)	Hydraulic Conductivity (m/s)
Falling-Head	1	$1.2 \times 10\text{-}7$
	6	$1.5 \times 10\text{-}8$
	12	$4.2 \times 10\text{-}9$
	25	-
	50	$1.1 \times 10\text{-}9$
	100	$1.1 \times 10\text{-}9$
	200	$1.1 \times 10\text{-}9$

Table E4. Summary of saturated hydraulic conductivity tests on oil and gas exploration and production waste at the wet condition.

Method	Dry Unit Weight (kN/m3)	Effective Vertical Stress (kPa)	Void Ratio	Hydraulic Conductivity (m/s)
Constant-Head	14.05	1	0.84	6.6×10-6
Falling-Head	14.47	3	0.79	1.3×10-7
	14.63	6	0.77	1.8×10-8
	14.95	17	0.73	5.4×10-9
	15.39	40	0.68	2.6×10-9
	15.89	90	0.63	1.3×10-9
	16.56	189	0.56	5.4×-10
	17.23	389	0.50	2.8×-10

Table E5. Summary of saturated hydraulic conductivity tests on the mixture of 80%MSW with 20% oil and gas exploration and production waste at the as-received condition.

Method	Dry Unit Weight (kN/m3)	Effective Vertical Stress (kPa)	Void Ratio	Hydraulic Conductivity (m/s)
Constant-Head	3.40	1	3.06	5.7×10-5
	3.62	5	2.82	4.7×10-5
	3.81	11	2.63	3.9×10-5
	4.13	24	2.34	2.7×10-5
	4.58	49	2.02	1.4×10-5
	5.19	98	1.66	5.7×10-6
	6.00	198	1.30	9.5×10-7
Falling-Head	7.04	397	0.96	2.4×10-7

Table E6. Summary of saturated hydraulic conductivity tests on the mixture of 80% MSW with 20% E&PW at the wet condition.

Method	Dry Unit Weight (kN/m3)	Effective Vertical Stress (kPa)	Void Ratio	Hydraulic Conductivity (m/s)
Constant-Head	3.12	1	3.43	6.0×10^{-5}
	3.28	5	3.21	5.5×10^{-5}
	3.48	11	2.97	4.6×10^{-5}
	3.80	24	2.63	3.5×10^{-5}
	4.30	49	2.21	2.2×10^{-5}
	4.97	98	1.78	8.6×10^{-6}
	5.87	198	1.35	2.0×10^{-6}
Falling-Head	7.07	395	0.95	1.1×10^{-7}

Table E7. Summary of saturated hydraulic conductivity tests on the mixture of 60% MSW with 40% E&PW at the as-received condition.

Method	Dry Unit Weight (kN/m3)	Effective Vertical Stress (kPa)	Void Ratio	Hydraulic Conductivity (m/s)
Constant-Head	3.85	1	3.06	5.6×10^{-5}
	4.06	5	2.85	5.1×10^{-5}
	4.28	11	2.65	4.4×10^{-5}
	4.61	24	2.39	3.3×10^{-5}
	5.11	49	2.06	1.5×10^{-5}
	5.73	98	1.73	4.8×10^{-6}
	6.51	196	1.40	9.1×10^{-7}
Falling-Head	7.33	396	1.13	8.9×10^{-8}

Table E8. Summary of saturated hydraulic conductivity tests on the mixture of 60% MSW with 40% E&PW at wet condition.

Method	Dry Unit Weight (kN/m3)	Effective Vertical Stress (kPa)	Void Ratio	Hydraulic Conductivity (m/s)
Constant-Head	3.73	1	3.19	6.2×10-5
	3.95	5	2.96	5.4×10-5
	4.16	11	2.76	4.5×10-5
	4.52	24	2.46	3.3×10-5
	5.07	49	2.08	1.9×10-5
	5.81	98	1.69	6.1×10-6
	6.75	198	1.32	1.4×10-6
Falling-Head	7.80	396	1.00	9.0×10-8

Table E9. Summary of saturated hydraulic conductivity tests on the mixture of 40% MSW with 60% E&PW at the as-received condition.

Method	Dry Unit Weight (kN/m3)	Effective Vertical Stress (kPa)	Void Ratio	Hydraulic Conductivity (m/s)
Constant-Head	5.68	5	2.17	6.1×10^{-5}
	5.88	11	2.06	4.9×10^{-5}
	6.25	24	1.88	4.3×10^{-5}
	6.89	49	1.62	3.3×10^{-5}
	7.71	98	1.34	1.7×10^{-5}
Falling-Head	8.76	196	1.06	4.6×10^{-6}
	9.65	396	0.87	5.4×10^{-7}

Table E10. Summary of saturated hydraulic conductivity tests on the mixture of 40% MSW with 60% E&PW at the wet condition.

Method	Dry Unit Weight (kN/m3)	Effective Vertical Stress (kPa)	Void Ratio	Hydraulic Conductivity (m/s)
Constant-Head	4.81	1	2.75	6.0×10-5
	4.98	5	2.62	5.1×10-5
	5.17	11	2.48	4.0×10-5
	5.42	24	2.33	2.8×10-5
	5.90	49	2.05	1.5×10-5
	6.54	98	1.75	4.8×10-6
	7.33	197	1.46	6.8×10-7
Falling-Head	8.29	396	1.17	5.7×10-8

Table E11. Summary of saturated hydraulic conductivity tests on the mixture of 20% MSW with 80% E&PW at as-received condition.

Method	Dry Unit Weight (kN/m3)	Effective Vertical Stress (kPa)	Void Ratio	Hydraulic Conductivity (m/s)
Constant-Head	7.83	1	1.71	6.3×10-5
	8.06	5	1.64	5.7×10-5
	8.30	11	1.56	5.1×10-5
	8.64	24	1.46	4.4×10-5
	9.24	49	1.30	3.2×10-5
	10.09	99	1.11	1.0×10-5
Falling-Head	11.08	197	0.92	1.3×10-6
	12.29	396	0.73	9.9×10-8

Table E12. Summary of saturated hydraulic conductivity tests on the mixture of 20% MSW with 80% E&PW at the wet condition.

Method	Dry Unit Weight (kN/m3)	Effective Vertical Stress (kPa)	Void Ratio	Hydraulic Conductivity (m/s)
Constant-Head	8.40	1	1.53	5.5×10^{-5}
	8.55	5	1.48	3.9×10^{-5}
	8.77	11	1.42	3.3×10^{-5}
	9.09	24	1.34	2.4×10^{-5}
	9.56	49	1.22	1.3×10^{-5}
	10.13	98	1.10	2.9×10^{-6}
Falling-Head	10.98	197	0.94	4.1×10^{-7}
	12.07	394	0.76	3.3×10^{-8}

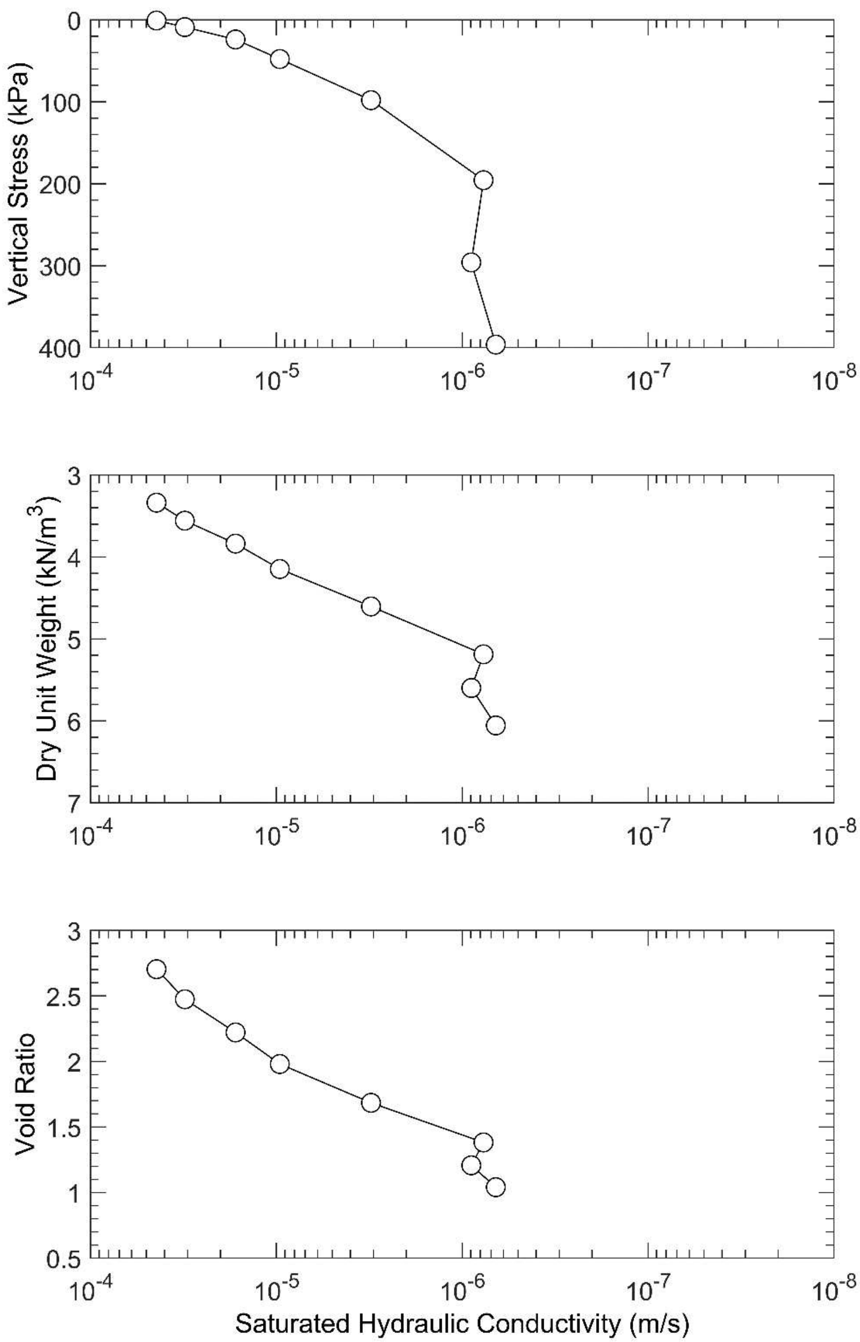

Fig. E1. Summary of saturated hydraulic conductivity tests on municipal solid waste (MSW).

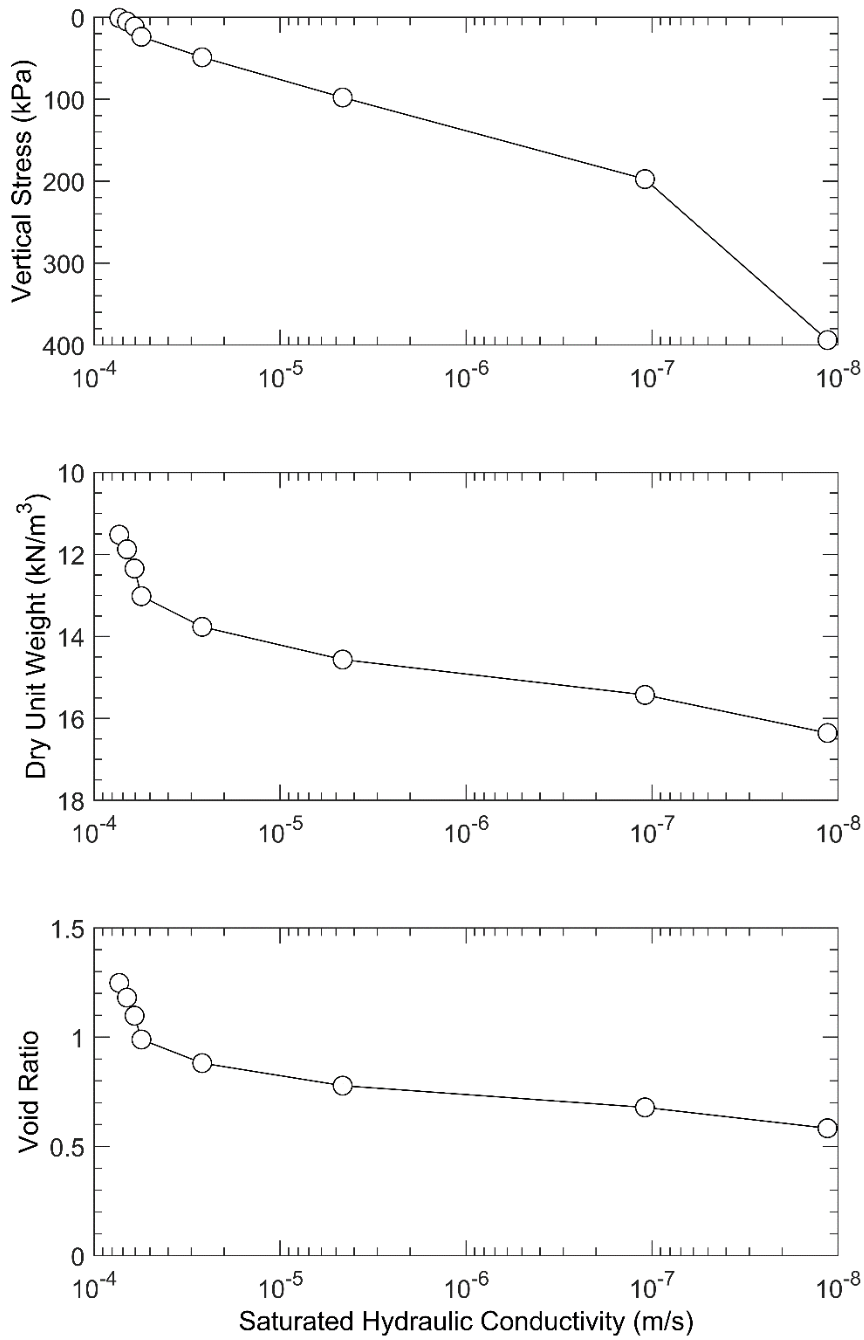

Fig. E2. Summary of saturated hydraulic conductivity tests on E&PW at the as-received condition.

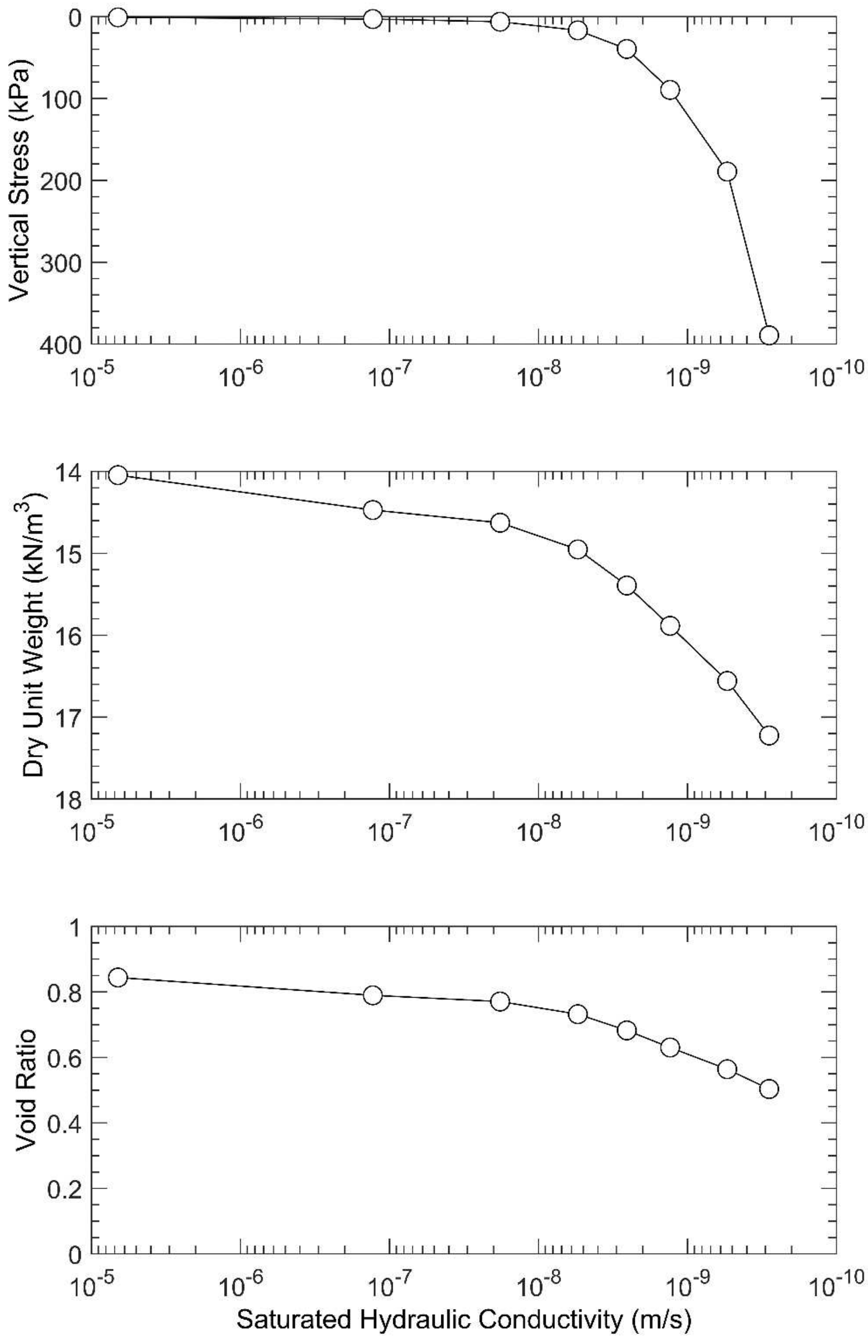

Fig. E3. Summary of saturated hydraulic conductivity tests on E&PW at the wet condition.

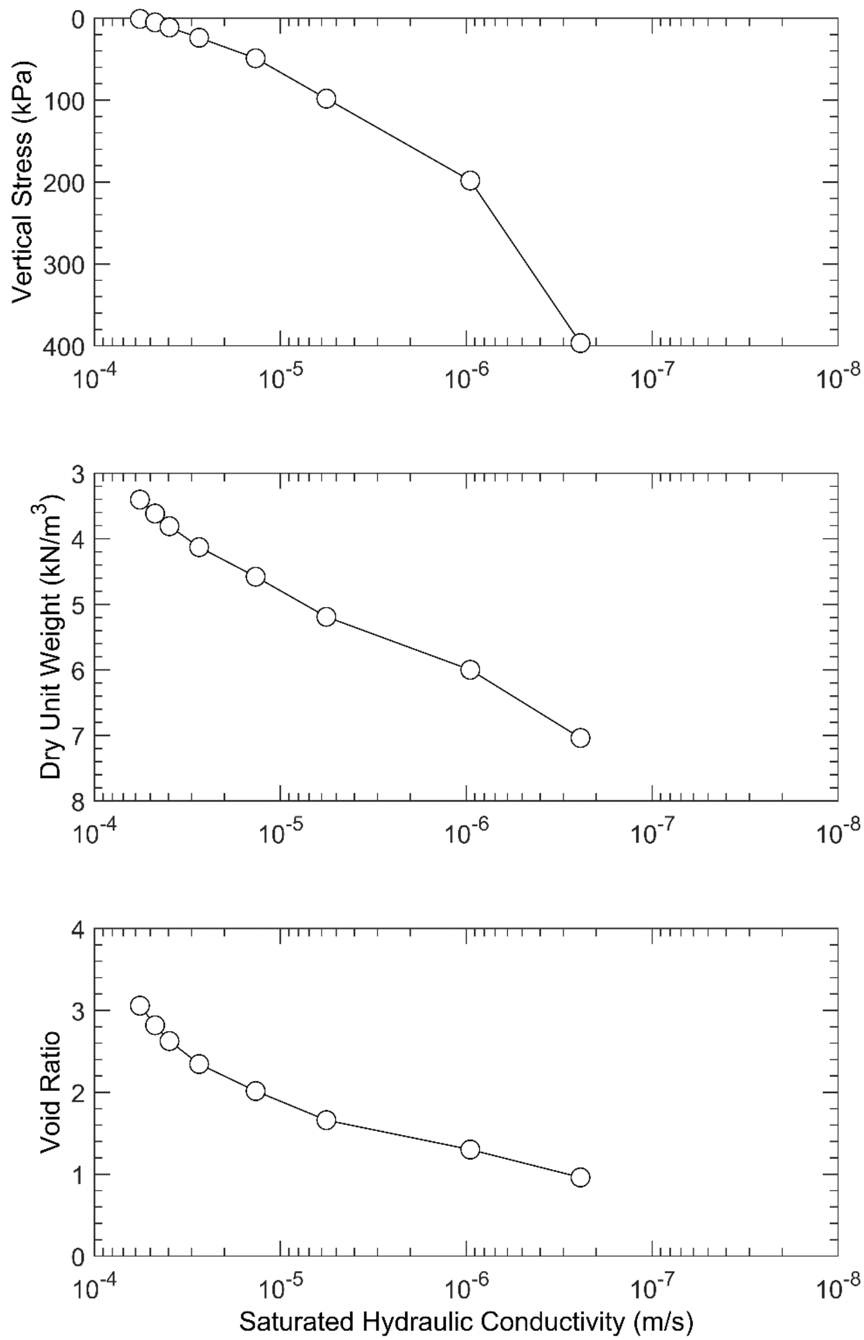

Fig. E4. Summary of saturated hydraulic conductivity tests on the mixture of 80% MSW with 20% E&PW at the as-received condition.

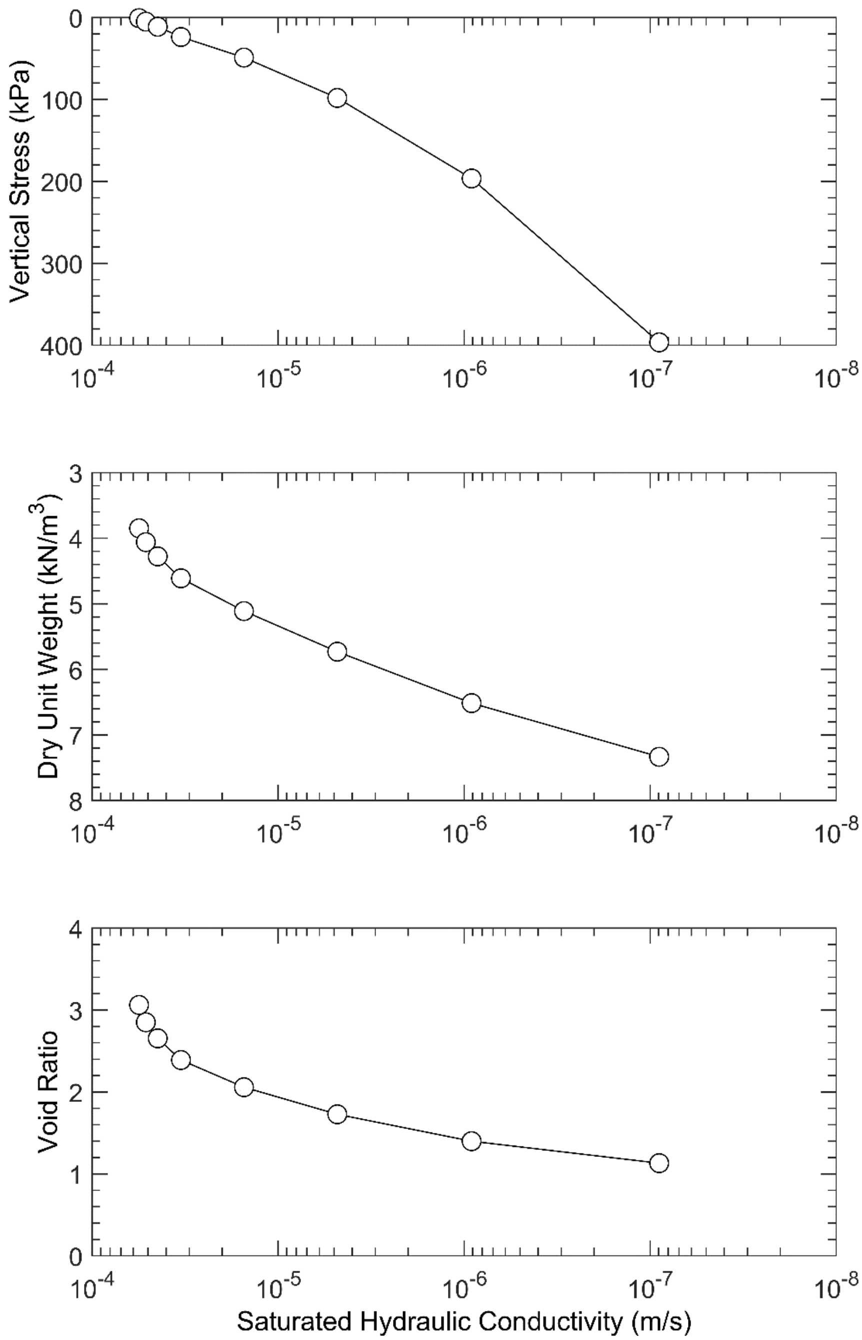

Fig. E5. Summary of saturated hydraulic conductivity tests on the mixture of 60% MSW with 40% E&PW at the as-received condition.

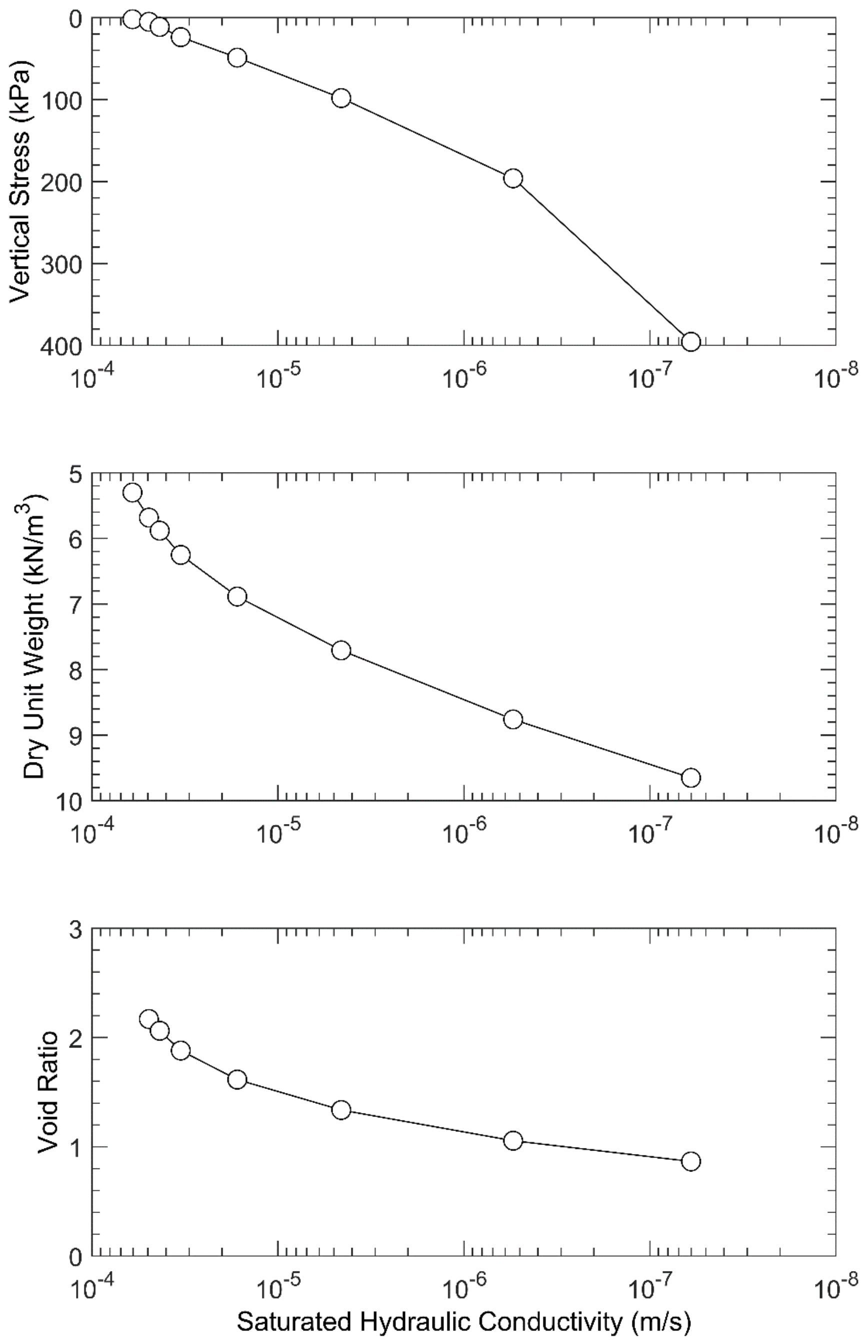

Fig. E6. Summary of saturated hydraulic conductivity tests on the mixture of 40% MSW with 60% E&PW at the as-received condition.

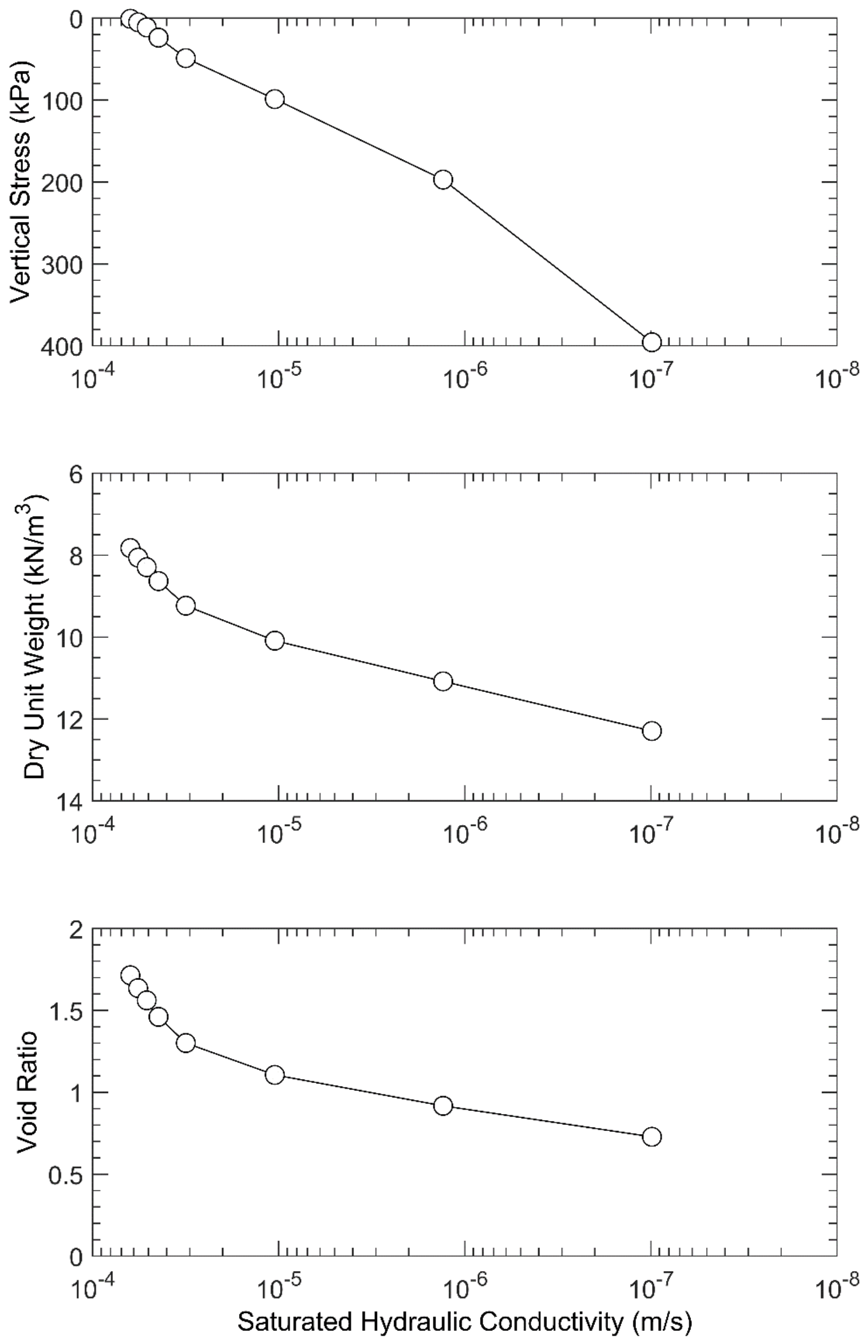

Fig. E7. Summary of saturated hydraulic conductivity tests on the mixture of 20% MSW with 80% E&PW at the as-received condition.

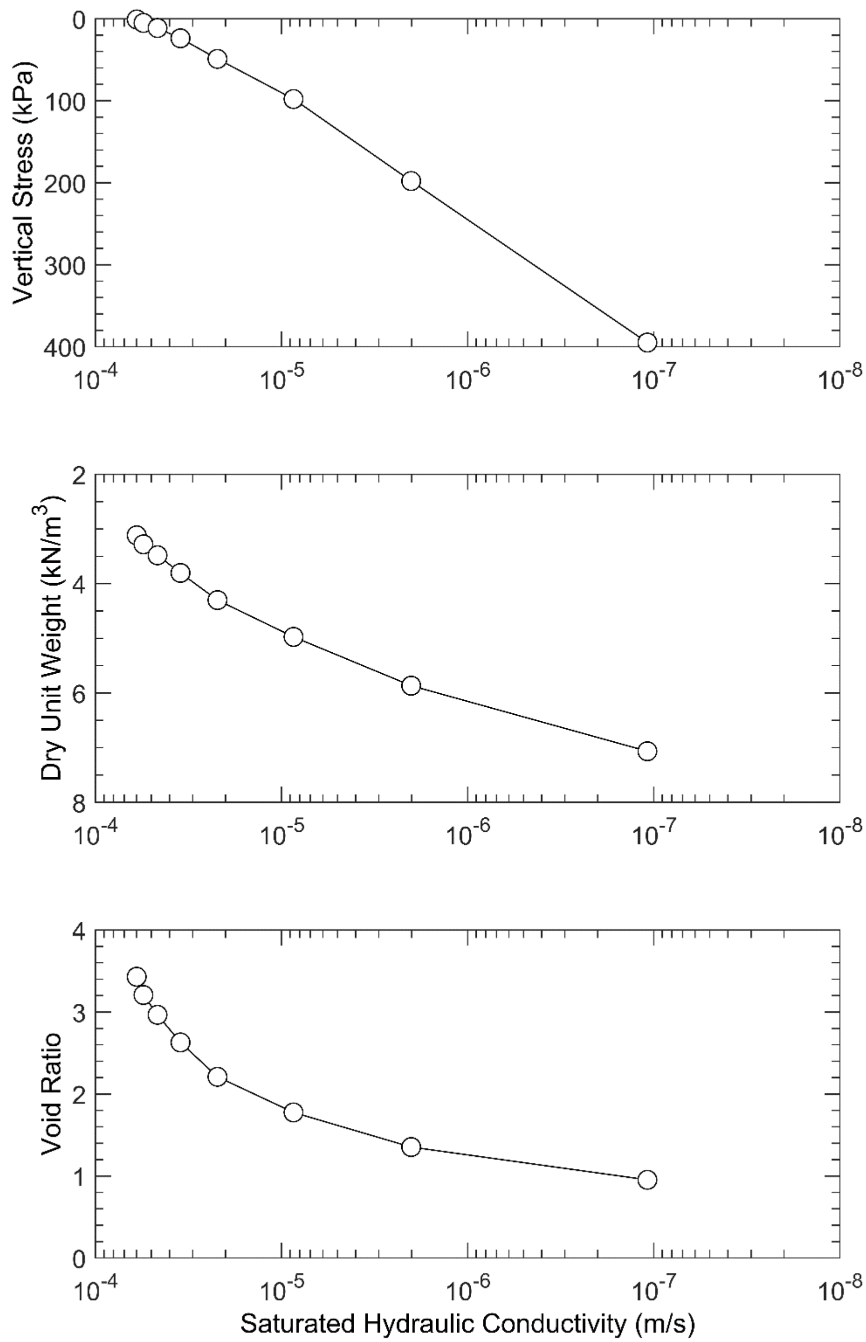

Fig. E8. Summary of saturated hydraulic conductivity tests on the mixture of 80% MSW with 20% E&PW at the wet condition.

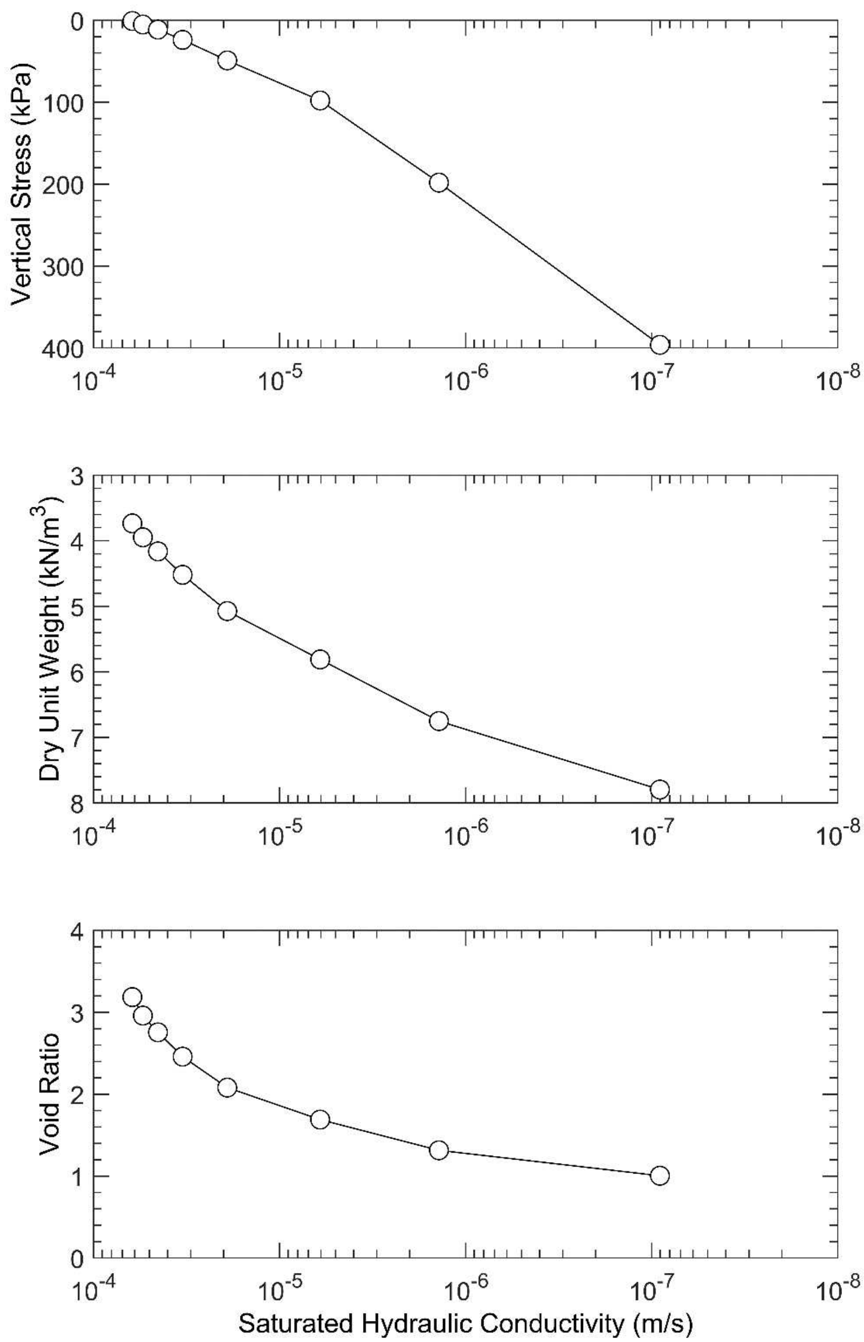

Fig. E9. Summary of saturated hydraulic conductivity tests on the mixture of 60% MSW with 40% E&PW at the wet condition.

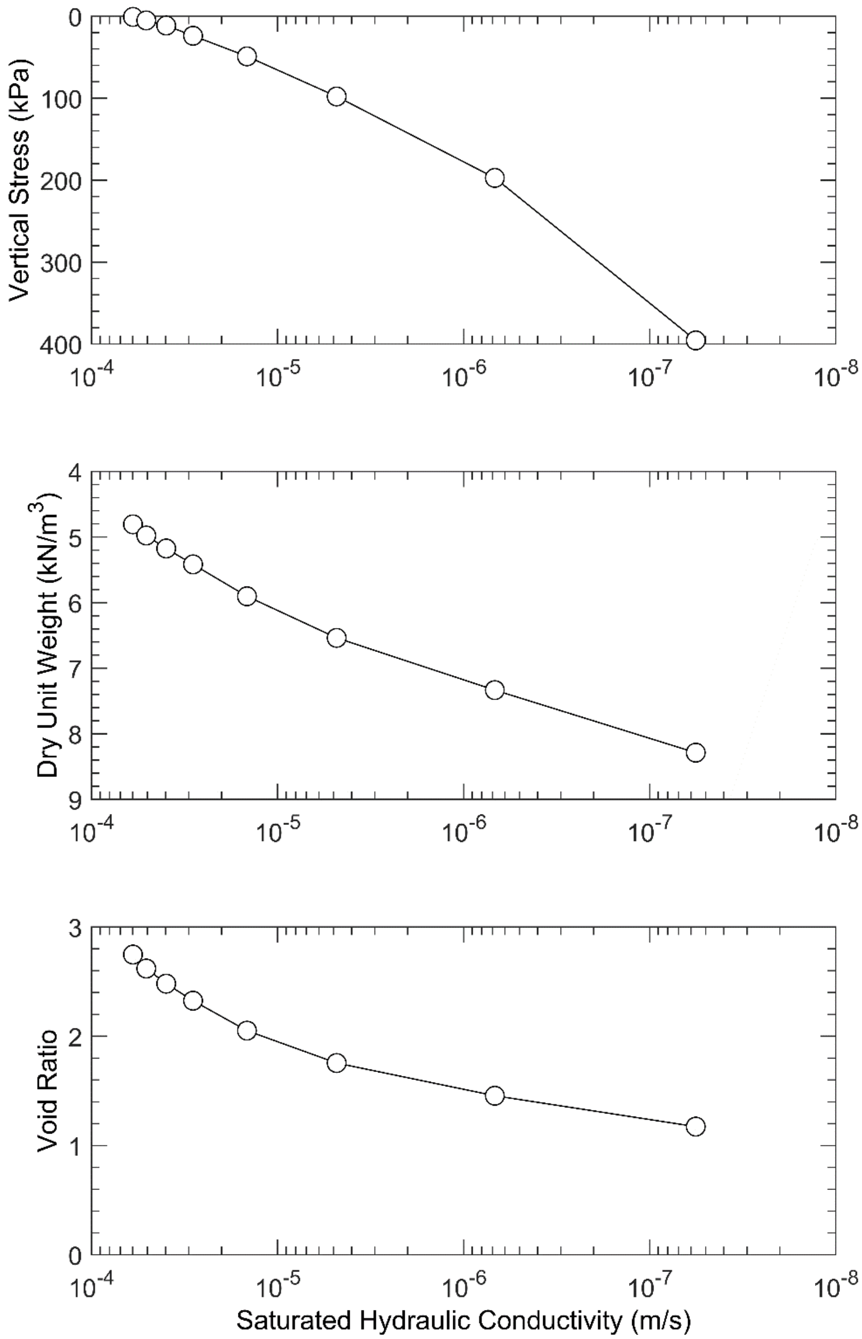

Fig. E10. Summary of saturated hydraulic conductivity tests on the mixture of 40% MSW with 60% E&PW at the wet condition.

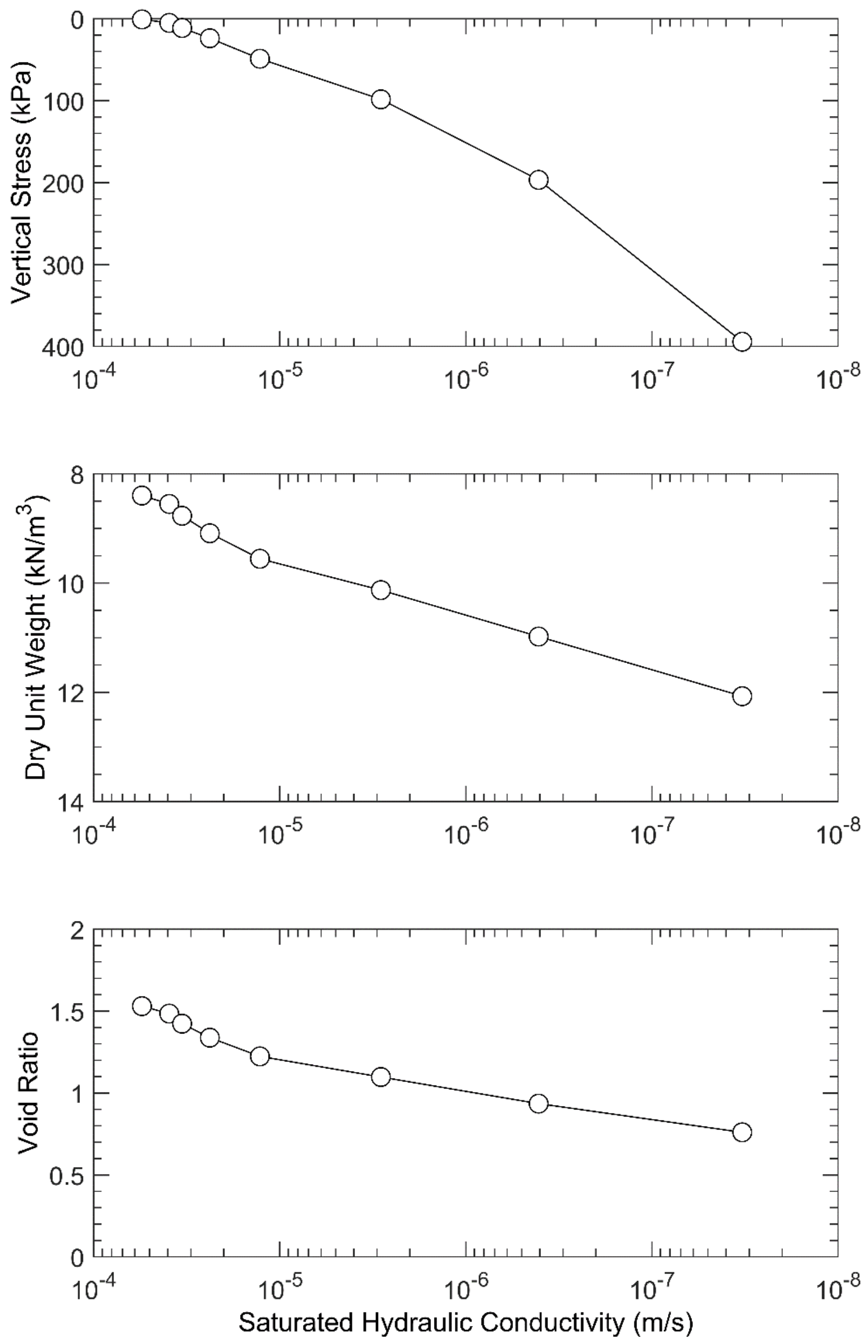

Fig. E11. Summary of saturated hydraulic conductivity tests on the mixture of 20% MSW with 80% E&PW at the wet condition.